

STATUS OF THESIS

Title of thesis

NOVEL OFDM SYSTEM BASED ON DUAL-TREE COMPLEX
WAVELET TRANSFORM

I MOHAMED HUSSIEN MOHAMED NERMA

hereby allow my thesis to be placed at the Information Resource Center (IRC) of Universiti Teknologi PETRONAS (UTP) with the following conditions:

1. The thesis becomes the property of UTP
2. The IRC of UTP may make copies of the thesis for academic purposes only.
3. This thesis is classified as

Confidential

Non-confidential

If this thesis is confidential, please state the reason:

The contents of the thesis will remain confidential for _____ years.

Remarks on disclosure:

Endorsed by

Signature of Author

Signature of Supervisor

Permanent Address: House No. 484,
Square 1, Khartoum, Sudan.

Name of Supervisor: AP. Dr. Varun
Jeoti Jagadish.

Date: _____

Date: _____

UNIVERSITI TEKNOLOGI PETRONAS

DISSERTATION TITLE: NOVEL OFDM SYSTEM BASED ON DUAL-TREE
COMPLEX WAVELET TRANSFORM.

by

MOHAMED HUSSIEN MOHAMED NERMA

The undersigned certify that they have read, and recommend to the Postgraduate Studies Programme for acceptance this thesis for the fulfilment of the requirements for the degree stated.

Signature: _____

Main Supervisor: AP. Dr. Varun Jeoti Jagadish _____

Signature: _____

Co-Supervisor: AP. Dr. Nidal S. Kamel _____

Signature: _____

Head of Department: Dr. Nor Hisham Bin Hamid _____

Date: _____

NOVEL OFDM SYSTEM BASED ON DUAL-TREE COMPLEX WAVELET
TRANSFORM

by

MOHAMED HUSSIEN MOHAMED NERMA

A Thesis

Submitted to the Postgraduate Studies Programme

as a Requirement for the Degree of

DOCTOR OF PHILOSOPHY

ELECTRICAL AND ELECTRONIC ENGINEERING

UNIVERSITI TEKNOLOGI PETRONAS

BANDAR SERI ISKANDAR,

PERAK

MAY 2010

DECLARATION OF THESIS

Title of thesis

NOVEL OFDM SYSTEM BASED ON DUAL-TREE COMPLEX
WAVELET TRANSFORM.

I MOHAMED HUSSIEN MOHAMED NERMA

hereby declare that the thesis is based on my original work except for quotations and citations which have been duly acknowledged. I also declare that it has not been previously or concurrently submitted for any other degree at UTP or other institutions.

Witnessed by

Signature of Author

Signature of Supervisor

Permanent address: House No. 484,
Square 1, Khartoum, Sudan.

Name of Supervisor
AP. Dr. Varun Jeoti Jagadish

Date : _____

Date : _____

To my Beloved Parents, Darling wife (Gamiela), Sweetheart Son (Moayid), and Precious Brothers and Sisters

ACKNOWLEDGEMENTS

In the name of Allah the most Compassionate and the most Merciful, who has favored me with countless blessings. May Allah accept our good deeds and forgive our shortcomings.

I would like to express my high gratitude to my advisors, AP. Dr. Varun Jeoti Jagadish and AP. Dr. Nidal S. Kamel for the endless hours of help, suggestions, ideas and advice during the development of this thesis.

My greatest gratitude and thankfulness are to my family:

My mother with her love and prayers backed me up and helped me to reach my goal.

My father (*May Allah forgive him and have mercy on him*) taught me the respect of science and encouraged me to seek knowledge and get higher education.

My greatest love and thanks are to my wife. Her love, care, and prayers were of great motivation and inspiration. She showed extreme patience and understanding through my studies and she was always there to help me in any way she could.

My special thanks are to my brothers and sisters. They were of great motivation and inspiration.

My greatest gratitude and thankfulness are to the members of postgraduate office for helpfulness, all the lecturers of electrical and electronic engineering department for their advices and all my friends in Universiti Teknologi PETRONAS for sharing experiences

In conclusion, I recognize that this research would not have been possible without the financial assistance of Universiti Teknologi PETRONAS (UTP), the Department of Electrical and Electronics Engineering.

Mohamed Hussien.

ABSTRACT

The demand for higher and higher capacity in wireless networks, such as cellular, mobile and local area network etc, is driving the development of new signaling techniques with improved spectral and power efficiencies. At all stages of a transceiver, from the bandwidth efficiency of the modulation schemes through highly nonlinear power amplifier of the transmitters to the channel sharing between different users, the problems relating to power usage and spectrum are aplenty. In the coming future, orthogonal frequency division multiplexing (OFDM) technology promises to be a ready solution to achieving the high data capacity and better spectral efficiency in wireless communication systems by virtue of its well-known and desirable characteristics.

Towards these ends, this dissertation investigates a novel OFDM system based on dual-tree complex wavelet transform (DTCWT) called DTCWT-OFDM. Traditional OFDM implementations use common Fourier filters for data modulation and demodulation via the inverse fast Fourier transform (IFFT) and the FFT operations respectively. Recent research has demonstrated that improved spectral efficiency can be obtained by using wavelet filters owing to their superior spectral containment properties. This has motivated the design of OFDM systems based on discrete wavelet transform (DWT) and also based on wavelet packet transform (WPT). As all the characteristics of OFDM modulated signals directly depend on the set of waveforms arising from using a given wavelet filter, several authors foresaw wavelet theory as good platform on which to build OFDM waveform bases.

Accordingly, in this work the DTCWT is used as a new platform to build a new OFDM system that can meet the stringent requirements of the future wireless communication systems. In the proposed system, the DTCWT is used in place of FFT in the conventional OFDM system. The proposed system has all the benefits of WPM system over conventional OFDM system, but it also shows performance improvement over WPM system. Investigated under perfect synchronization assumption, it is shown that its PAPR is better, its PSD containment is better, its performance in the

presence of nonlinear power amplifier is better, and its BER performance is also better. These improvements are attributed to two distinct properties of the DTCWT filters – the unique impulse response and shift-invariance of the filters. For the same length of filters in WPM and DTCWT, the design requirements of the DTCWT filters produce better impulse response and hence the better PAPR results. At the same time, the shift invariance property of DTCWT causes improvement in BER performance over WPM system which is shift-variant. This is demonstrated with the help of average BER when propagation is through frequency-selective Rayleigh channels.

Finally, it is shown that the proposed OFDM system does not suffer from higher computational complexity than OFDM and WPM system as fast FFT-like algorithms exist for computing DTCWT.

ABSTRAK

Permintaan untuk keupayaan lebih tinggi dan lebih tinggi dalam rangkaian-rangkaian wayarles, seperti kawasan tempatan yang selular, lincah dan tempatan dan sebagainya, memandu pembangunan baru memberi isyarat teknik-teknik dengan meningkat spektrum dan kecekapan kuasa. Pada semua peringkat seorang penghantar terima, daripada lebar jalur kecekapan modulasi itu merangka melalui amat amplifier kuasa tak linear penghantar itu untuk perkongsian saluran antara pengguna lain, masalah-masalah itu berkaitan untuk penggunaan tenaga dan spektrum banyak sekali. Dalam masa depan kedatangan, pemultipleksan pembahagian frekuensi ortogon (OFDM) janji-janji teknologi menjadi satu penyelesaian kesediaan untuk mencapai data tinggi keupayaan dan kecekapan spektrum lebih baik dalam sistem telekomunikasi wayarles oleh kebaikan nya ciri-ciri terkenal dan elok.

Ke hujung ini, disertasi ini menyiasat sebuah novel sistem OFDM berdasarkan dua pokok gelombang kecil kompleks mengubah (DTCWT) dipanggil DTCWT-OFDM. Pelaksanaan OFDM tradisional menggunakan Fourier biasa ditapis untuk modulasi data dan pengenyahmodulan melalui puasa songsang jelmaan Fourier (IFFT) dan operasi-operasi FFT masing-masing. Penyelidikan baru-baru ini telah menunjukkan yang meningkat kecekapan spektrum boleh didapati dengan menggunakan gelombang kecil penapis disebabkan atasan mereka ciri-ciri pembendungan spektrum. Ini telah bermotivasi reka bentuk bagi OFDM sistem-sistem berdasarkan gelombang kecil diskret mengubah (DWT) dan juga berlandaskan paket gelombang kecil mengubah (WPT). Sebagai semua ciri-ciri OFDM mengubah isyarat-isyarat secara langsung bergantung set bentuk gelombang itu muncul daripada menggunakan satu turas gelombang kecil yang dianugerahkan, beberapa pengarang melihat teori gelombang kecil sebagai platform baik pada yang untuk membina bentuk gelombang OFDM berdasarkan.

Maka, dalam kerja ini DTCWT adalah digunakan seperti sebuah platform baru untuk membina satu sistem OFDM baru yang boleh berjumpa syarat-syarat ketat sistem

telekomunikasi wayarles akan datang. Dalam sistem yang dicadangkan, DTCWT adalah digunakan sebagai ganti FFT dalam sistem OFDM konvensional. Sistem yang dicadangkan mempunyai semua faedah-faedah sistem WPM mengenai sistem OFDM konvensional, tetapi ia juga menunjukkan perbaikan prestasi mengenai sistem WPM. Disiasat di bawah penyegerakan sempurna andaian, ia ditunjukkan yang nya PAPR adalah lebih baik, pembendungan JPanya adalah lebih baik, prestasinya dalam kehadiran amplifier kuasa tak linear adalah lebih baik, dan prestasi BERnya adalah juga lebih baik. Peningkatan-peningkatan ini dianggap berpunca daripada dua kekayaan berbeza DTCWT turas - sambutan impuls unik dan anjakan ketakberubahan penapis itu. Untuk serupa panjang meresapi WPM dan DTCWT, keperluan-keperluan rekabentuk penapis DTCWT menghasilkan sambutan impuls lebih baik dan oleh itu keputusan-keputusan PAPR lebih baik. Pada masa yang sama, anjakan ketakberubahan harta bagi sebab-sebab DTCWT pemajuan dalam prestasi BER mengenai sistem WPM yang adalah anjakan kelainan. Ini ditunjukkan dengan bantuan purata itu BER apabila pembiakan selesai frekuensi memilih Rayleigh menyalurkan.

Akhirnya, ia ditunjukkan yang dicadangkan sistem OFDM tidak menghadapi kerumitan pengiraan lebih tinggi daripada OFDM dan WPM sistem kerana algoritma FFT-like cepat wujud untuk pengkomputeran DTCWT.

In compliance with the terms of the Copyright Act 1987 and the IP Policy of the university, the copyright of this thesis has been reassigned by the author to the legal entity of the university,

Institute of Technology PETRONAS Sdn Bhd.

Due acknowledgement shall always be made of the use of any material contained in, or derived from, this thesis.

© Mohamed Hussien Mohamed Nerma, 2010

Institute of Technology PETRONAS Sdn Bhd

All rights reserved.

TABLE OF CONTENTS

LIST OF TABLES	XVI
LIST OF FIGURES	xvii
LIST OF ABBREVIATIONS	xx
LIST OF SYMBOLS	xxvii
CHAPTER 1 INTRODUCTION	1
1.1 Motivation	1
1.2 Wavelet Based Signal Processing Architecture and Application	2
1.3 Significance and Objective of the Thesis	4
1.4 Research Methodology and Scope	7
1.5 Contributions	7
1.6 Organization of the Thesis	8
CHAPTER 2 OFDM, WPM AND RELATED LITERATURE.....	10
2.1 Introduction	10
2.2 OFDM System	12
2.2.1 Principle of OFDM.....	12
2.2.2 OFDM System Implementation	14
2.2.3 OFDM System Design	17
2.2.3.1 Considerations.....	17
2.2.3.2 Requirements	17
2.2.3.3 Parameters	18
2.2.4 Benefits and Drawbacks of OFDM	18
2.2.5 Applications of OFDM.....	19
2.2.6 OFDM System Model	21
2.2.6.1 Continuous Time System Model.....	21
2.2.6.2 Discrete Time System Model.....	24
2.2.7 Wavelets in Multicarrier Modulation	26
2.3 Wavelet Packet Modulation (WPM).....	27

2.3.1 Introduction	27
2.3.2 Overview of Wavelet Transform and Multiresolution Analysis	28
2.3.3 Wavelet Packet and Wavelet Packet Trees.....	31
2.3.4 The DWT and DWPT Operations	34
2.4 Underlying Structure of the OFDM and WPM Systems	36
2.4.1 Underlying Structure of OFDM System.....	36
2.4.2 Underlying Structure of WPM System.....	37
2.5 Wavelet Based OFDM (WOFDM)	40
2.6 Drawback of Common Discrete Wavelet Transform.....	43
2.7 Review of Related Research	44
2.7.1 MCM	44
2.7.2 OFDM.....	45
2.7.3 WPM.....	46
2.7.4 OFDM based on Complex Wavelet.....	53
CHAPTER 3 DT \mathbb{C} WT AND THE OFDM SYSTEM BASED ON IT	55
3.1 Introduction	55
3.2 Shortcomings of Wavelet Transform.....	56
3.2.1 Shift Variance.....	56
3.2.2 Oscillations	56
3.2.3 Lack of Directionality.....	56
3.2.4 Aliasing.....	56
3.3 The Solution	57
3.4 The Dual-Tree Complex Wavelet Transform (DT \mathbb{C} WT).....	58
3.4.1 Dual-Tree Framework	60
3.4.2 Half Sample Delay Condition	62
3.4.3 Filter Design for DT \mathbb{C} WT.....	62
3.4.3.1 First Method	63
3.4.3.2 Second Method	63
3.4.4 DT \mathbb{C} WT Filters Choice.....	63

3.5 Underlying Structure of the DTCWT-OFDM System	65
3.6 Analysis of DTCWT-OFDM System	69
3.6.1 Power Spectrum Density	69
3.6.2 Peak-to-Average Power Ratio	70
3.6.2.1 Effect of the Nonlinear HPA	70
3.6.2.2 DTCWT-OFDM and nonlinear HPA	74
3.6.3 Bit Error Rate	76
3.6.4 Computational Complexity	76
3.6.5 Channel Estimation and Synchronization	76
CHAPTER 4 RESEARCH METHODOLOGY AND RESULTS	78
4.1 Performance Metric Parameters and Research Methodology	79
4.1.1 For the OFDM System	84
4.1.2 For the WPM System	84
4.1.3 For the DTCWT-OFDM System	85
4.2 Peak-to-Average Power Ratio	85
4.2.1 Peak Envelope	86
4.2.2 CCDF	89
4.2.2.1 Typical Comparison	89
4.2.2.2 Study of use of different filters in DTCWT	90
4.2.2.3 Study on use of different number of subcarriers	92
4.3 Power Spectrum Density	95
4.3.1 Power Spectrum Density without the HPA	95
4.3.2 Power Spectrum Density with the HPA	96
4.3.2.1 Spectrum Re-growth	97
4.3.2.2 Input Power Back-off	97
4.4 Bit Error Rate	102
4.4.1 Bit Error Rate without the HPA	102
4.4.1.1 BER in AWGN	102
4.4.1.2 BER in Rayleigh Flat Fading Channel	103

4.4.1.3 Study of BER with different wavelet filters.....	104
4.4.2 Bit Error Rate with HPA	106
4.5 Study of the Shift Invariance Property.....	110
4.6 Complexity Analysis.....	114
CHAPTER 5 CONCLUSION AND FUTURE WORK.....	116
5.1 Dissertation Summary and Contributions.....	116
5.2 Future Work.....	118
PUBLICATIONS.....	120
 Conference Papers.....	120
 Journal Papers	120
 Book Chapters.....	121
BIBLIOGRAPHY.....	122
APPENDIX A.....	132
APPENDIX B.....	135
APPENDIX C.....	139
APPENDIX D.....	142
APPENDIX E.....	147

LIST OF TABLES

Table 2.1 Data rates provided by existing communication systems.....	20
Table 2.2 Orthogonal frequency division multiple modulation based systems.....	21
Table 3.1 Approximations to CCDF of PAPR.	74
Table 4.1 Main channel properties of the 10-tap model.	84
Table 4.2 Simulation parameters.	86
Table 5.1 Comparison of DT-CWT-OFDM, WPM and the conventional OFDM systems.....	118

LIST OF FIGURES

Figure 1.1 Wavelet domain signal processing.	3
Figure 1.2 Wavelet domain pre-processing.	4
Figure 2.1 Classification of the MCM systems.	12
Figure 2.2 Block diagram of a generic MCM transmitter.	13
Figure 2.3 Comparison between conventional FDM (a) and OFDM (b).	14
Figure 2.4 OFDM symbol with cyclic prefix (CP).	16
Figure 2.5 Basic OFDM transmitter and receiver.	17
Figure 2.6 Simplified continuous time baseband OFDM model.	22
Figure 2.7 Subcarrier spectrum of OFDM system.	24
Figure 2.8 BER performance of theoretical BPSK and OFDM using BPSK in AWGN channel.	26
Figure 2.9 Two stage analysis filter banks or wavelet decomposition.	30
Figure 2.10 Two stage synthesis filter bank or wavelet reconstruction.	31
Figure 2.11 Analysis and synthesis filters using H, G, H^l, G^l operators.	33
Figure 2.12 Wavelet packet trees: (a) DWPT/analysis tree, (b) IDWPT/synthesis Tree.	34
Figure 2.13 Subband decomposition.	35
Figure 2.14 Time frequency tiling of the WT.	36
Figure 2.15 Time frequency tiling of the WPT.	36
Figure 2.16 Functional block diagram of the OFDM system.	37
Figure 2.17 Functional block diagram of the WPM system.	38
Figure 2.18 WPM: (a) Modulation (IDWPT) and (b) Demodulation (DWPT) trees.	39
Figure 2.19 Wavelet based MCM structure.	41
Figure 2.20 Frequency response of seven spectrally contiguous subchannel pulse sequence for OFDM transmission.	42
Figure 2.21 Frequency response of seven spectrally contiguous subchannel pulse sequence for WOFDM transmission.	43
Figure 3.1 Dual-tree discrete CWT (DTDCWT) analysis (demodulation) FB.	59

Figure 3.2 Inverse dual-tree discrete CWT (IDTCWT) synthesis (modulation) FB.	60
Figure 3.3 Real and imaginary parts of complex coefficients from the upper and lower tree respectively.....	64
Figure 3.4 DTCWT decomposition and reconstruction.....	65
Figure 3.5 Functional block diagram of OFDM based on DTCWT system.....	66
Figure 3.6 A typical power amplifier response.....	71
Figure 3.7 AM/AM characteristic of the SSPA.....	72
Figure 3.8 AM/AM and AM/PM characteristic of the TWTA.....	73
Figure 3.9 Functional block diagram of OFDM based on DTCWT system with HPA.	75
Figure 4.1 Flow charts of the simulation procedures of the considered systems.	83
Figure 4.2 Envelope of the OFDM, WPM and DTCWT-OFDM systems.	87
Figure 4.3 Envelope of the 16 subcarriers using FT.....	88
Figure 4.4 Envelope of the 16 subcarriers using WT.	88
Figure 4.5 CCDF for the OFDM, WPM and DTCWT-OFDM systems.....	89
Figure 4.6 Effect of using different set of filters in design of the DTCWT-OFDM....	90
Figure 4.7 Effect of using different set of filters in design of the WPM system.	92
Figure 4.8 CCDF results for the OFDM using different subcarriers (N).....	93
Figure 4.9 CCDF results for the WPM using different subcarriers (N).....	94
Figure 4.10 CCDF results for the DTCWT-OFDM using different subcarriers (N). ..	95
Figure 4.11 PSD for the OFDM, WPM and DTCWT-OFDM systems.....	96
Figure 4.12 PSD for the OFDM, WPM and DTCWT-OFDM systems in presence of nonlinear SSPA.....	98
Figure 4.13 PSD for the OFDM, WPM and DTCWT-OFDM systems in presence of nonlinear TWTA.....	99
Figure 4.14 PSD for the OFDM, WPM and DTCWT-OFDM systems in presence of nonlinear SSPA and TWTA.	100
Figure 4.15 PSD of the considered systems. OFDM (IBO = 10.9 dB), WPM (IBO = 6.8 dB), DTCWT-OFDM (IBO = 5.5 dB).....	101
Figure 4.16 PSD of the considered systems. OFDM (IBO = 10.9 dB), WPM (IBO = 6.8 dB), DTCWT-OFDM (IBO = 5.5 dB).....	102

Figure 4.17 BER performance of DTCW-OFDM using BPSK and 16-QAM in AWGN channel.	103
Figure 4.18 BER performance of DTCW-OFDM using BPSK and 16-QAM in a 10-tap Rayleigh channel.	104
Figure 4.19 BER performance of DTCW-OFDM using BPSK and 16-QAM in AWGN channel for different type of filters.	105
Figure 4.20 BER performance of WPM using BPSK in AWGN channel for different type of filters.....	106
Figure 4.21 BER performance of DTCWT-OFDM using BPSK and 16-QAM in the presence of SSPA.	108
Figure 4.22 BER performance of DTCWT-OFDM using BPSK and 16-QAM in the presence of TWTA.	109
Figure 4.23 BER performances of the OFDM, WPM and DTCWT-OFDM systems using 10.9 dB, 6.8 dB and 5.5 dB of IBO respectively.	110
Figure 4.24 BER performance of the DTCWT-OFDM using BPSK in frequency selective channel.....	111
Figure 4.25 BER performance of the DTCWT-OFDM using 16-QAM in frequency selective channel.....	112
Figure 4.26 BER performance of the DTCWT-OFDM using BPSK with different values of the tap delay.	113
Figure 4.27 BER performance of the DTCWT-OFDM using 16-QAM with different values of the tap delay.	114

LIST OF ABBREVIATIONS

ACI	Adjacent Channel Interference
ADC	Analog to Digital Converter
ADSL	Asynchronous Digital Subscriber Line
AM/AM	Amplitude Modulation-Amplitude Modulation
AM/PM	Amplitude Modulation-Phase Modulation
ASCET	Adaptive Sine Modulated / Cosine Modulated Filter Bank Equalizer for Transmultiplexers
AWGN	Additive White Gaussian Noise
BER	Bit Error Rate
BPSK	Binary Phase Shift Keying
BWA	Broadband Wireless Access
CCDF	Complementary Cumulative Distribution Function
CHT	Complex Haar Transform
CIR	Channel Impulse response
CLT	Central Limit Theorem
CMFB	Cosine Modulated Filter Banks
CNR	Carrier to Noise Ratio
COFDM	Coded OFDM
CP	Cyclic Prefix
CR	Cognitive Radio
CWOFDM	Coded Wavelet Based OFDM

CCWP	Complex Wavelet Packet
CCWT	Complex Wavelet Transform
CWT	Continuous Wavelet Transform
DAB	Digital Audio Broadcasting
DCT	Discrete Cosine Transform
DCT-OFDM	DCT Based OFDM
DDTCCWT	Discrete Dual-Tree Complex Wavelet Transform
DFT	Discrete Fourier Transform
DFT-OFDM	DFT Based OFDM
DMT	Discrete Multi Tone
DSL	Digital Subscriber Line
DSP	Digital Signal Processing
DTCWT	Dual-Tree Complex Wavelet Transform
DTCWT-OFDM	DTCWT Based OFDM
DTDCWT	Dual-Tree Discrete Complex Wavelet Transform
DTWT	Dual-Tree Wavelet Transform
DVB	Digital Video Broadcasting
DWMT	Discrete Wavelet Multitone
DWPT	Discrete Wavelet Packet Transform
DWPT-OFDM	DWPT Based OFDM
DWT	Discrete Wavelet Transform
DWT-OFDM	DWT Based OFDM
E_b/N_o	Energy per Bit to Noise Power Spectral Density Ratio

EDGE	Enhanced Data Rate for GSM Evolution
ETSI	European Telecommunications Standards Institute
FB	Filter Bank
FDE	Frequency Domain Equalizer
FDM	Frequency Division Multiplex
FEC	Forward Error Correction
FFT	Fast Fourier Transform
FFT-OFDM	FFT Based OFDM
FIR	Finite Impulse Response
FSK	Frequency Shift Keying
FT	Fourier Transform
GaAs-FET	Gallium Arsenide Field-Effect Transistor
GI	Guard Interval
GSM	Global System for Mobile Communication
HF	High Frequency
HIPERLAN2	High Performance Radio LAN Version 2
Home PAN	Home Phone Line Networking Alliance
HPA	High Power Amplifier
i.i.d	independent and identically distributed
IBO	Input Power Back-Off
ICI	Inter Carrier Interference
IDDT \mathcal{C} WT	Inverse Discrete Dual-Tree Complex Wavelet Transform
IDFT	Inverse Discrete Fourier Transform

IDTDCWT	Inverse Dual-Tree Discrete Complex Wavelet Transform
IDWPT	Inverse Discrete Wavelet Packet Transform
IDWT	Inverse Discrete Wavelet Transform
IEEE	Institute of Electrical and Electronics Engineers
IFFT	Inverse Fast Fourier Transform
ISI	Inter Symbol Interference
JPEG	Joint Photographic Experts Group
LAN	Local Area Network
LDPC	Low-Density Parity-Check
LDPC-CWOFDM	Low Density Parity Check Coded Wavelet Based OFDM
MACS	Multiple Access Communication Systems
MC-CDMA	MultiCarrier Code Division Multiple Access
MCM	MultiCarrier Modulation
M-D	MultiDimensions
MIMO	Multiple Input Multiple Output
ML	Maximum Likelihood
MLSE/SIC	Maximum-Likelihood Sequence Estimation/Successive Interference Cancellation
MRA	Multi Resolution Analysis
MWPM	Multiwavelet Packet Modulation
NBI	Narrow Band Interference
OBO	Output Back-off
OFDM	Orthogonal Frequency Division Multiplexing

OFDMA	Orthogonal Frequency Division Multiple Access
ONBs	Orthonormal Bases
OOB	OutOff Band
PAPR	Peak to Average Power Ratio
PCCC	Parallel Concatenated Convolutional Code
PHY	Physical Layer
PLC	Power Line Communication
PR	Perfect Reconstruction
PSAM	Pilot Symbol Assisted Modulation
PSD	Power Spectrum Density
PSK	Phase Shift Keying
QAM	Quadrature Amplitude Modulation
QMF	Quadrature Miror Filter
QoS	Quality of Service
QPSK	Quadrature Phase Shift Keying
RF	Radio Frequency
RS	Reed-Solomon
SC	Single Carrier
SC-OFDM	Single Carrier OFDM
SC-WPM	Single Carrier WPM
SNR	Signal to Noise Ratio
SSB	Single Side Band
SSPA	Solid State Power Amplifier

STBC	Space Time Block Coding
STC	Space Time Code
STFT	Short Time Fourier Transform
TCWOFDM	Turbo Coded Wavelet based OFDM
TDM	Time Division Multiplexing
TWT	Travelling Wave Tube
TWTA	Travelling Wave Tube Amplifier
UWB	Ultra Wideband
UWT	Undecimated Wavelet Transforms
VLSI	Very Large Scale Integration
WCC	Woven Convolutional Codes
WCDMA	Wideband Code Division Multiple Access
WiFi	Wireless Fidelity
WiMAX	Worldwide Interoperability for Microwave Access
WLAN	Wireless Local Area Network
WM	Wavelet Modulation
WMCM	Wavelet Based MCM
WOFDM	Wavelet OFDM
WPDM	Wavelet Packet Division Multiplexing
WPM	Wavelet Packet Modulation
WPT	Wavelet Packet Transform
WPTP	Wavelet Packet Tree Pruning
WSSUS	Wide Sense Stationary Uncorrelated Scattering

WT

Wavelet Transform

LIST OF SYMBOLS

τ_{max}	Maximum Delay Spread
T_g	Length of CP
N	No. of Subcarriers
T_s	OFDM Symbol Time
N_g	Guard Interval
T	IFFT Symbol Period
T_{sym}	Effective Symbol Period
B	Bandwidth
$\phi(t)$	Scaling Function
a_{ok}	Scaling Function Coefficients
$\psi(t)$	Wavelet Function
$d_{j,k}$	Wavelet Function Coefficients
$x(t)$	Continuous Time Transmitted Signal
$y(t)$	Continuous Time Received Signal
$h(t)$	Channel Impulse Response
$w(t)$	AWGN Noise
$\theta(t)$	Phase difference
f_c	Carrier Frequency
$g(A)$	AM/AM function
$\Phi(A)$	AM/PM function
V_m	Nested Subspaces
w_m	Wavelet Space
m	Scaling Index
k	Translation Index
$h(k)$	Low-Pass Filter
$g(k)$	High-Pass Filter

A_0	Saturation output Amplitude
P_0	Maximum output Power
P_s	Mean output Power of the Transmitted Signal
α	Roll-off Factor
$\delta(k)$	Kronecker Delta Function
σ^2	Noise Variance
$R_e[x]$	The Real Part of x
$I_m[x]$	The Imaginary Part of x

CHAPTER 1

INTRODUCTION

1.1 Motivation

Doubtlessly, the considerable growth in the demand of mobile devices supporting high data rate and high bandwidth multimedia communications has posed many challenges to current wireless technologies and architectures in terms of supporting these higher data rate transmission while conserving the limited bandwidth and power resources [1], [2]. Particularly, the power constraints determined by the size of the batteries in mobile devices and the scarcity of the finite spectrum resources are the most limiting among all the other transmission requirements [3]. To overcome the limitations in current hardware architectures and the limited utilization of the scarce radio spectrum, there is an urgent need for more efficient communication technologies. At present, the power constraints are overcome by use of the technologies for a better battery and more linear and efficient front-end high power amplifiers – that are both, unluckily, very expensive [4].

By improving the efficiency with which the spectrum resource is utilized, by developing techniques allowing for better spectrum-sharing among users, and by widening the upper-most range of usable spectrum the bandwidth constraints can be greatly improved [5], [6]. A variety of solutions have been brought upon by digital signal processing (DSP) techniques to address power and bandwidth issues in current transceiver designs [2]. This work is an effort in the same direction wherein efficient signal-processing methods are developed that address the aforesaid issues at the transceiver. In this work, a novel multi-carrier technique based on efficient complex wavelet signal processing is investigated for more effective utilization of the spectrum and power in wireless transceiver than what is available.

A significant amount of research has been carried out applying wavelets to almost all aspects of digital wireless communication systems [7], [8], [9] be they data compression, source and channel coding, signal de-noising, channel modeling, or design of transceivers. The flexibility and the ability to represent the signals more accurately than other bases are the main property of wavelets encouraging these applications.

These properties of wavelets also make them very suitable for signal processing in modern communication systems such as multicarrier modulation (MCM) systems and multiple antenna systems [7], [10]. Also, the versatility of wavelet bases makes them strong contenders for variety of applications in future wireless communication systems such as wireless channel modeling, interference mitigation, orthogonal frequency division multiplexing (OFDM) modulation, multiple access, ultra wideband communications, wireless networks and cognitive radio (CR) intelligent wireless communication system [7], [10]. This work build on this premise by further investigating the potential of deploying, in particular, complex wavelets in the design of an MCM system.

In this thesis, the use of complex wavelet based OFDM technology to address power and bandwidth efficiency problems in modern wireless communication systems is investigated. Specifically, dual-tree complex wavelet transform (DTCWT)¹ is made use of for designing a novel OFDM system, i.e., an OFDM system based on DTCWT (DTCWT-OFDM) is proposed.

1.2 Wavelet Based Signal Processing Architecture and Application

The wavelet transform (WT) is a class of generalized Fourier transform (FT) with basis-functions localized well in both time and frequency domains. This transform provides a way to analyze the signals by examining the coefficients (or weights) of the WT. In traditional wavelet theory, WT facilitates the decomposition of the signal of interest into a set of basis waveforms, called wavelets (small waves) [11], [12]. As an extension of WT, the wavelet packet transform (WPT), has also been developed and used in signal processing and digital modulation schemes [7], [13]. Commonly, in

¹ We use the complex number symbol \mathbb{C} in CWT to avoid confusion with the often used acronym CWT for the continuous wavelet transform.

the WT based processing, a signal is decomposed into a set of coefficients and the coefficients are then utilized based on the desired attributes of the signal. In system-identification problems, these wavelet coefficients provide information about the time varying frequency content of the signal analyzed. An explicit example in wireless communications is the modeling of a time varying channel impulse response [7]. The WT has the property that it concentrates the information about the desired characteristics of the analyzed signal in only a few coefficients, while the remaining coefficients have negligible magnitudes. This makes the processing of signals in the wavelet domain computationally efficient.

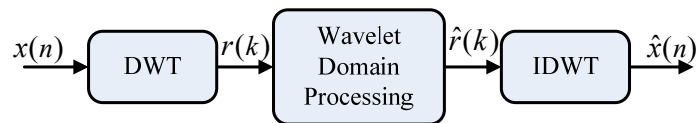


Figure 1.1 Wavelet domain signal processing.

Relying on the type of application, there are different ways in which the versatile power of WT based signal processing can be used. For example, joint photographic experts group committee (JPEG2000) stipulates its use in image compression, and, WiMAX as wavelet packet modulation (WPM) [7]. Figure 1.1 shows a functional diagram of the wavelet domain signal processing operation. In this figure, the discrete time input signal, $x(n)$, is decomposed into a set of coefficients, $r(k)$, using the discrete wavelet transform (DWT). The coefficients are then processed via thresholding and/or scaling to produce a new set of coefficients, $\hat{r}(k)$, which are stored or used to reconstruct, using the inverse DWT (IDWT), the signal, $\hat{x}(n)$, with the desired properties. The process of approximating the original signal, $x(n)$, can make use of the best basis- functions-selection algorithm to force the decomposition to obtain the desired characteristics of the signal [12].

Another popular approach for taking advantage of the WT is in the pre-processing and post-processing stages as shown in Fig. 1.2. In this approach, a signal, $x(n)$, is modified using the WT to get an intermediate signal, $y(n)$, prior to being input into the system or channel. In fact, the pre-processed signal, $y(n)$, may be the signal $\hat{r}(k)$ or $\hat{x}(n)$, the output from the wavelet domain signal processing block shown in

Fig. 1.1. Both the transform domain processing and pre-processing techniques can be used for various applications from multiple-input and multiple-output (MIMO) systems to CR. In this research work, the pre-processing and post-processing is utilized using, respectively, IDTCWT and DTTCWT in the OFDM system.



Figure 1.2 Wavelet domain pre-processing.

1.3 Significance and Objective of the Thesis

The design of efficient digital communication systems is a challenge which is affected by a number of factors such as the available technology, the channel characteristics, the type of service aimed for (e.g., data, speech, video, images, facsimile, etc.), new ideas in research, the acceptable cost of the system, and regulations. The driving force behind this challenge today for future digital communication systems is the requirement for higher data rates and systems capable of supporting many different types of services with different bit error probability and delay requirements.

To this end, OFDM is one of the best candidates and is fast becoming the de-facto standard for present and future high speed communication systems. OFDM is a MCM technique that divides the digital data stream to be transmitted into a number of parallel bit streams, and utilizing these to modulate a number of subcarriers.

In OFDM system, subchannels are obtained with an orthogonal transformation using inverse discrete Fourier transform (IDFT) [14] on each block of data. The DFT/IDFT exhibits the desired orthogonality and can be implemented efficiently using the fast Fourier transform (FFT) algorithm. Orthogonal transformations are used so that at the receiver side, simply, the inverse transformation can be applied to demodulate the data without error in the absence of noise. Efficient modulation and coding methods can be utilized in the individual subchannels to approach the capacity of the channel. OFDM schemes use rectangular pulses for data modulation. Therefore, a given subchannel has significant spectral overlap with a large number of adjacent subchannels. Hence, subchannel isolation is preserved only for channels which

introduce virtually no distortion. But typical channels are far from ideal, and introduce interference that reduces system performance.

One of the key ideas behind the OFDM realization is the use of guard interval (GI) that contains a cyclic prefix (CP), which is used to overcome the intersymbol interference (ISI) caused by the delay spread of the channel [15], [16] and make the OFDM system realizable using DFT/IDFT. The large number of subchannels/subcarriers makes the task of equalization at the receiver a simple scalar multiplication/division (frequency domain equalization). However, this performance comes at the cost of i) poor spectral concentration of the subcarriers and ii) certain loss of spectral efficiency. These are the characteristics of Fourier (rectangular) filters.

An alternative approach to conventional OFDM is based on DWT that makes use of wavelet filters that have better time-scale localization property. This leads to highly structured and thus efficiently realizable transmission signal sets. Currently, wavelet based OFDM has gained popularity in the literature. DWT-OFDM can better combat narrowband interference (NBI) and is inherently more robust with respect to intercarrier interference (ICI) than conventional FFT filters due to very high spectral containment properties of the wavelet filters. As DWT-OFDM systems do not rely on cyclic prefix, the data rates can surpass those of FFT based OFDM systems.

A wavelet packet (WP) is a generalization of wavelets, in that each octave frequency band of the wavelet spectrum is further subdivided into finer frequency bands by using the two scale relation repeatedly. The translates and dilates of each of these wavelet packets form an orthogonal basis allowing a signal to be decomposed into many wavelet packet components. A signal maybe represented by a selected set of wavelet packets without using every wavelet packet for a given level of resolution.

Wavelet packets offer a more affluent signal analysis than wavelet decomposition of a signal. It allows focus on any part in time-frequency domain in a more detailed way than is possible with ordinary wavelet transform. The good frequency characteristics and greater flexibility presented by WPT make it a very useful choice for high data rate OFDM transceiver in fading channel conditions than DWT. However, a major trouble with common WPT is its lack of shift-invariance. This means that, on shift of the input signal, the wavelet coefficients vary substantially. The signal-information in the subbands may even not be stationary so that the energy distribution across the

subbands may change. To overcome the problem of shift dependence, one possible method is to simply reject the subsampling causing the shift dependence. Techniques that exclude or partially exclude subsampling are known as cycle-spinning, oversampled filter banks or undecimated wavelet transforms (UWT). However, these transforms are redundant [17], which is not desirable in MCM systems as it increases the computational complexity many-fold.

As another option, one can use a non-redundant wavelet transform, called Dual-Tree Complex Wavelet Transform (DTCWT) that achieves approximate shift invariance [18]. This transform gives rise to complex wavelet coefficients that can be used to modulate the data stream in the same way that WPM do [19]. In this thesis, we use this DTCWT to design the OFDM system.

The general objective of this work is related to the application of DTCWT to design and evaluate a new OFDM system. The specific goals of this work can be summarized as:

- ❑ Establish an appropriate system model for the DTCWT based OFDM transceiver scheme.
- ❑ Carry out simulation based performance analysis of the DTCWT based OFDM system and compare with conventional OFDM (FFT based OFDM system) and Wavelet Packet Modulation (WPM) systems (WPT based OFDM system) under different scenario.
- ❑ Study peak-to-average power ratio (PAPR) performance of the transmitted signals of the above three systems.
- ❑ Study, under the assumption of perfect synchronization and no high power amplifier (HPA) at the transmitter, the power spectral density (PSD) and the bit error rate (BER) performance of these ideal systems in AWGN and Rayleigh channels.
- ❑ Study the impact of the presence of the HPA (both, the solid state high power amplifier (SSPA) and travelling wave tube amplifier (TWTA)) on PSD in terms of spectrum re-growth, input power back-off.
- ❑ Study the impact of the presence of the HPA on BER and average BER in flat fading and frequency-selective Rayleigh channels.
- ❑ Study the impact of approximate time-invariance of DTCWT on BER performance in the presence of frequency-selective Rayleigh channel as

compared to time-varying WPT.

- Find out the implementation complexity of the proposed system and compare it with those of the conventional OFDM and WPM systems.

1.4 Research Methodology and Scope

To verify the capability of the proposed system, a couple of comparisons are performed with the conventional OFDM and WPM systems for various metric parameters like PSD, PAPR, BER and average BER and computational complexity. Among various performance metric parameters, these parameters reflect the true nature of wavelet filters and their impact on the system performance.

The systems model includes transmitter and receiver side and Rayleigh channel in between are simulated in the presence of AWGN under the assumption of perfect synchronization. The simulations are carried out under a MATLAB[®] (7.6) R2008a environment. The blocks are implemented by MATLAB[®] functions using personal computer running Windows XP service pack 3 on Intel[®] Pentium[®] 4 2.8GHz processor, and 2GB of RAM.

1.5 Contributions

There are many ways in which wavelet theory has advanced the field of wireless communications. In this work, particular emphasis is placed upon the application of wavelets to transmission technologies. The main contributions of this work are:

1. Design of a new MCM transceiver scheme based on DTCWT. It is shown that the proposed system, while retaining all the good performance of WPM over conventional OFDM, can achieve better PAPR performance than both.
2. Analysis of system performance of DTCWT-OFDM relative to those of OFDM and WPM, both, in the presence and absence of nonlinear HPA. The PSD and the BER and average BER performance of the systems under both AWGN and Rayleigh channels are analyzed. It is shown that the proposed system has lower input power back-off, lower out-of-band attenuation and better BER performance in the presence of HPA.
3. It is also shown that the complexity of the system is lower than that of the

conventional OFDM and WPM systems.

1.6 Organization of the Thesis

The following outlines the organization of this thesis and describes the contents of each chapter.

Chapter 1 introduces the background and motivation of this research work with the comprehensive description of the central theme of this research, and how the idea of wavelet based signal processing is made use of. The main contributions of this work are also listed.

Starting with the conventional OFDM, chapter 2 provides an introduction to OFDM and WPM systems. After a brief history on origin of MCM, this chapter describes the principles of OFDM and how it can be generated and received illustrating OFDM digital implementation scheme by using FFT and its counterpart, the IFFT. Moreover, it gives details of the cyclic prefix (CP) and explains how it helps avoid inter-symbol interference (ISI) in dispersive channels. It also illustrates the benefits and drawbacks of OFDM. Then, it introduces the basic concept of WT, multiresolution analysis (MRA), wavelets and scaling functions, then the representation of the DWT, WPT and subcoding. These are followed by the underlying structure of OFDM and WPM systems. Following that the OFDM system based on wavelet i.e., WOFDM is introduced, and finally, this chapter concludes with a review of the related research work.

Chapter 3 introduces the problems and shortcomings related to use of real WT and the concept of DTCWT. Some important issues related to DTCWT such as the dual-tree (DT) framework, half sample delay condition, filter design and choice of the DTCWT filters are also described. Then the proposed systems model with complete transmitter and receiver architectures is presented. The issue of PAPR is investigated and the impact of nonlinear HPA in the proposed system is also investigated.

The performance of the PSD, PAPR, BER, average BER and computational complexity for the proposed system are quantified in chapter 4 through simulation in the MATLAB[®] computing environments using BPSK and 16 QAM with Haar (also known as Daubechies-1 (db1), db3, db9 and db13 and different filters in the design of DTCWT. These results are shown for different number of subcarriers in AWGN and

Rayleigh channel and compared with those of OFDM and WPM systems. The results of the PSD, CCDF BER, average BER, spectrum re-growth and input power pack-off in the present and absent of HPA for the OFDM, WPM and DTCWT-OFDM systems are also analyzed. Moreover, the computational complexity of the above systems is also investigated.

Finally, chapter 5 concludes the thesis with the summary of major features of the research presented. The chapter also presents avenues for further and possible future research work in this field.

Appendix A addresses the m-file of the MATLAB® function to perform the one dimension IDTCWT. Appendix B presents the m-file of the MATLAB® function to perform the two dimensions IDTCWT. Appendix C described the m-file of the MATLAB® function to perform the one dimension DTCWT. Appendix D details the m-file of the MATLAB® function to perform the two dimensions DTCWT. Finally, Appendix E show the coefficients of the DTCWT filters

CHAPTER 2

OFDM, WPM AND RELATED LITERATURE

This chapter presents a detailed background of conventional OFDM system and the WPM system so the system-design of DT-CWT based OFDM system can be presented systematically later. It also presents the related literature that captures the work done in the area of OFDM, WPM and complex wavelet based OFDM systems. The chapter begins with an introduction to multicarrier modulation (MCM) systems in section 2.1, followed by a presentation of the general principles of OFDM system in section 2.2. The discussions of the OFDM system implementation and design are discussed in section 2.2.2 and 2.2.3, respectively. Benefits and drawbacks of OFDM system are discussed in section 2.2.4 along with a summary of various applications of OFDM in section 2.2.5. In section 2.2.6 continuous and discrete-time OFDM system model are discussed, while section 2.2.7 discusses the wavelet in MCM. An overview of wavelet transform and multi-resolution analysis (MRA) are discussed in 2.3.1 and 2.3.2, respectively. The wavelet packet (WP) and wavelet packet transform (WPT) are presented in section 2.3.3, followed by discussions on sub-coding in section 2.3.4. The underlying structure of OFDM and WPM systems are illustrated in section 2.4. Then, section 2.5 presents the wavelet based OFDM (WOFDM) system and section 2.6 discusses the drawback of common discrete wavelet. This chapter is concluded with section 2.7 wherein a comprehensive description of the related literature of this research work is given.

2.1 Introduction

MCM schemes, such as OFDM, are used in modern communication systems due to their resilience to frequency selective channels. MCM systems can broadly be categorized into wired and wireless systems as shown in Fig. 2.1. The MCM

techniques can be classified by the block-transform used, such as: FFT, DWT, WPT, cosine-modulated filter bank (CMFB), and complex wavelet transform (CWT). Among the complex wavelet based systems, this work proposes the dual-tree complex wavelet transform (DTCWT) based system.

Besides the advantage of their resilience to frequency selective wireless channels, the MCM systems provide good protection against co-channel interference and impulsive parasitic noise and are less sensitive to sample timing offsets than single systems are. In addition to these advantages the channel equalization becomes simpler than by using adaptive equalization techniques with single carrier (SC) systems. However, despite their significant advantages, MCM techniques also suffer from a high PAPR of multicarrier signal. When passed through nonlinear, power-efficient amplifiers at the transmitter, high PAPR signals generate unacceptable levels of out-of-band (OOB) distortions leading to spectral re-growth. This forces the amplifiers to operate in the more linear regions of the amplifier gain with lower peak-to-peak signal level amounting to high input power back-off. At the same time, it requires larger frequency guard bands leading to poor utilization of the power and spectrum. To alleviate the problem of PAPR in OFDM and WPM (a generalization of OFDM based on WPT) systems, several techniques have been proposed, which can basically be divided into three categories. First, the signal distortion techniques – these techniques basically reduce the peak amplitudes by nonlinearly distorting the OFDM signal at or around the peaks.

Examples of distortion techniques are peak cancellation, peak windowing, and clipping [20]. The second group is coding techniques that use a particular forward-error correcting code set that excludes OFDM symbols with large PAPR [20]. The third group is based on scrambling each OFDM symbol with different scrambling sequences and selecting that sequence that gives the smallest PAPR [20]. PAPR reduction schemes based on precoding, a digital signal processing (DSP) solution, are also deployed [21], [22], [23].

Synchronization is another drawback of the MCM systems. The MCM systems are quite sensitive to frequency offset and phase noise resulting in inter-carrier interference (ICI) and inter-symbol interference (ISI). So a system designer should select a robust algorithm so that, at the receiver side, the errors can be easily corrected. At the receiver, there exist carrier frequency offset, symbol timing offset,

and sampling clock errors, which have to be estimated and compensated. Usually, the frequency offset and timing errors are more dominant than the sampling clock inaccuracy. For example in the OFDM systems, the main synchronization parameters to be estimated are detection of the frame, the starting time of the FFT window (timing synchronization), and the frequency offset due to the inaccuracies of the transmitter and receiver oscillators, and the Doppler shift of the mobile channel. These two synchronization tasks have to be performed before the OFDM receiver can demodulate the subcarriers. In addition, if coherent demodulation is used, the receiver also needs an estimate of the channel to equalize the distortion caused by the channel.

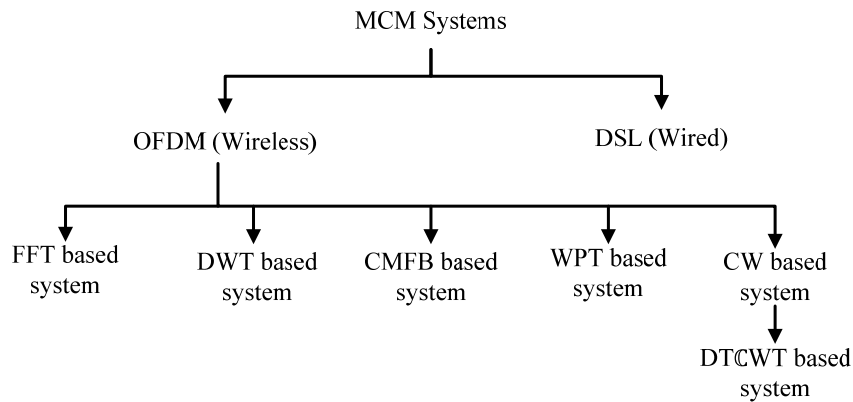


Figure 2.1 Classification of the MCM systems.

2.2 OFDM System

2.2.1 Principle of OFDM

The idea of orthogonal frequency division multiplexing (OFDM) comes from multicarrier modulation (MCM) transmission technique. The principle of MCM is to partition the input bit stream into numerous parallel bit streams and then use them to modulate several sub carriers as shown in Fig. 2.2. Each subcarrier is separated by using the guard band to prevent the subcarrier from overlapping with each other. On the receiver side, bandpass filters are used to separate the spectrum of individual subcarriers. OFDM is a special form of spectrally efficient MCM technique, which employs densely spaced orthogonal subcarriers and overlapping spectrums. The use of bandpass filters is not required in OFDM because of the orthogonal nature of the

subcarriers. Hence, the available bandwidth is used very efficiently without causing the ICI.

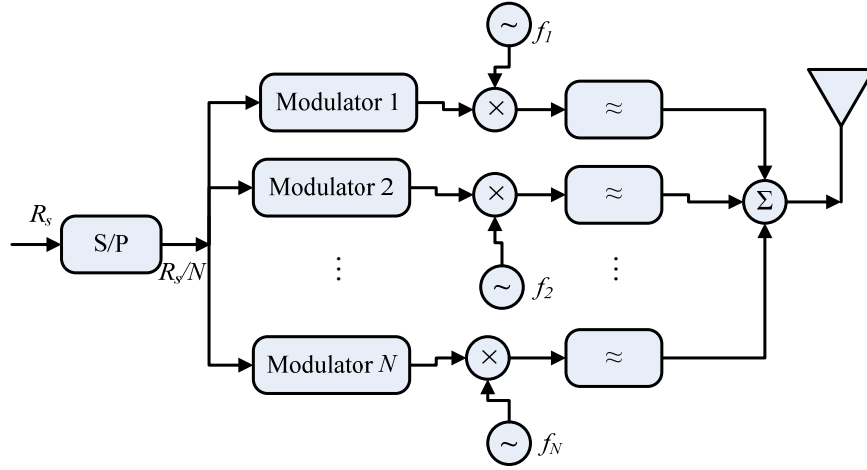


Figure 2.2 Block diagram of a generic MCM transmitter.

At first in classical parallel data system, the total signal frequency band is divided into N non-overlapping frequency subchannels. Every subchannel is modulated with a separate symbol, and then the N subchannels are multiplexed in the frequency-domain. It seems good to avoid spectral overlap of channels to ICI, but this kind of modulation, has the problem of inefficient use of the available spectrum. To solve this inefficiency the proposed suggestions are to use parallel data and frequency division multiplex (FDM), with overlapping subchannels, Fig. 2.3 (a). Using the overlapping MCM, the required bandwidth is greatly reduced, Fig. 2.3 (b).

Fig. 2.3 elucidates an essential concept about OFDM, the concept of orthogonality. In OFDM, the orthogonality between subcarriers should fulfill these two properties as shown in Fig. 2.3(b) :

- Each subcarrier should, accurately, have an integer number of cycles in the symbol duration, T_s .
- The number of adjacent subcarriers should be separated by exactly $1/T_s$.

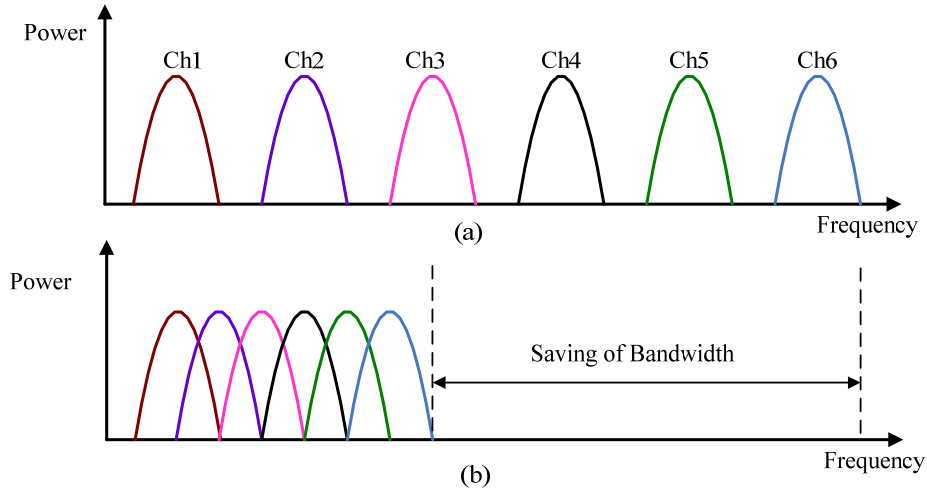


Figure 2.3 Comparison between conventional FDM (a) and OFDM (b).

In a system, following the above mentioned properties, it is possible that the sidebands of each subcarrier overlap, yet we receive the total signal without adjacent carrier interference.

It is still possible to recover the individual subcarrier despite their overlapping spectrum provided that the orthogonality is maintained. The orthogonality is accomplished by performing fast Fourier transform (FFT) on the input stream. Because of the grouping of multiple low data rate subcarriers, OFDM provides a composite high data rate with long symbol duration. Depending on the channel coherence time, this reduces or completely eliminates the risk of intersymbol interference (ISI), which is a common phenomenon in multipath channel environment with short symbol duration. The use of cyclic prefix (CP) in OFDM symbol can reduce the effect of ISI even more [20], but it also introduces a loss in signal to noise ratio (SNR) and reduction in data rate.

2.2.2 OFDM System Implementation

The principle of OFDM, basically a multicarrier modulation (MCM) technique, was already known in the 50's and 60's. But, the system implementation was delayed due to technological difficulties, primarily the difficulty of digital implementation of FFT/inverse FFT (IFFT), which was not easy at that time. In 1965, Cooley and Tukey were

proposed the algorithm for FFT calculation [24] and afterward its efficient implementation on chip makes the OFDM into application. The digital implementation of OFDM system is achieved by using the mathematical operations called discrete Fourier transform (DFT) and its equivalent part inverse DFT (IDFT). These two operations are extensively used for transforming data between the time-domain and frequency-domain. In case of OFDM, these transforms can be seen as mapping data onto orthogonal subcarriers. In order to perform frequency-domain data into time-domain data, IDFT connects the frequency-domain input data with its orthogonal basis functions, which are sinusoids at certain frequencies. In other words, this correlation is alike to mapping the input data onto the sinusoidal basis functions. In practice, OFDM systems employ combination of FFT and IFFT blocks which are mathematical equivalent version of the DFT and IDFT.

At the transmitter side, an OFDM system handles the source symbols as though they are in the frequency-domain. These symbols are fed to an IFFT block which brings the signal into the time-domain. If the N numbers of subcarriers are selected for the system, the basis functions for the IFFT are N orthogonal sinusoids of distinct frequency and IFFT receive N symbols at a time. Each of N complex valued input symbols determines the amplitude and phase of the sinusoid for that subcarrier.

Before transmission, a CP is inserted at the beginning of the OFDM symbol to avoid interference between consecutive symbols. The CP is a copy of the last part of the OFDM symbol, which is appended to the front of transmitted OFDM symbol [20], and it makes the transmitted signal periodic. Hence, the linear convolution performed by the channel looks like a cyclic convolution to the data if the CP is longer than channel impulse response (CIR) and the CIR does not change during one OFDM symbol interval. It means, the length of the CP T_g must be chosen as longer than the maximum delay spread of the target multipath environment.

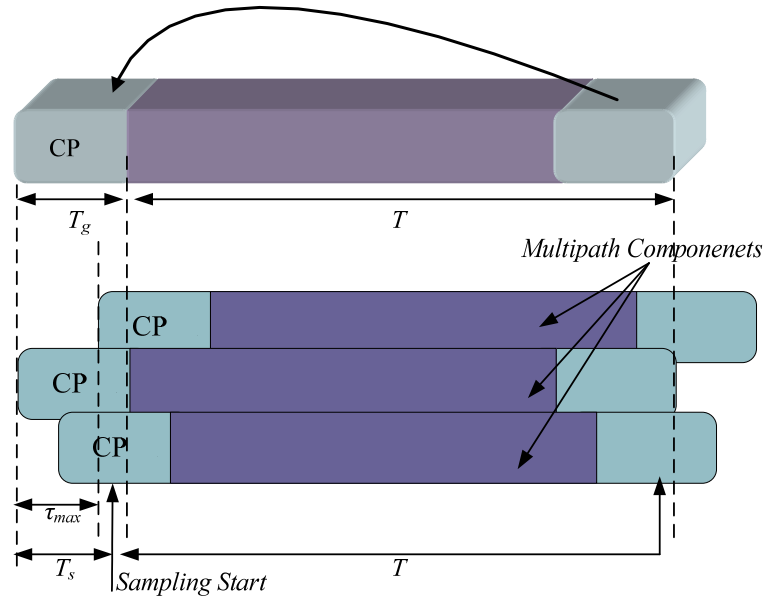


Figure 2.4 OFDM symbol with cyclic prefix (CP).

Figure 2.4 depicts the benefits arise from CP insertion, certain position within the CP is chosen as the sampling starting point at the receiver, which satisfies the criteria $\tau_{max} < T_s < T_g$, where τ_{max} is the maximum multipath spread. Once the above condition is satisfied, there is no ISI since the previous symbol will only have effect over samples within $[0, \tau_{max}]$. And it is also clear from the figure that sampling period starting from T_s will encompass the contribution from all the multipath components so that all the samples experience the same channel and there is no ICI.

The output of the IFFT is the summation combination of all N sinusoids and makes up a single OFDM symbol. The length of the OFDM symbol is extended by the so called cyclic extension or a guard interval (GI) N_g , now the OFDM symbol is $(N + N_g)T$ where T is the IFFT input symbol period. In this way, IFFT block offers a simple way to modulate data onto N orthogonal subcarriers.

At the receiver side, the receiver removes the CP part and performs the FFT with the remainder of the received samples. The FFT block accomplishes the reverse process on the received signal and carries it back to the frequency-domain. The block diagram in Fig. 2.5 depicts the exchange between frequency-domain and time-domain in an OFDM system.

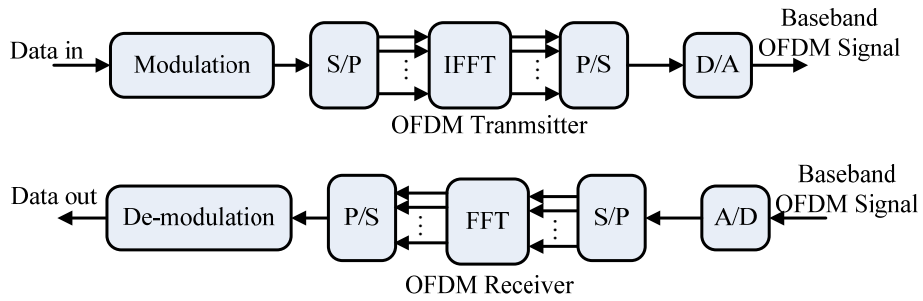


Figure 2.5 Basic OFDM transmitter and receiver.

Proper coding design is usually employed in wireless OFDM systems to achieve a reasonable error probability. Coding in OFDM can be implemented in the time and frequency domains such that both dimensions are utilized to achieve better immunity against frequency and time selective fading. For example, the combination of a Reed-Solomon outer code and a rate-compatible convolutional inner code along with proper time/frequency interleaving constitutes a powerful concatenated coding strategy [25]. Other advanced coding techniques, such as turbo codes and low-density parity-check (LDPC) codes, also seem promising for some multicarrier applications [26], [27], [28].

2.2.3 OFDM System Design

2.2.3.1 Considerations

OFDM system design issues aim to reduce the data rate at the subcarriers, therefore, the symbol duration increases and as a result, the multipath effects are reduced effectively. The insertion of higher valued CP will achieve good results against combating multipath effects but at the same time it will increase the loss of energy. Thus, a tradeoff between these two parameters must be done to obtain a reasonable system design.

2.2.3.2 Requirements

OFDM system depends on the following four requirements: [29]

- Available bandwidth: The bandwidth has a significant role in the selection of number of subcarriers. Large amount of bandwidth will allow obtaining a large number of subcarriers with reasonable CP length.

- Required bit rate: The system should be able to offer the data rate required for the specific purpose.
- Tolerable delay spread: An user background specific maximum tolerable delay spread should be known a priori in determining the CP length. T_{max} .
- Doppler values: The effect of the Doppler shift owing to the user movement should be taken into account.

2.2.3.3 Parameters

The design parameters are resulting according to the system requirements. The design parameters for an OFDM system are as follows [20]

- Number of subcarriers: it have been stated earlier that the selection of large number of subcarriers will help to fighting multipath effects. But, at the same time, this will increase the synchronization complexity at the receiver side.
- Symbol duration and CP length: An ideal choice of ratio between the CP length and symbol duration should be selected, so that multipath effects are combated and not significant amount bandwidth is lost due to CP.
- Subcarrier spacing: Subcarrier spacing will depend on available bandwidth and number of subcarriers used. But, this must be chosen at a level so that synchronization is achievable.
- Modulation type per subcarrier: The performance requirement will determine the selection of modulation scheme. Adaptive modulation can be used to support the performance requirements in changing environment.
- Forward error correction (FEC) coding: A suitable selection of FEC coding will make sure the robustness of the channel to the random errors.

2.2.4 Benefits and Drawbacks of OFDM

In the above section, we have shown how an OFDM system combats the ISI and reduces the ICI. In addition to these benefits, there are other benefits of OFDM system that are listed hereunder:

- High spectral efficiency because of overlapping spectra.
- Simple implementation by FFT.

- Low receiver complexity as the transmitter battle the channel effect to some extends.
- Suitable for high data rate transmission.
- High flexibility in terms of link adaptation.
- Low complexity multiple access schemes such as orthogonal frequency division multiple access (OFDMA).
- Efficient way of dealing with multipath delay spread.
- By dividing the channel into narrowband flat fading sub-channels, OFDM is more resistant to frequency selective fading than single carrier (SC) system are.
- In moderately slow time varying channel, it is possible to significantly improve the capacity by adapting the data rate per subcarrier according to the SNR of that particular subcarrier.
- Using adequate channel coding and interleaving one can recover symbol lost due to the frequency selectivity of the channel.
- OFDM makes single frequency networks possible, which is especially attractive for broadcasting applications.
- It is possible to use maximum likelihood (ML) detection with reasonable complexity [30].

On the other hand, the few drawbacks an OFDM system suffers from are listed as follows:

- An OFDM system is highly sensitive to timing and frequency offsets [20]. Demodulation of an OFDM signal influenced by an offset in the frequency can lead to a high bit error rate.
- An OFDM system with large number of subcarriers will have a higher peak to average power ratio (PAPR) compared to SC system. High PAPR of a system makes the implementation of digital to analog conversion (DAC) and analog to digital conversion (ADC) extremely difficult [29].

2.2.5 Applications of OFDM

OFDM has achieved a big interest since the beginning of the 1990s [31] as many of the implementation difficulties have been overcome. OFDM has been used or

proposed for a number of wired and wireless applications. The first commercial use of OFDM technology was digital audio broadcasting (DAB) [29]. OFDM has also been utilized for the digital video broadcasting (DVB) [32]. OFDM under the acronym of discrete multitone (DMT) has been selected for asymmetric digital subscriber line (ADSL) [33]. The specification for wireless local area network (WLAN) standard such as IEEE² 802.11a and g, wireless fidelity (WiFi) [34], [35] and European telecommunications standards institute (ETSI) high performance radio local area network (LAN) version 2 (HIPERLAN2) [36] has employed OFDM as their physical layer (PHY) technologies. IEEE 806.16 worldwide interoperability for microwave access (WiMAX) standard for fixed/mobile broadband wireless access (BWA) IEEE 802.20 has also accepted OFDM for PHY technologies.

Table 2.1 Data rates provided by existing communication systems.

Data Rates	Systems
1-10 Kbps	Pagers
10-100 Kbps	1G/2G cellular systems
100-500 Kbps	2.5G cellular systems (e.g., enhanced data rate for global system for mobile communication (GSM) evolution (EDGE)); IEEE 802.15.4 (ZigBee)
1-10 Mbps	3G cellular systems (e.g., wideband code division multiple access (WCDMA)); IEEE 802.11; Bluetooth; asynchronous digital subscriber line (ADSL); Data over Cable
10-100 Mbps	IEEE 802.11b; IEEE 802.11 a/g; IEEE 802.16 (WiMAX); very high data rate digital subscriber line (VDSL)
100-500 Mbps	IEEE 802.11n; IEEE 802.15.3a; HomePlug; home phone line networking alliance (HomePNA).
0.5-2 Gbps	IEEE 802.15.3c
10-20 Gbps	WirelessHD

Table 2.1 summarizes some of existing communication systems and their supported data rate ranges. Table 2.2 lists systems from Table 2.1 that use OFDM for communications. Depending on the system requirements, 64-1024 subcarriers have

² *The Institute of Electrical and Electronics Engineers*

been used and constellation size up to 32768 for the modulation of the individual subcarriers.

Table 2.2 Orthogonal frequency division multiple modulation based systems.

System	Maximum number of subcarriers	Modulations
IEEE 802.11 a/g	64	BPSK; QPSK; 16 QAM; 32 QAM; 64 QAM
IEEE 802.11 n	128	BPSK; QPSK; 16 QAM; 32 QAM; 64 QAM
IEEE 802.16	2048	BPSK; QPSK; 16 QAM; 64 QAM
IEEE 802.15.3a	128	QPSK
IEEE 802.15.3c	256	BPSK - 64 QAM
HomePlug	1024	BPSK - 1024 QAM
ADSL/VDSL	4096	BPSK - 32768 QAM

2.2.6 OFDM System Model

The system model described herein uses a simplified model with the following assumptions: OFDM symbol duration with cyclic prefix (CP) is $T = T_g + T_{sym}$, where T_{sym} is the effective symbol duration and T_g , the length of CP. T_g also stands for guard interval. The frequency separation between adjacent subcarriers is equal to the inverse of the effective symbol interval T_{sym} , which is the minimum frequency separation required to achieve orthogonality between two subcarriers. A total of N subcarriers are used with total bandwidth of $B = N/T_{sym}$ Hz. The transmitter and receiver are assumed perfectly synchronized and the fading is slow enough for the channel to be considered constant during one OFDM symbol.

2.2.6.1 Continuous Time System Model

The first MCM systems design did not make use of digital modulation and demodulation. The continuous time OFDM model illustrated in Fig. 2.6 below is considered for convenience, which in practice is digitally synthesized [37].

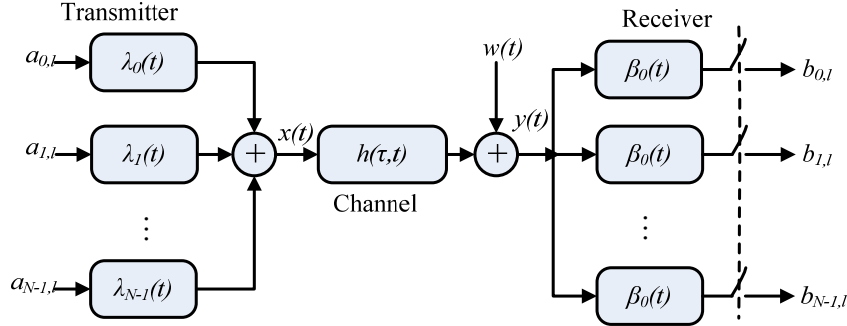


Figure 2.6 Simplified continuous time baseband OFDM model.

The RF model of the OFDM signal is expressed as

$$x_{RF,l}(t - lT) = \begin{cases} R_e \left\{ \lambda(t - lT) \sum_{k=0}^{N-1} a_{k,l} e^{j2\pi(f_c + \frac{k}{T_{sym}})(t-lT)} \right\} & lT - T_{win} - T_g \leq t \leq lT + T_{sym} + T_{win} \\ 0 & \text{otherwise} \end{cases} \quad (2.1)$$

where f_c is the carrier frequency, $a_{k,l}$ is the signal constellation point, l is the index on subcarrier, and $\lambda(t)$ is the transmitter pulse shape defined as

$$\lambda_k(t) = \begin{cases} \frac{1}{\sqrt{T_{sym}}} e^{j\frac{2\pi kt}{T_{sym}}} & -T_g < t < T_{sym} \\ 0 & \text{otherwise} \end{cases} \quad (2.2)$$

Finally, the continuous sequence of the transmitted OFDM symbol can be written as

$$x_{RF,l}(t) = \sum_{l=-\infty}^{\infty} x_{RF,l}(t - lT) \quad (2.3)$$

The baseband transmitted signal for l^{th} OFDM symbol using the baseband carrier frequencies with index k , (i.e., $f_k = k/T_{sym}$) is expressed as

$$x_l(t) = \sum_{k=0}^{N-1} a_{k,l} \lambda_k(t - lT) \quad (2.4)$$

When an infinite sequence of OFDM symbols is transmitted, the output of the transmitter is a superposition of individual OFDM symbols

$$x(t) = \sum_{l=-\infty}^{\infty} x_l(t) = \sum_{l=-\infty}^{\infty} \sum_{k=0}^{N-1} a_{k,l} \lambda_k(t - lT) \quad (2.5)$$

The influence of the time dispersive, multipath fading radio channel is expressed by

its lowpass equivalent CIR, $h(t, \tau)$. Then with the assumption that the channel delay spread is within $[0, T_g]$, the received signal $y(t)$ after the CP is removed will be

$$y(t) = \int_0^{T_g} h(t, \tau)x(t - \tau)d\tau + w(t) \quad (2.6)$$

where $w(t)$ is zero mean additive white Gaussian noise (AWGN) in the channel with double sided power spectral density of $N_0/2$.

The OFDM receiver uses bank of filters matched to the transmitter waveforms given by

$$\beta_k(t) = \begin{cases} \lambda_k^*(T - t) & \text{if } t \in [0, T - T_g] \\ 0 & \text{otherwise} \end{cases} \quad (2.7)$$

And the sampled output of the m^{th} receiver filters which are matched to the effective part of the symbol $[T_g, T]$, is given by

$$\begin{aligned} b_m &= \frac{1}{\sqrt{T_{sym}}} \int_0^{T_{sym}} y(t)e^{-j\frac{2\pi kt}{T_{sym}}} dt \\ &= \frac{1}{T_{sym}} \sum_0^{N-1} a_m H_m \int_0^{T_{sym}} e^{j\frac{2\pi m\tau}{T_{sym}}} e^{-j\frac{2\pi kt}{T_{sym}}} dt + W_m \end{aligned} \quad (2.8)$$

where H_m expressed as

$$H_m = \int_{T_g}^T h(\tau)e^{-j\frac{2\pi m\tau}{T_{sym}}} d\tau \quad (2.9)$$

is the sampled frequency response of the channel at the m^{th} subcarrier frequency, and $W_m = \int_{T_g}^T w(T - t)\lambda_k^*(t)dt$ is the noise part. Since the transmitter waveforms $\lambda_k(t)$'s are orthogonal, i.e.,

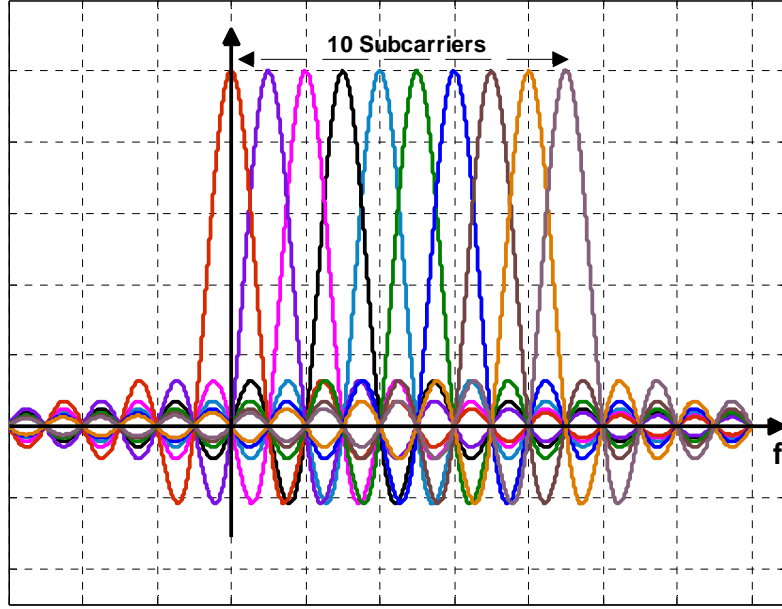


Figure 2.7 Subcarrier spectrum of OFDM system.

$$\int_{T_g}^T \lambda_k(t) \lambda_m^*(t) dt = \frac{1}{T_{sym}} \int_{T_g}^T e^{j\frac{2\pi mt}{T_{sym}}} e^{-j\frac{2\pi kt}{T_{sym}}} dt = \delta[k - m] \quad (2.10)$$

where $\delta[k]$ is the Kronecker delta function [38], Eq. (2.8) can be simplified to

$$b_m = a_m H_m + W_m \quad (2.11)$$

The rectangular transmitter pulse shapes result in a $\sin(x)/x$ shaped frequency response for each channel as shown in Fig. 2.7 above. The sidelobes for the $\sin(x)/x$ function decay as $1/f^2$ which is not efficient and thus windowing is required to reduce the sidelobe energy.

2.2.6.2 Discrete Time System Model

The discrete-time system model can be obtained from its continuous-time model by sampling at time intervals $t_n = nT_s$, where $T_s = T_{sym}/N$. The normalized discrete-time transmitted signal with CP of length $N_g = T_g/T_s$ is given as [37], [39], and [40]

$$x(n) = \frac{1}{\sqrt{N}} \sum_{k=0}^{N-1} a_k e^{j\frac{2\pi kn}{N}} \quad n \in [N_g, N-1] \quad (2.12)$$

Equation (2.10) is an N -point IDFT of a discrete data sequence $x[k]$, $0 \leq k \leq N-1$, which can be efficiently implemented using IFFT algorithm.

Since the signal bandwidth is limited to W , the wide sense stationary uncorrelated scattering (WSSUS) channel can also be modeled as a tapped delay line with random taps. Here also, with the same assumption that $N_g \geq L$, the total delay of the channel coefficients, $h(n, l)$, the received discrete signal, after the CP is removed, is given by

$$y(n) = \sum_{l=0}^L h(n, l)x(n-l) + w(n) \quad n \in [0, N-1] \quad (2.13)$$

where $w(n)$ is complex zero mean Gaussian random variable with variance $N_0/2$. Then, to demodulate the symbols on different subcarriers, we perform FFT on $y(n)$, and obtain

$$Y_m = X_m H_m + W_m \quad (2.14)$$

where W_m is white Gaussian noise Fourier transformed.

If the channel coefficients H_m are equal, that is the channel is time invariant over one OFDM symbol period, there will be no ICI.

The purpose of communication being the recovery of transmitted symbols a_k 's, it can be seen that these can be estimated from Eq. (2.14) simply by dividing y_k at each subcarrier by channel response h_k – popularly known as a zero-forcing equalizer. A typical bit error rate (BER) performance of an OFDM system is given in Fig. 2.8 that shows the symbols are as accurately recovered as they do in BPSK system.

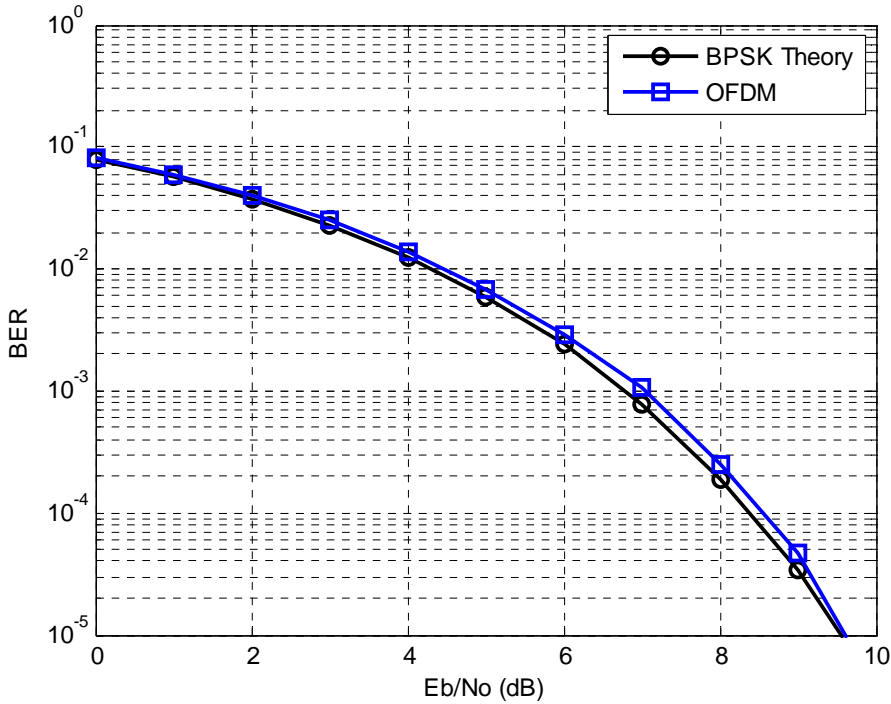


Figure 2.8 BER performance of theoretical BPSK and OFDM using BPSK in AWGN channel.

2.2.7 Wavelets in Multicarrier Modulation

The major drawback of the OFDM system is the rectangular window used, which creates high side lobes. Moreover, the pulse shaping function employed to modulate each sub-carrier broadens to infinity in the frequency-domain [41]. This leads to high interference and lower performance levels. The result of wave-shaping of OFDM signal on ISI and ICI is detailed in [42]. In [43] the optimal wavelet is designed for OFDM signal so as to minimize the maximum of total interference. The wavelet transform has a more longer basis functions and can offer a higher degree of side lobe suppression [13]. With the promise of greater flexibility and ameliorated performance against channel effects, wavelet based basis functions have emerged as strong contender for MCM in wireless channels.

In the conventional OFDM system, the ISI and ICI are reduced by adding a GI using CP to the head of the OFDM symbol. Adding CP can largely reduce the spectrum efficiency. Wavelet based OFDM systems do not need CP [7], thereby enhancing the spectrum efficiency. According to the IEEE broadband wireless standard 802.16.3

[44], avoiding the CP gives Wavelet OFDM an advantage of roughly 20% in bandwidth efficiency. Furthermore, as pilot tones are not required for the wavelet based OFDM system, they perform better in comparison to existing OFDM systems like 802.11a or HiperLAN, where four out of fifty two sub-bands are used for pilots. This gives WOFDM another 8% advantage over typical OFDM implementations [7].

2.3 Wavelet Packet Modulation (WPM)

2.3.1 Introduction

The transform of a signal is no more than another form of representing the signal. In Fourier theory a signal can be represented as the sum of a possibly infinite series of sinusoids, which is referred to as a Fourier expansion. Fourier expansion works well with time-invariant signals. For a time-varying signal, a complete characterization in the frequency-domain should include the time aspect, resulting in the time-frequency analysis of a signal. In the past, several solutions have been developed which, more or less, are able to represent a signal in the joint time-frequency domain. They include the short time Fourier transform (STFT) and wavelet transform (WT) [5].

The WT, however, gives the time-scale representation of the signal where scale relates to frequency in an indirect way. There has been intensive research on wavelets. In particular, Mallat [45] and Meyer [46] discovered a close relationship between wavelet and multi resolution analysis (MRA), which leads to a simple way of calculating wavelet functions. Their work also established a connection between wavelet and digital filter-bank. Daubechies developed a systematic technique for generating finite duration orthogonal wavelets with finite impulse response (FIR) filter banks [47].

The major conclusions of current studies on WT point to development of several new applications. One of the promising applications of wavelet transforms is in the area of digital wireless communications where they can be used to generate waveforms that are suitable for transmission over wireless fading channels.

2.3.2 Overview of Wavelet Transform and Multiresolution Analysis

In wavelet and wavelet packet transforms, a signal usually in time-domain is represented as a weighted sum of translates and dilates of a mother wavelet. The translations and dilations of a wavelet function provide the means for constructing orthonormal basis of wavelets spanning the space $L^2(R)$ of square integrable functions. They can be grouped by their dilation or scaling constants into the disjoint subsets spanning the orthogonal subspaces of $L^2(R)$ [12]. These subsets corresponding to different scales and represent the signal at different resolution levels give rise to MRA [12], [48]. Wavelet Transforms can be classified as continuous wavelet transforms (CWT) or DWT. A continuous time signal can be represented in the wavelet-domain as

$$x(t) = \sum_{j,k \in Z} d_{j,k} \psi_{j,k}(t) = \sum_{k \in Z} a_{o,k} \phi_{o,k}(t) + \sum_{j=0}^{\infty} \sum_{k \in Z} d_{j,k} \psi_{j,k}(t) \quad (2.15)$$

where Z is the set of integers. The orthonormal basis functions $\phi_{jk}(t) = 2^{\frac{j}{2}} \phi(2^j t - k)$ are derived from the scaling function $\phi(t)$, and the wavelet functions $\psi_{j,k}(t) = 2^{\frac{j}{2}} \psi_{j,k}(2^j t - k)$ constitute an orthonormal basis derived from the mother wavelet $\psi(t)$. In wavelet terminology, the scaling functions $\phi_{j,k}(t)$, for $j, k = 1, 2, 3, \dots$, span the subspace $V_j \subset V_{j+1}$ and the wavelet function $\psi_{j,k}(t)$, for $j, k = 1, 2, 3, \dots$, span the subspace $w_j \subset V_{j+1} - V_j$. These subspaces constitute a MRA on $L^2(R)$. The time-domain input $x(t)$, is represented by the wavelet coefficients $a_{o,k}$ and $d_{j,k}$, where k and j determine the time-domain shift and scale of the mother wavelet, respectively, resulting in the different resolution levels and thus different subspaces. When the infinite sums over scale are truncated and limited to J , we get:

$$x(t) = \sum_{j=0}^J \sum_k d_{j,k} \psi_{j,k}(t) \quad (2.16)$$

The equation (2.16), describes the signal $x(t)$ in terms of the bandpass filters whose bandwidth and center frequency are increased by the factor 2^j . The discretization in time of $x(t)$ results in $x(n)$, and the WT projects this signal on the wavelet subspace w_j as follows:

$$x_j(n) = \sum_{k \in \mathbb{Z}} a_{o,k} \phi_{0,k}(n) + \sum_{k \in \mathbb{Z}} d_{j,k} \psi_{j,k}(n) \quad (2.17)$$

The discrete wavelet coefficients $a_{o,k}$, and $d_{j,k}$ can be approximated in the discrete domain and this gives rise to the DWT as follows [49]:

$$a_{o,k} = \sum_n x(n) \phi_{0,k}(n) \quad (2.18)$$

$$d_{j,k} = \sum_n x(n) \psi_{j,k}(n) \quad (2.19)$$

In practice, the discrete wavelet transforms are realized as a finite impulse response (FIR) filter by using the convolution of the input signal with a combination of a lowpass and highpass filter. The lowpass filter, $h(k)$, and the highpass filters, $g(k)$, are derived from the wavelet function, $\psi_{j,k}(t)$, and scaling function, $\phi_{0,k}(t)$, as follows [49]:

$$h(k) = \frac{1}{\sqrt{2}} \langle \phi\left(\frac{t}{2}\right), \phi(t-k) \rangle \quad (2.20)$$

$$g(k) = \frac{1}{\sqrt{2}} \langle \psi\left(\frac{t}{2}\right), \phi(t-k) \rangle \quad (2.21)$$

where $\langle . , . \rangle$ is the inner product of functions. Thus from (2.20) and (2.21), the filters $h(k)$ and $g(k)$ are obtained by dilating, time shifting and sampling the original mother wavelet. These filters are then used for designing the orthonormal basis for subspaces V and w if the following conditions are satisfied [49]:

$$\begin{aligned} |H(w)|^2 + |H(w + \pi)|^2 &= 2 \\ |G(w)|^2 + |G(w + \pi)|^2 &= 2 \\ G(w)H(w)^* + G(w + \pi)H(w + \pi)^* &= 0 \end{aligned} \quad (2.22)$$

where $H(w)$ and $G(w)$ are the discrete Fourier transforms of $h(k)$ and $g(k)$, respectively. The decomposition of the input signal is achieved by first filtering the input signal by $h(n)$ and $g(n)$ and then downsampling the outputs of both filters. It can be mathematically expressed as

$$cA_1(n) = \sum_{k=0}^L h(k)x(2n+k) \quad (2.23)$$

$$cD_1(n) = \sum_{k=0}^L g(k)x(2n+k) \quad (2.24)$$

where $cA_1(n)$ are the scaling coefficients for the approximation portion, $cD_1(n)$ are the wavelet coefficients for the detail portion, and L is the length of the wavelet filters. Expression (2.23) and (2.24) represent the first level of the wavelet decomposition. The subsequent levels are obtained by further filtering the approximation (or detail) portions of the first level discrete wavelet transforms. For example, the second level coefficients are obtained by further decomposition of the coefficients obtained from the first level decomposition as follows:

$$cA_2(n) = \sum_{k=0}^L h(k)cA_1(2n+k) \quad (2.25)$$

$$cD_2(n) = \sum_{k=0}^L g(k)cA_1(2n+k) \quad (2.26)$$

where $cA_1(n)$ and $cD_1(n)$ are the first level wavelet transforms, $cA_2(n)$ and $cD_2(n)$ are the second level wavelet transforms, and L is the length of the wavelet filters. This decomposition process is illustrated in Fig. 2.9.

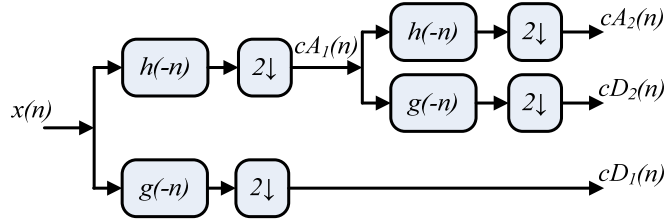


Figure 2.9 Two stage analysis filter banks or wavelet decomposition.

Generally, the approximation coefficients for level $m+1$ are obtained from the previous level m coefficients as follows:

$$cA_{m+1}(n) = \frac{1}{\sqrt{2}} \sum_k h(k)cA_m(2n+k) = \frac{1}{\sqrt{2}} \sum_k h(k-2n)cA_m(k) \quad (2.27)$$

Similarly, the coefficients for level $m+1$ are obtained from the previous level m coefficients as follows:

$$cD_{m+1}(n) = \frac{1}{\sqrt{2}} \sum_k g(k)cA_m(2n+k) = \frac{1}{\sqrt{2}} \sum_k g(k-2n)cA_m(k) \quad (2.28)$$

The equations (2.27) and (2.28) represent the multiresolution decompositions algorithm. The algorithm is the first half of the fast wavelet transform. The vector containing the sequence $(1/\sqrt{2})h(k)$ represents the lowpass filters which lets through low signal frequencies and hence a smoothed version of the signal, and the highpass filter $(1/\sqrt{2})g(k)$ which lets through the high frequency corresponding to the signal details. In the reverse direction, the reconstruction of cA_m from cA_{m+1} and cD_{m+1} can be obtained from the reconstruction algorithm shown in Fig. 2.10 and is expressed as

$$cA_{m-1}(n) = \frac{1}{\sqrt{2}} \sum_k h(n-2k)cA_m(k) + \frac{1}{\sqrt{2}} \sum_k g(n-2k)cD_m(k) \quad (2.29)$$

This operation is also carried out recursively, leading to the IDWT. The further decomposition of both approximation Eq. (2.23), and the detail Eq. (2.24), lead to the discrete WPT (DWPT).

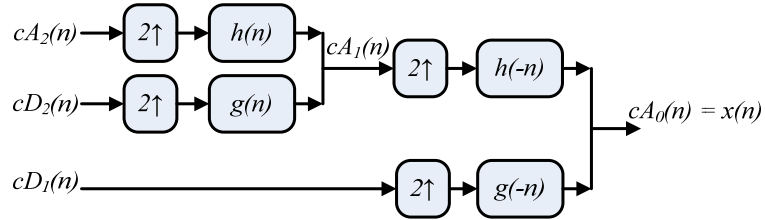


Figure 2.10 Two stage synthesis filter bank or wavelet reconstruction.

2.3.3 Wavelet Packet and Wavelet Packet Trees

As a generalization of wavelets, wavelet packets are basis functions that localize in both time and frequency domains. As with wavelets, they are constructed using quadrature mirror filter (QMF) pairs $h(n)$ and $g(n)$, satisfying the following conditions [50], [51]:

$$\sum_{n=-\infty}^{\infty} h(n) = 2 \quad (2.30)$$

$$\sum_{n=-\infty}^{\infty} h(n) h(n - 2k) = 2\delta(k) \quad (2.31)$$

$$g(n) = (-1)^n h(L - n - 1) \quad (2.32)$$

where $\delta(\cdot)$ is the delta function, $h(n)$ and $g(n)$ are the low- and highpass filters, respectively, and L is the span of the filters. The QMFs $h(n)$ and $g(n)$ are recursively used to define the sequence of basis functions $\phi_n(t)$, called wavelet packets as follows:

$$\phi_{2n}(t) = \sum_{k \in \mathbb{Z}} h(k) \phi_n(2t - k) \quad (2.33)$$

$$\phi_{2n+1}(t) = \sum_{k \in \mathbb{Z}} g(k) \phi_n(2t - k) \quad (2.34)$$

Wavelet packets have the following orthogonality properties:

$$\langle \phi_n(t - j), \phi_n(t - k) \rangle = \delta(j - k) \quad (2.35)$$

$$\langle \phi_{2n}(t - j), \phi_{2n+1}(t - k) \rangle = 0 \quad (2.36)$$

The first property states that each individual wavelet packet is orthogonal to all the nonzero integer translates of itself. While the second property states that pairs of wavelet packets from the same parent are orthogonal to all translates.

Another way to conceptualize the wavelet and wavelet packet transforms is by viewing them as operators. Based on $h(n)$ and $g(n)$, and corresponding reversed filters $h(-n)$ and $g(-n)$, four operators H^{-1}, G^{-1}, H and G are defined and can be used to construct a wavelet packet tree. H and G are the down-sampling convolution operators and H^{-1} and G^{-1} are up-sampling deconvolution operators. The four operators performing on the sequence of samples $x(n)$ are defined as follows [50]:

$$H\{x\}(2n) = \sum_{k \in \mathbb{Z}} x(k) h(k - 2n) \quad (2.37)$$

$$G\{x\}(2n) = \sum_{k \in \mathbb{Z}} x(k) g(k - 2n) \quad (2.38)$$

$$H^{-1}\{x\}(n) = \sum_{k \in \mathbb{Z}} x(k)h(n - 2k) \quad (2.39)$$

$$G^{-1}\{x\}(n) = \sum_{k \in \mathbb{Z}} x(k)g(n - 2k) \quad (2.40)$$

Figure 2.11 shows the construction of these operators. H and G can be used to decompose (analyze) any discrete function, $x(n)$, on the space $L^{-1}(Z)$ into two orthogonal subspaces and are similar to the decomposition and reconstruction operations depicted earlier in Fig. 2.9 and Fig. 2.10. Each decomposition (H or G) step causes in two coefficient vectors each being half the length of the input vector, keeping the total length of the data unchanged. This operation can be refined by cascading the operators for multiple steps. In this iterative decomposition procedure, the size of the output coefficient vectors are reduced at each step by a factor of 2 and eventually these output vectors become scalars. This decomposition process, using H and G , is called the discrete WPT (DWPT) and represents the wavelet analysis process. The decomposition is reversible process and the inverse DWPT (IDWPT) can be used to reconstruct the original input vector from the coefficients vectors.

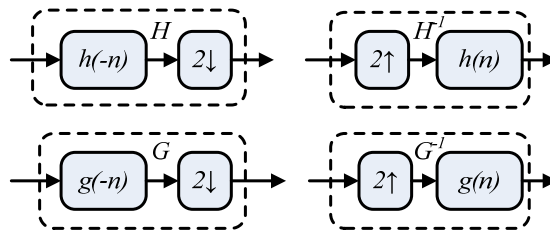


Figure 2.11 Analysis and synthesis filters using H, G, H^{-1}, G^{-1} operators.

The IDWPT is referred to as the synthesis process. This is in line with similar interpretations of the DFT and IDFT operators. The IDWPT is a sequence of upsampling filtering processes defined by the operators H^{-1} and G^{-1} . As the reverse operators to H and G , H^{-1} and G^{-1} each operator takes a input vector of size n and outputs a vectors of size $2n$. The operation at each node that join the outputs from H^{-1} and G^{-1} , in Fig. 2.11, represents the addition of vectors of the same size, producing a output vectors of size $2n$.

The DWPT and IDWPT operations are usually represented by a wavelet packet tree as shown in Fig. 2.12. In this dissertation, one of the application for the IDWPT in Fig. 2.12 is to generate (synthesize) the waveform going into the channel representing a set of QAM or PSK symbols $\{a_0, a_1, \dots, a_{N-1}\}$. This process, referred to as WPM can be viewed as a synthesis operation representing the data symbols as weighted and shifted version of the basis functions, $\phi_j[k]$, which is similar to the generation of the OFDM signals.

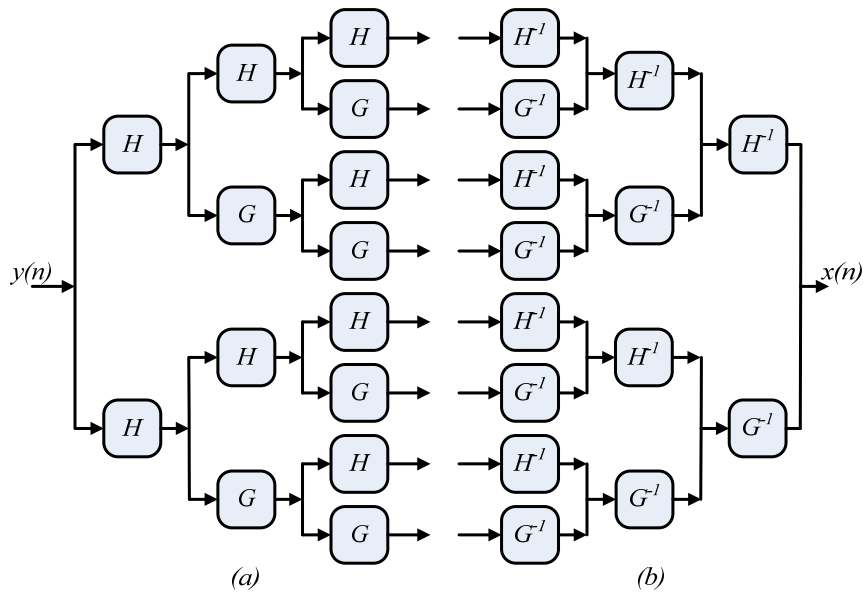


Figure 2.12 Wavelet packet trees: (a) DWPT/analysis tree, (b) IDWPT/synthesis Tree.

2.3.4 The DWT and DWPT Operations

In the frequency-domain, the DWT and DWPT operations are equivalent to the decomposition of the input signal into subbands. This is also called subband coding, where the signal to be coded is successively split into high and low frequency components. In the continuous time-domain of WT and WPT, the hierarchical arrangement of the filters, $h(t)$ and $g(t)$ (corresponding to $h(n)$ and $g(n)$ in the discrete time-domain), gives rise to a series of filter banks, iteratively dividing the input signal into two equal parts in each step.

The high-pass components contain the smallest details and hence are not usually processed any further, as in the case of the DWT. However, the low-pass components still contain some details, and therefore it can be split again. The dyadic splitting operation can be repeated until the desired degree of resolution is obtained. The process of dividing the spectrum is graphically displayed in Fig. 2.13. If the high-pass components are also split in subsequent steps, the subband coding is equivalent to the decomposition using the DWPT. The advantage of the iterative and dyadic implementation of wavelet subband decomposition is that only two filters are needed. The outputs of the filters are approximation and detail components of the WT, and they represent the low and high band portions of the original input signal. If the approximation selection of the WT is used for the further decomposition, then the high portion of the bandwidth will be split. In this manner, the decomposition of the input signal can be arbitrary and the subband decomposition can be customized to best suit the desired goal of the system [7].

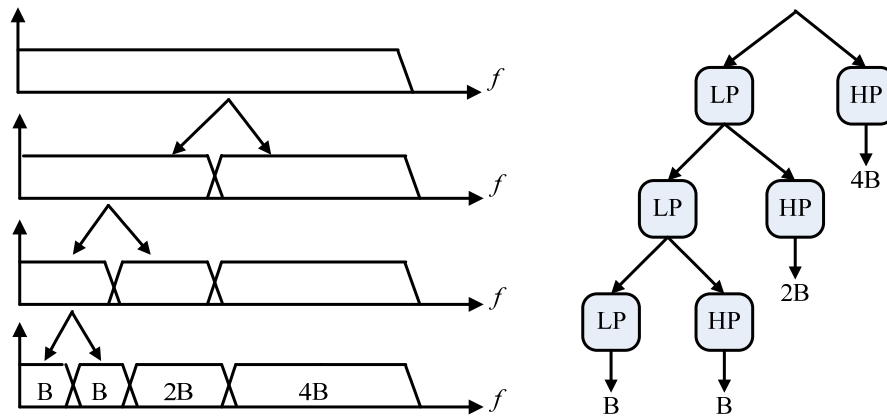


Figure 2.13 Subband decomposition.

The frequency decomposition of signals alone does not fully capture the essence of the time-frequency plane with the wavelets' time frequency "boxes". Figure 2.14 [52], shows the time-frequency box of scaling functions in WT, with a time and a frequency width scaled respectively for different basis functions.

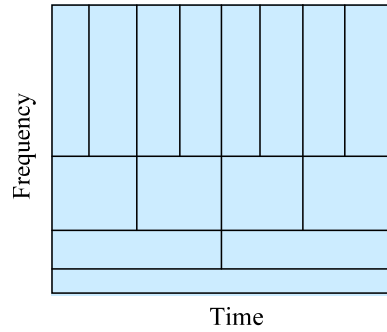


Figure 2.14 Time frequency tiling of the WT.

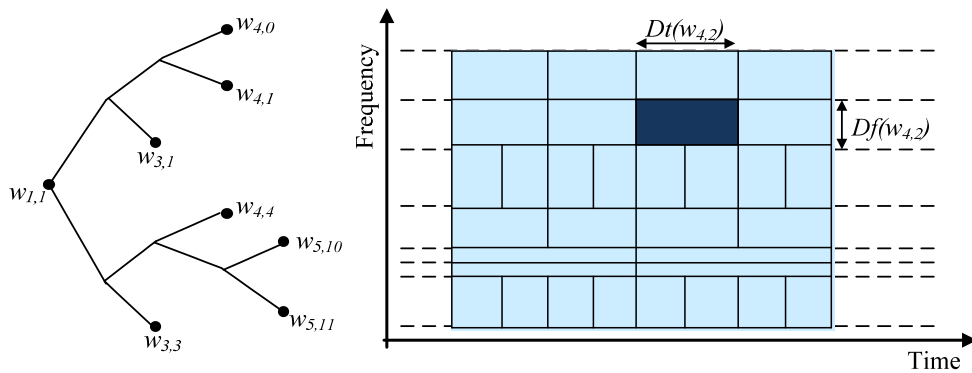


Figure 2.15 Time frequency tiling of the WPT.

A wavelet packet basis divides the frequency axis in different intervals of varying sizes. The time-frequency boxes are obtained by translating in time the wavelet packets covering each frequency interval in order to cover the whole time-frequency plane representing the signal of interest as illustrated in Fig. 2.15 [13]. This tiling is determined by the deployment of the appropriate tree representing the WPT.

2.4 Underlying Structure of the OFDM and WPM Systems

2.4.1 Underlying Structure of OFDM System

OFDM is an efficient MCM scheme for wireless, frequency selective communication channels. In the baseband equivalent OFDM transmitter with N subcarriers, N

modulation symbols (usually from PSK or QAM constellations) in the m -th data frame, $a^m[k]$ where $k = 0, 1, \dots, N-1$, are mapped over the interval $[0, T]$ onto the continuous time OFDM signal, $x(t)$, as follows:

$$x(t) = \frac{1}{N} \sum_{k=0}^{N-1} a[k] e^{j2\pi k f_0 t} \quad t \in [0, T] \quad (2.41)$$

where $f_0 = 1/T$, $j = \sqrt{-1}$, T is the symbol duration, and for brevity of notation, indexing of the frames (m) is dropped.

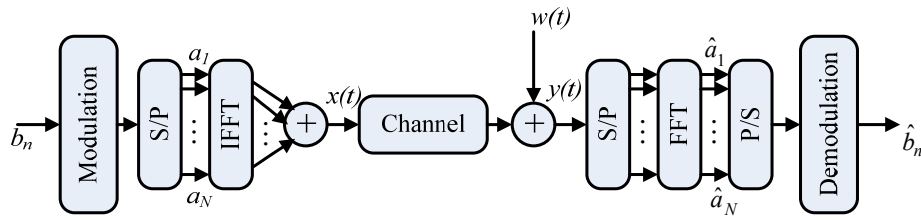


Figure 2.16 Functional block diagram of the OFDM system.

The discrete time version of Eq. (2.41), referred to as the OFDM frame, is formed by sampling $x(t)$ at the Nyquist rate $\frac{1}{T}$ at N time instances $t = n \frac{T}{N}$ to get:

$$x[n] = \frac{1}{N} \sum_{k=0}^{N-1} a[k] e^{j2\pi kn/N} \quad (2.42)$$

where $n = 0, 1, \dots, N-1$. In Eq. (2.42), OFDM symbols $x[n]$ are related to modulation symbols $a[k]$ through an IDFT. When N is a power of two, the IDFT can be evaluated using the computationally efficient IFFT.

Figure 2.16 shows a functional block diagram of an OFDM system in the discrete time-domain. On the receiver side, the FFT is used for decoupling the subcarrier followed by a demodulator to detect the signaling points.

2.4.2 Underlying Structure of WPM System

Analogous to OFDM, WPM also known as wavelet packet division multiplexing (WPDM) is another viable MCM technique with high bandwidth efficiency and flexibility in adaptive channel coding schemes [13]. WPM has been a serious

contender to OFDM in WiMAX proposals and has a lot of potential in cognitive radio (CR) systems. Unlike OFDM, which divides the communication channel into orthogonal subchannels of equal bandwidth, WPM uses an arbitrary time-frequency plane tiling to create orthogonal subchannels of different bandwidths and symbol rates [50].

The WPM synthesis equation for discrete time representation of the waveform going into the channel or HPA is very similar to that of OFDM, where the discrete functions, $\phi_k[n]$, replaces the N finite duration complex exponentials $\exp(j2\pi kn/N)$ in (2.2). The Nyquist sampled version of the transmitted signal, $x[n]$, is constructed as the sum of M waveforms $\phi_k[n]$ individually modulated with the specially indexed QAM or PSK symbols as follows [13]:

$$x[n] = \sum_i \sum_{j=0}^{M-1} a_{i,j} \phi_j[n - iM] \quad (2.43)$$

where $a_{i,j}$ is a constellation encoded i -th data symbol modulating the j -th wavelet packet basis function. A functional block diagram of the WPM system is shown in Fig. 2.17.

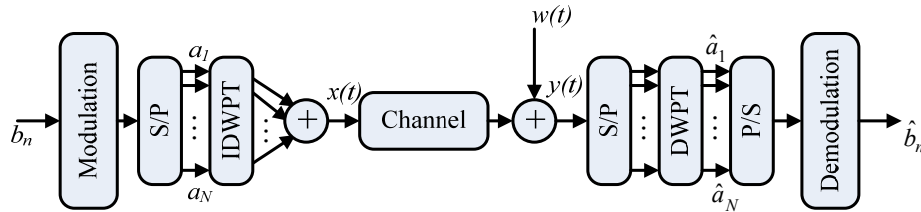


Figure 2.17 Functional block diagram of the WPM system.

The IDWPT in Eq. (2.23) synthesizes a discrete representation of the transmitted signal as sum of M waveforms shifted n time that embed information about the data symbols, $a_{i,j}$. These waveforms are built by successive iterations of H^{-1} and G^{-1} operations as discussed before. In the WPM system, the IDWPT synthesis operation is represented by Fig. 2.18 (a).

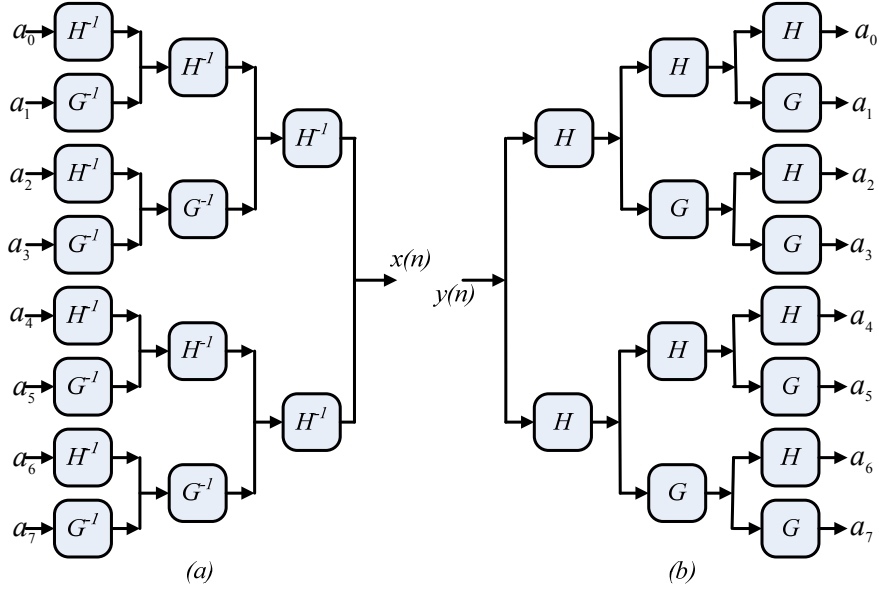


Figure 2.18 WPM: (a) Modulation (IDWPT) and (b) Demodulation (DWPT) trees.

Similar to the OFDM system, at the transmitter side an IDWPT block is used in place of the IFFT block, while at the receiver a DWPT block is used in the place of the FFT block. The IDWPT block work in a similar fashion to an IFFT; it takes QAM symbols at the input and outputs them as parallel time frequency “subcarriers”.

The properties (2.35) and (2.36) of wavelet packet basis functions $\phi_j[k]$, guarantee the orthogonality of the subcarriers irrespective of the time-frequency tiling widths and is the motivation behind the algorithms presented in this chapter. The DWPT at the receiver recovers the transmitted symbols $(a_{i,j})$, through the analysis formula exploiting the orthogonality properties of the DWPT and is schematically represented in Fig. 2.18 (b). At the receiver side we obtain:

$$r(n) = x(n) * h(n) + w(n) = \sum_k h(k)x(n - k) + w(n) \quad (2.44)$$

where $h(n)$ denotes the channel impulse response and $w(n)$ is the noise.

$$r(n) = \sum_k h(k) \sum_i \sum_{j=0}^{M-1} a_{i,j} \phi_j[n - k - iM] + w(n) \quad (2.45)$$

In the absence of noise and for known channel at receiver, the constellation symbols

$a_{i,j}$ can be estimated as follows:

$$x(n) = \sum_j \langle x(n), \phi_j(n) \rangle \phi_j(n) \quad (2.46)$$

where $x(n) = \sum_j a_j \phi_j(n)$, thus

$$x(n-k) = \sum_j \langle x(n-k), \phi_j(n) \rangle \phi_j(n) \quad (2.47)$$

Now the received signal is

$$r(n) = \sum_k h(k)x(n-k) = \sum_k h(k) \sum_j \langle x(n-k), \phi_j(n) \rangle \phi_j(n) \quad (2.48)$$

$$\begin{aligned} \langle r(n), \phi_m^* \rangle &= \left\langle \sum_k h(k) \sum_j \langle x(n-k), \phi_j(n) \rangle \phi_j(n), \phi_m^* \right\rangle \\ &= \sum_k h(k) \langle x(n-k), \phi_m(n) \rangle \end{aligned} \quad (2.49)$$

By deconvolution $a_m = \langle x(n-k), \phi_m(n) \rangle$ can be obtained.

2.5 Wavelet Based OFDM (WOFDM)

In wavelet based OFDM (WOFDM), the IFFT and FFT blocks are simply replaced by an inverse discrete wavelet transform (IDWT) and discrete wavelet transform (DWT), respectively [53]. In Fourier based OFDM, there are M independent quadrature amplitude modulation (QAM) or phase shift keying (PSK) subchannels via a $k = 2M$ point IFFT operation (when the conjugate symmetry condition is imposed). The real wavelet transform (WT) converts real numbers to real numbers, and hence real constellation must be used in each subchannel. To keep the same data rate in wavelet systems, K independent subchannels are multiplexed together via a K point IDWT.

Perfect spectral containment requires ideal brickwall filters, which are not physically realizable due to the infinite length of their impulse responses. It is desirable, however, to be as close as possible to brickwall filters, to have a high degree of spectral containment, and limit the effects of ICI. The filter bank (FB) structure accomplishing this MCM by DWT is shown in Fig. 2.19.

In OFDM employing Fourier filters, the overlap factor is equal to 1, thus the pulse waveforms for different symbol blocks do not overlap in time. However, for wavelet OFDM (WOFDM), the overlap factor is greater than 1, hence the pulse waveforms overlap in time. In Fourier filter banks, the prototype filter is simply a rectangular window. In the wavelet case, the set of N bandpass pulses β_k ; $0 \leq k \leq N - 1$ and their time shifts by integer multiples of N provide an orthonormal set of waveforms for transmission of the sequence of symbol blocks [53].

Due to higher spectral containment between subchannels, WOFDM is better able to overcome the effects of narrowband interference (NBI) and is inherently more robust with respect to ICI than traditional Fourier filters [53]. WOFDM is implemented via overlapped waveforms to preserve data rate. Thus the use of CP does not make sense in this context. Without the CP, the data rate in wavelet systems can surpass those of Fourier implementations, one of its key motivating factors.

Computational complexity is another key issue. Due to the high data rates required in modern applications, low complexity is imperative. Both Fourier and wavelet (for which there is a uniform frequency decomposition) transforms have a computational complexity of $O(N \log_2 N)$, where N is the rank of the transform, or the number of subchannels [54].

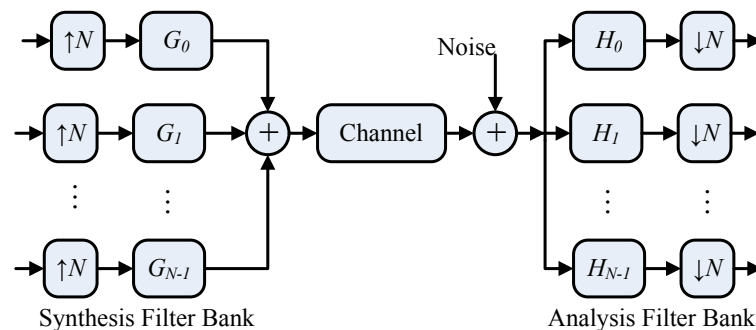


Figure 2.19 Wavelet based MCM structure.

The first sidelobe of the Fourier filter has a magnitude 14 dB smaller than the main lobe. On the other hand, For the wavelet filter, the first sidelobe has a magnitude 45 dB below the main lobe [53], as shown in Figs. 2.20 and 2.21, respectively.

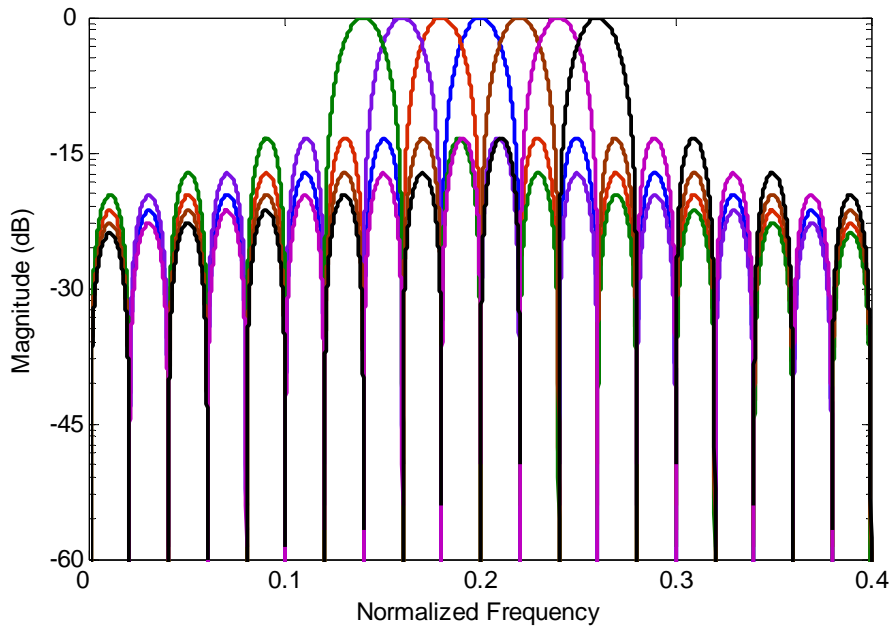


Figure 2.20 Frequency response of seven spectrally contiguous subchannel pulse sequence for OFDM transmission.

The great reduction in sidelobe levels is the main motivation behind the recent trend of using wavelet filters in OFDM systems. Wavelet filters provide better spectral containment than their Fourier counterparts. When orthogonality between carriers is lost, after the transmitted signal passes through a non-uniform channel, the amount of interference between carriers in wavelet systems is much lower than in Fourier systems, since the sidelobes contain less energy.

The improved spectral containment reduces ICI. Reducing the ICI without the need for a CP is an attractive feature of WOFDM. It permits data rates to be pushed past those of Fourier OFDM, which relies heavily on the CP and 1-tap equalizer to mitigate the effects of ICI.

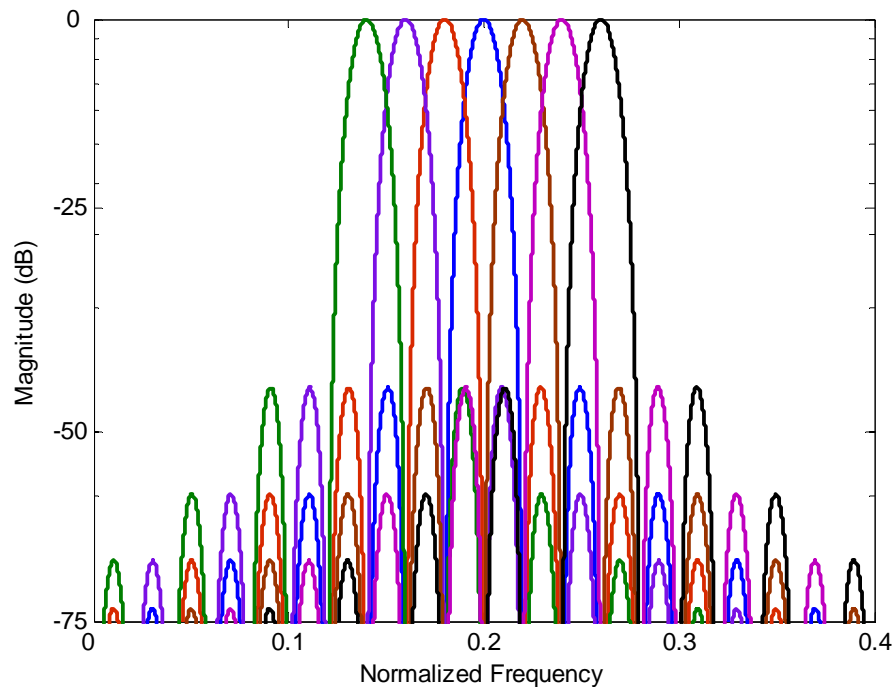


Figure 2.21 Frequency response of seven spectrally contiguous subchannel pulse sequence for WOFDM transmission.

2.6 Drawback of Common Discrete Wavelet Transform

As we mentioned before, an alternative approach to conventional OFDM is based on DWT, which leads to highly structured and thus efficiently realizable transmission signal sets. WOFDM has gained popularity in the literature recently. Due to very high spectral containment properties of wavelet filters, WOFDM can better combat NBI and is inherently more robust with respect to ICI than traditional FFT filters. Since there is no CP present in wavelet implementation the data rates can surpass those of FFT implementations.

A wavelet packet is a generalization of wavelets in that each octave frequency band of the wavelet spectrum is further subdivided into finer frequency bands by using the two scale relation repeatedly. The translates of each of these wavelet packets form an orthogonal basis. We can decompose a signal into many wavelet packet components.

A signal maybe represented by a selected set of wavelet packets without using every wavelet packet for a given level of resolution.

Wavelet packets offer a richer signal analysis than wavelet decomposition of a signal. It's allow to focusing on special parts in time-frequency domain in a more detailed way than is possible with ordinary wavelet transform. The good frequency characteristics and greater flexibility offered by WPT make it an attractive choice for high data rate OFDM transceiver in fading channel conditions than DWT. However, a major problem of common WPT is its lack of shift invariance. This means that on shift of the input signal, the wavelet coefficients vary substantially. The signal information may even not be stationary in the subbands so that the energy distribution across the subbands may change. To overcome the problem of shift dependence, one feasible approach is to simply omit the subsampling causing the shift dependence. Techniques that omit or partially omit subsampling are known as cycle spinning, oversampled filter banks or UWT. However, these transforms are redundant [17], which is not desirable in MCM.

As an alternative, we used a non-redundant wavelet transform that achieves approximate shift invariance [18]. This transform yields to complex wavelet coefficients that modulate the data stream in the same way that WPM do [19]. In this thesis we used the DT \mathbb{C} WT to achieve this property.

2.7 Review of Related Research

2.7.1 MCM

The principle of transmitting data in parallel using multiple carriers on the same channel dates back more than 40 years. The first systems using MCM were military high frequency (HF) radio links in the late 1950s and early 1960s [55].

- One of the first systems using MCM is the Kineplex [55] in 1957 a single side band (SSB) HF FDM system with closely spaced tones operating at 3kbps. The paper describing the Kineplex system also shows its bit error rate vs. signal to noise ratio performance with frequency shift keying (FSK) modulation.
- Another similar MCM system is the Kathryn modem in 1965 [56], which transmits large number of subcarriers, each BPSK modulated, in SSB mode.

- In 1966, Chang presented a theoretical analysis of the performance of an orthogonal multiplexing data transmission scheme subject to a number of degrading factors like sampling error, phase error and developed a simple formula for computing ICI and ISI [57].
- The following year Zimmerman et. al. in 1967 presented the Kathryn modem with all its capabilities including variable transmission rate, channel coding. The frequency multiplexing is implemented using Fourier transform based on analog signal processing [58].

2.7.2 OFDM

OFDM is a special form of MCM with densely spaced sub-carriers and overlapping spectra. Its main idea was patented by Chang, from the Bell Labs, in 1966, but it was only after the paper by Bingham in 1990 that it got its due popularity [59].

- The earliest prominent work on system description and the performance analysis of multicarrier systems is carried out in 1967 by Saltzberg [60]. The system described uses infinitely long symbols that are strictly band-limited with orthogonal subcarriers overlapping in frequency. He concluded by pointing out that the design trend in multicarrier systems should be towards reducing crosstalk between adjacent channels rather than on perfecting the individual channels.
- A major paper by Weinstein and Ebert [14] in 1971 described the use of DFT for generating overlapping orthogonal subcarriers implemented using efficient signal processing and eliminating the bank of subcarrier oscillators. They also used raised cosine window function in time domain and guard interval (GI) between symbols for combating ISI and ICI. In 1985 Cimini also carried out analysis and simulation of DFT based OFDM system using pilot-based correction for combating the effects of multipath propagation and ICI on narrow-band digital mobile channel [16].
- Steendam and Moeneclaey in 1999 investigated the effect of the number of subcarriers and the guard time duration on the performance of OFDM systems operating on a frequency-selective time-selective channel [61].

- In 1999 Intern Kim et. al. analyzed the combined influence of ISI and ICI on the performance of Reed-Solomon (RS) coded OFDM system [62]. They went on to observe that there is an optimum number of subcarriers that minimizes the decoding error probability of the RS code for each channel state.

2.7.3 WPM

An MCM system based on WPT is called wavelet packet modulation (WPM). Actually, the wavelet theory as applied to MCM systems has been well studied in pervious works in 1995 [63] and in 1997 [64]. However, the applications were limited to only the wired transmission and the waveform used was only that of a real wavelet.

- In 1998, Heather Newlin presented a paper on the ongoing developments of the use of wavelets in the field of communication. He presented a variety of wavelet communication applications and he discussed the application of wavelet in modulation, receivers, and in multiple access communication systems (MACS) [67].
- Michael et. al. in 1994 showed that the extra degree of freedom that is achieved by using overlappable filters make discrete wavelet multi tone (DWMT) system potentially superior to the discrete multi tone (DMT) system for ADSL and other applications [68].
- An analytical method for evaluating the performance of the DWMT and the DMT systems has been outlined in 1995 by Sandberg and Tzannes [53]. They summarized that, the DWMT system is more robust than the other multicarrier implementations with regard to ICI, and to narrowband channel disturbances.
- Then in 1995, Lindsey and Jeffrey developed a useful method of wavelet packet basis functions for digital modulation. Through a simple example they showed that the WPM is a superior method for orthogonally multiplexed digital communication [50].
- Again in 1997, Lindsey [64], presented a generalized multirate wavelet based modulation format for orthogonally multiplexed communication system utilizing multidimensional signaling techniques. This generalized framework affords an complete library of basis sets with increased flexibility in time-frequency partitioning.

- Weimin et. al. in 1997 verified from simulation that, the WPM system does support the multirate services, and the performance of multirate services transmission system with wavelet packets combined with multirate filtering technology is more robust than the conventional SC system in AWGN and single tone interference scenario. Also it's better than the FFT based MCM system [69].
- In 1997, Sablatash et. al. explained the relationship of FB trees to wavelet packet trees for subspaces, decimation operations, and coordinates of the projections of a function onto the subspaces. They proposed design and implementation of wavelet packet based FB trees for multiple access communications. Two designs for the FBs are summarized and the equations for the designs are provided [70].
- Akansu and Xueming in 1998 investigated the performance of OFDM and DWMT techniques for single and multi tone interference. They showed that DWMT has a superior performance than OFDM for these interference environments due to its limitation of spectral overlap between his subcarriers [71].
- In 2000, Wong et. al. derived an expression for the probability error for a WPDM scheme in the presence of both impulsive and Gaussian noise sources and demonstrated that the WPDM can provide greater immunity to impulsive noise than both a time division multiplexing (TDM) scheme and an OFDM scheme [72].
- Bouwel et. al. in 2000 studied the implementation of wavelet packet in MCM, and the effects this implementation has on the requirements imposed in the design of useable wavelets. They showed that the reconstructions imposed by the perfect reconstruction (PR) requirement necessitate the use of the bi-orthogonal wavelets [73].
- At the 5th international OFDM-workshop in 2000 Kozek et. al. [75] presented a comparison of wavelet type, Gabor-type (OFDM and DMT) and also Wilson-type (offset-QAM/OFDM) transmultiplexer structures. Using linear distortion (perturbation) caused by time-invariant channels as performance measure they concluded that Gabor structures show optimum perturbation stability

- In 2001, Manglani and Bell extended investigation to the performance of wavelet modulation (WM) in several time varying channels: Rayleigh, flat, slow fading channels and frequency-selective, slow fading channels. They conclude the following: WM performance in frequency selective channels is depend on the presence of ISI, WM performance in An AWGN channel is best at all signal to noise ratios (SNRs) and the performance in flat fading channel is better than a frequency-selective channel [74].
- Negash and Nikookar in 2002 proved that, comparing with the conventional OFDM, the Haar and Daubechies based orthonormal wavelets are capable of reducing the power of ISI and ICI, which were caused by the loss in orthogonality between the carriers as a result of the multipath wireless channel [3].
- Daly et. al. in 2002 outlined a fast tree selection algorithm which achieves the optimum WPM tree for the case of a finite complexity transceiver. And they found that the optimum WPM outperforms conventional multichannel systems of equal complexity for ISI channels [51].
- In 2002, Sun and Daniel proposed a power line communication (PLC) system using DWMT modulation and adaptive algorithm to design a liner traversal equalizer for the proposed communication system. They verified that, the proposed system gives a significant improvement over the conventional OFDM approach [77].
- Charina and Kozek in 2002 presented analytical results, numerical estimation, and numerical simulation showing that, the wavelet based affine MCM schemes are unfit for communication through dispersive time invariant channels as given in digital subscriber line (DSL) and some wireless communication environments [82].
- Couturier et. al. in 2003 presented DWMT as MCM using cosine modulated filter banks (CMFB) to create a wavelet basis. They used a Nyquist filter to implement this modulation and built a fast algorithm to perform it efficiently. They found that the WM is more resistant to parasite radio frequency (RF) [78].
- Zhang et. al. in 2003 proposed Turbo Coded Wavelet based OFDM (TCWOFDM) and low density parity check (LDPC) coded wavelet based

OFDM (LDPC-CWOFDM). They compared the BER of these two systems in different code parameters on AWGN channel. They showed that, TCWOFDM performs better than LDPC-CWOFDM [80].

- Okamoto et. al. in 2003 outlined a multimode transmission using WPM and OFDM, which can be applied to multiple transmission environments. Using the different characteristics between WPM and OFDM in fading and inference environments, good performance was obtained in both environments [81].
- In 2003, Koga et. al. introduced wavelet based OFDM (WOFDM) for PLC, they showed that, WOFDM is a better MCM scheme for PLC compared to OFDM due to its better localized orthogonal subchannels in frequency-domain. Also, they showed its BER characteristic in AWGN and its carrier to noise ratio (CNR) property with an imitated transmission channel [83].
- Similarly in 2004, Zhang et. al. presented their findings of comparison, on DFT-OFDM and DWT-OFDM on three different channel models and showed that, generally, BER performance of DWT-OFDM is better than that of DFT-OFDM [76].
- Mingli and Jacek in 2004 presented a multiwavelet packet modulation (MWPM). Compared to OFDM, they showed that, the bandwidth efficiency of MWPM is increased r times with multiplicity of r . In addition, they proved that the effects of frequency selective wireless channel and high PAPR in OFDM can be mitigated in the new scheme by properly designing the MWPM dyadic structure [84].
- Mingli and Jacek again in 2004 proposed a practical implementation of MWPM transceiver by employing the matrix filter banks. They showed the effectiveness of the MWPM by evaluating the performance of MWPM in both AWGN and Rayleigh flat channels [85].
- Also in 2004, Zhao et. al. outlined the comparisons of coded OFDM (COFDM) and uncoded OFDM system with different orthogonal bases - like DFT and DWT on AWGN and multipath fading channel. They showed that WOFDM and coded WOFDM (CWOFDM) perform much better than DFT-OFDM and DFT-COFDM on AWGN channel respectively. But on multipath fading channel DFT-OFDM performs superior than WOFDM in certain SNR conditions, and vice versa [86].

- Anwar et. al. in 2004 investigated the PAPR of wavelet based transmultiplexer for high speed digital communication system. Their computer simulation results clarified that Haar wavelet based transmultiplexer exhibit low PAPR values when frequency domain spreading is achieved by using Hadamard code [87].
- Aicha et. al. in 2004 analyzed the PAPR of WPDM signals. Simulation results showed that minimum PAPR is obtained using Haar wavelet. They also proposed a technique based on different mapping for the different users to decreases the PAPR. The obtained PAPR gain was about 3dB [88].
- In 2005, Baig et. al. give the performance comparison of conventional DFT with DWPT in an OFDM transceiver. They used Haar and Daubechies wavelets for DWPT in a multipath fading and frequency selective fading channel. They showed that DWPT-OFDM outperforms DWT-OFDM, at the same time, DWT-OFDM outperforms DFT-OFDM [89].
- Sakakibara et. al. in 2005 considered applying WPM to satellite communications. They showed that, the BER performance of WPM in fading channel is better than that for OFDM. They proposed the SC WPM (SC-WPM) method that applies the principle of SC-OFDM to WPM to remedy the PAPR [90].
- Antony and Petri in 2005 studied the performance of WPM for transmission over wireless channels. They conclude that the WPM is a viable alternative to OFDM and it should be considered for future communication systems [13].
- Abad et. al. in 2005 analyzed and compared the performance obtained in power line networks when using OFDM and DWMT modulations. They showed that, due to multipath, OFDM performance is better than DWMT performance in PLC. Furthermore, in some cases, when the multipath effect is high, high speed communications cannot be established using DWMT [91].
- In 2006, Zhao et. al. presented a new coded wavelet based MCM (WMCM) system by using woven convolutional codes (WCC) as channel coding scheme. They showed that, increasing the number of decoding iterations of WCC-WMCM cannot bring so much coding gain in the low regions of the energy per bit to noise power spectral density ratio (E_b/N_0), but, it greatly

improve the performance of WCC-WMCM in the middle to high regions of E_b/N_0 [79].

- In 2006, Ameen and Hadi modeled and simulated DWT-OFDM over Rayleigh selective fading mobile radio channel, and proposed a turbo DWT-OFDM to improve the BER performance of the system. They used parallel concatenated convolutional code (PCCC) and showed that, the proposed turbo DWT-OFDM system gives enhancement in BER performance over the uncoded DWT-OFDM and the classical turbo FFT-OFDM [92].
- In 2007, Gautier et. al. showed that the wavelet packet based MCM is more robust to narrow band interference (NBI) than the conventional OFDM modulation. Also they showed that, for multipath transmission, the use of complex wavelet outperforms the use of real one and outperforms the OFDM modulation when CP technique is not used [93].
- In 2007, Izumi et. al. investigated the equalization technique for WOFDM applied to PLC. They applied adaptive sine modulated / cosine modulated FB equalizer for transmultiplexers (ASCET) to WOFDM and evaluated its performance over the multipath power line channel. They conclude that the performance of OFDM with guard interval (GI) can be approximately equivalent to that of W-OFDM with ASCET [94].
- Maki et. al. in 2007 enhanced the WPM to improve the performance in multipath fading environments by using complex Haar transform (CHT) with exponential term. They analyzed frequency-domain equalizer (FDE) in WPM, and compared the calculation complexity with OFDM. They showed that the calculation cost of WPM increases linearly, while the BER performance was largely improved using FDE compared with OFDM in 10-path static fading environments [95].
- Shuzheng et. al. in 2007 addressed the multiwavelet packet based OFDM. They showed that, the proposed MWPM gives better spectral efficiency compared with conventional OFDM system. Taking the effects of both ISI and ICI into account, they proved that the proposed MCM system is incomparably superior to the conventional OFDM system [96].
- Baro and Ilow in 2007 proposed wavelet packet tree pruning (WPTP) for reduction of PAPR in WPM systems. In their technique, a full wavelet packet

tree is dynamically pruned via joining and splitting of terminal nodes to achieve a minimum PAPR. The complementary cumulative distribution function (CCDF) of the PAPR modified signal showed about a 3.5 dB improvement over the original WPM signal [21]. They are also proposed a WPTP technique with multiple nodes and multiple pass processing to reduce the PAPR in WPM system. The CCDF of the PAPR optimized signal showed about 5 dB improvement over the original WPM signal [22].

- In 2008, Baro and Ilow again in [23], introduced a new PAPR reduction method in OFDM system by deploying wavelet packet pre-processing. They use joint inverse DWPT (IDWPT) and Inverse DFT (IDFT). The proposed method preserves the average transmitted energy at the same time maintains the integrity of the transmitted information. The CCDF of PAPR of the proposed scheme achieves about 5.5 dB reductions in PAPR over traditional OFDM system at clipping probability of 10^{-4} .
- Galli et. al. in 2008 compared OFDM and W-OFDM with respect to some specific aspects of power line channel. They conclude that, W-OFDM is better MCM scheme compared to OFDM because it exhibits higher transmission efficiency, deeper notches, robustness to narrowband interference (NBI), and lower circuit cost as fewer carriers than conventional or windowed OFDM need to be used [97].
- Gupta et. al. in 2008 studied the BER performance of conventional DFT-OFDM system and compared it with those of DWT-OFDM and discrete cosine transform (DCT) OFDM (DCT-OFDM) systems. They showed that Haar wavelet based scheme yields the lowest average bit error probability and the performance of DFT-OFDM and DWT (Haar)-OFDM with quadrature phase shift keying (QPSK) is better than binary PSK (BPSK) modulation format [98].
- In 2008, Kumbasar and Kucur represented a way to reduce the PAPR in WOFDM system by searching for a better wavelet packet tree structures. These better wavelet tree structures were obtained by using a brute force search algorithm. Numerical and simulation results showed that, these structures produced a lower PAPR values than conventional Mallat structures without any degradation in BER performance for the same bandwidth

occupancy and does not introduce any additional complexity to the WOFDM system [99].

2.7.4 OFDM based on Complex Wavelet

Some researchers suggested using the complex wavelet in order to overcome the drawbacks of the OFDM systems based on DWT and DWPT.

- In 1998, Adhikary and Reddy showed that the complex wavelet packet (CWP) based MCM scheme yields lower average bit error probability compared to the DFT based scheme. And they conclude that the improved performance of the complex wavelet packet based scheme is because of the spectrally contained nature of the CWP bases which are under the control of the designer [100].
- Zhang and Bi in 2001 developed a maximum-likelihood sequence estimation / successive interference cancellation (MLSE/SIC) detector to retrieve the transmitted CWP based OFDM (CWPOFDM) symbols. They showed that the performance of CWPOFDM without CP is close to or superior to that of DFT based OFDM (DFTOFDM) with CP, at price of a little increased computational complexity [101].
- In 2003, Wang and Zhang presented a general design method for a new OFDM system based on orthogonal M-band complex valued filter banks (FBs), which have more flexible frequency response and more suitable to deal with complex valued signals present in wireless systems. In their simulation results they show that designed filter bank (FB) has better performance over DFT-based FB and DWMT system. In case of average power of interference they also show that it can be further reduced by using longer filters in the proposed M-band complex valued FBs [102].
- Gautier and Lienard in 2006 proposed a new wavelet based MCM which uses complex wavelet. They showed that the use of complex wavelet outperforms the use of real one and outperforms the OFDM when the CP technique is not used in both time and frequency dispersive channel transmission [11].
- Finally in 2009, Xiangbin and Guangguo developed a new MC-CDM system based on CWP and space time block codes (STBC). The performance of their system is better than the space time coded (STC) MC-CDMA based on

wavelet packet and close or superior to the traditional MC-CDMA with CP. In addition, their system with two transmit antennas utilizing STBC can realize full diversity and full transmission rate, successfully enhance system capacity and improve the ability against channel fading and various interference [103].

From the above literature review, we can deduce that, based on the good time frequency localization of the wavelets, many authors suggest building an OFDM system based on wavelet. However, the drawback of the common DWT and DWPT is also recognized to be certain lack of shift invariance [18] in the transform. The solution of this problem lies, among others, in using \mathbb{C} WT and \mathbb{C} WPT [18] and [93].

Here, it would be worthwhile to mention that no research has, as yet, suggested using the dual-tree complex wavelet transform (DTCWT) – a transform that has all the desired properties of common wavelets with desired property of approximate shift-invariance. Accordingly, this work proposes to explore the use of this transform and introduce a new OFDM system based on it.

CHAPTER 3

DTCWT AND THE OFDM SYSTEM BASED ON IT

In the preceding chapters, a comprehensive overview of the conventional OFDM system, the WPM system and the related literature were presented. This chapter begins with a brief history of using wavelet in wireless communications and introduction to DTCWT in section 3.1, followed by the description of the problems and shortcoming related to real WT in section 3.2 and the solution is given in section 3.3. Section 3.4 presented a comprehensive description of the DTCWT, followed by discussing the underlying structure of DTCWT-OFDM system in section 3.5. Finally, sections 3.6 discuss the all analysis issues of the proposed system such as PSD, PAPR, BER, implementation complexity, etc.

3.1 Introduction

Since early 1990s, the WT and WPT have been receiving increased attention in modern wireless communications [50]. A number of modulation schemes based on wavelets have been proposed [11], [13], [50], [63], [64], [73], [93], [101] and [104]. However, both WT and WPT suffer from four fundamental but intertwined shortcomings - oscillations, shift-variance, aliasing, and lack of directionality. The solution to these four problems is, among others, to use complex wavelets. In this thesis, we will focus particularly on the dual-tree complex wavelet transform (DTCWT). The DTCWT was introduced by Kingsbury [105], and detailed out by him in [106], [107], [108], [109], as two real DWTs. It is, relatively, a recent enhancement to the DWT, with important additional properties. Unlike DWT, it is nearly shift-invariant; satisfies PR condition using short linear phase filters; has limited redundancy; has efficient, $O(N)$, computation – only twice the simple DWT

for 1-D (2^m times for m -D), and has good directional selectivity in two and higher dimensions.

3.2 Shortcomings of Wavelet Transform

Regardless of its efficient computational algorithm and sparse representation, the wavelet transform suffers from some fundamental but intertwined shortcomings [106].

3.2.1 *Shift Variance*

Due to small shift of the signal, the oscillation pattern of the wavelet coefficient can hugely disconcert. The shift variance complicates the wavelet domain processing. Consequently, algorithms must be made capable of coping with the wide range of possible wavelet coefficient patterns caused by shifted singularities [107], [110], [111], [112], [113].

3.2.2 *Oscillations*

The oscillating of the wavelet coefficients (positive and negative around singularity) complicates the wavelet based processing by making singularity extraction and signal modeling very defying [114]. Besides, the singularities yield large wavelet coefficients is magnified due to passing of the oscillating function through zero.

3.2.3 *Lack of Directionality*

While the alternating of the Fourier in higher dimensions correspond to highly directional plane waves, the standard tensor product construction of multidimension (M -D) wavelets produces a checkerboard pattern that is simultaneously oriented along several directions implying certain lack of directionality [106].

3.2.4 *Aliasing*

Under the condition that the wavelet and scaling coefficients are not changed, the inverse DWT cancels the aliasing that occur as a results of the wide spacing of the

wavelet coefficient samples. Any wavelet coefficient processing such as quantization, filtering, and thresholding perturbs the tender balance between the forward and inverse transforms, leading to artifacts in the reconstructed signal [106].

3.3 The Solution

Note that the Fourier transform does not suffer from these problems. Luckily, there is a simple solution to these four DWT shortcomings.

The DWT is based on real valued oscillating wavelets. However, the Fourier transform is based on complex valued oscillating sinusoids.

$$e^{j\theta t} = \cos(\theta t) + j\sin(\theta t) \quad (3.1)$$

The real and imaginary parts form a Hilbert transform pair i.e., they are 90° out of phase with each other.

Encouraged by the Fourier representation, imagine a Complex Wavelet Transform (CWT) with a complex valued scaling function and a complex valued wavelet function. If $\psi_c(t)$ is either of them, then it has similar representation as before. Therefore,

$$\psi_c(t) = \psi_r(t) + j\psi_i(t) \quad (3.2)$$

where, by analogy to Eq. (3.1), $\psi_r(t)$ is real and even and $j\psi_i(t)$ is imaginary and odd. Furthermore, if $\psi_r(t)$ and $\psi_i(t)$ form a Hilbert transform pair, then $\psi_c(t)$ is an analytic signal and supported on only one-half of the frequency axis.

Any CWT based on wavelets cannot closely possess the Hilbert transform/analytic signal properties. This means that as such CWT will not perfectly overcome the above mentioned DWT problems. The key face up in dual-tree wavelet design is thus the design of its two FBs to yield a complex wavelet and scaling function that are as close as possible to being analytic.

In the cost of only a moderate redundancy: $2 \times$ redundancy in 1-D (2^d for d -dimensional signals, in general). the DTCWT comes very close to mirroring the attractive properties of the Fourier transform, including a nearly shift-invariant magnitude with a simple near linear-phase encoding of signal shifts; substantially reduced aliasing; a smooth, non-oscillating magnitude; and directional wavelets in higher dimensions [106], [114], [115].

3.4 The Dual-Tree Complex Wavelet Transform (DTCWT)

The DTCWT employs two real DWTs with one DWT giving the real part of the transform while the other giving the imaginary part. The two real wavelet transforms use two different sets of filters, each satisfying the perfect reconstruction (PR) conditions. The two sets of filters are jointly designed so that the overall transform is approximately analytic. Let $h_0(n)$, $h_1(n)$ denote the low-pass/high-pass filter-pair for the upper FB and $g_0(n)$, $g_1(n)$ denote the low-pass/high-pass filter pair for the lower FB. $\psi_h(t)$ and $\psi_g(t)$ are the two real wavelets associated with each of the two real wavelet transforms. $\phi_h(t)$ and $\phi_g(t)$ are the two real scaling functions associated with each of the two real wavelet transforms. These filters are used to define the sequence of wavelet functions and scaling functions as follows:

$$\psi_h(t) = \sqrt{2} \sum_n h_1(n) \phi_h(2t - n) \quad (3.3)$$

$$\phi_h(t) = \sqrt{2} \sum_n h_0(n) \phi_h(2t - n) \quad (3.4)$$

where $h_1(n) = (-1)^n h_0(d - n)$. The wavelet function $\psi_g(t)$, the scaling function $\phi_g(t)$ and the high-pass filter for the imaginary part $g_1(n)$ are defined in similar way. The filters are designed so that the complex wavelet is approximately analytic in order to satisfy the PR conditions. Consistently, they are designed so that $\psi_g(t)$ and $\psi_h(t)$ form a Hilbert transform pair [106] i.e.,

$$\psi_g(t) = H\{\psi_h(t)\} \quad (3.5)$$

The analysis (decomposition or demodulation) and the synthesis (reconstruction or modulation) FBs used to implement the DTCWT and their inverses are illustrated in Figs. 3.1 and 3.2, respectively for a 4-level FB.

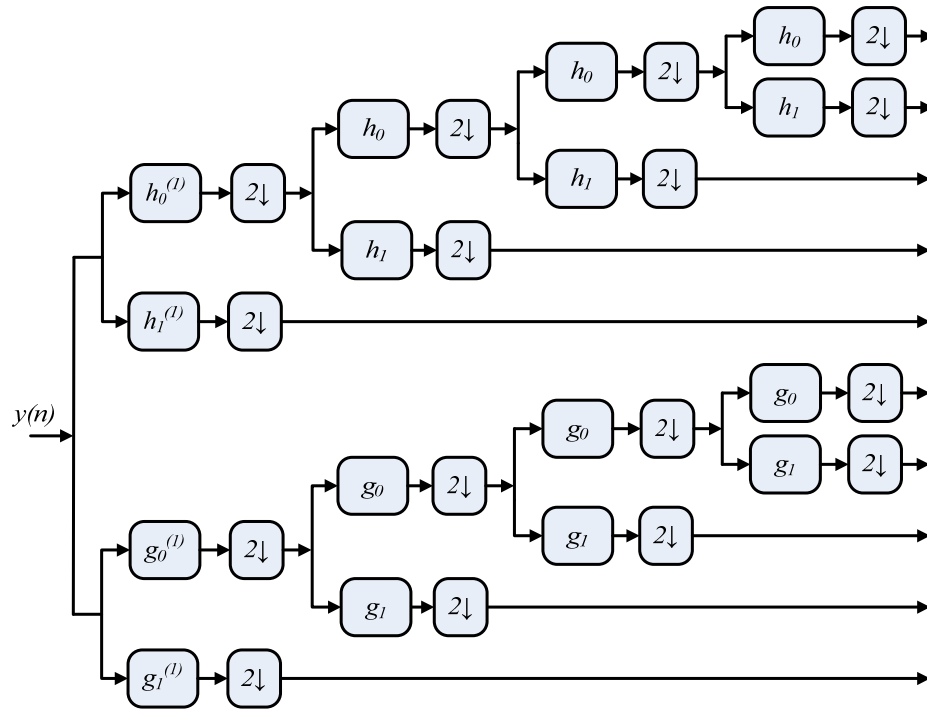


Figure 3.1 Dual-tree discrete CWT (DTDCWT) analysis (demodulation) FB.

In term of simplicity, the inverse dual-tree discrete complex wavelet transform (IDTDCWT) is as simple as the forward transform. To invert the transform, the real part and the imaginary part are inverted separately using bi-orthogonal filters $\tilde{h}_0, \tilde{h}_1, \tilde{g}_0, \tilde{g}_1$ designed for PR with the corresponding analysis filters h_0, h_1, g_0, g_1 respectively. It should be noted, however, that the DTDCWT requires the design of new filters. Primarily, it requires a pair of filter-sets so chosen that the corresponding wavelets form a Hilbert transform pair. Existing filters for wavelet transforms should not be used to implement both trees of the DTDCWT [106].

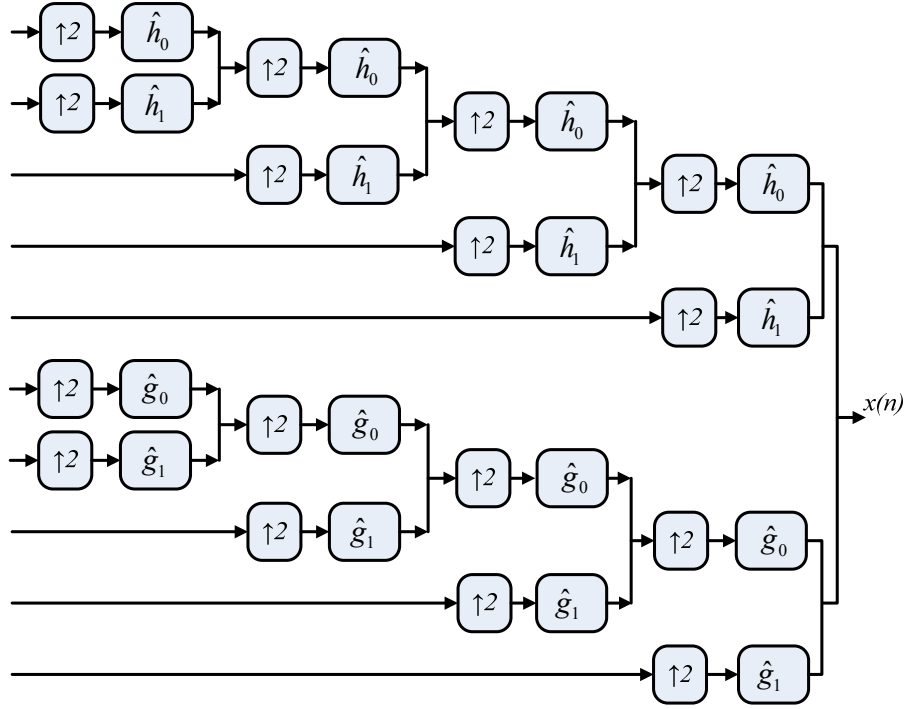


Figure 3.2 Inverse dual-tree discrete CWT (IDTDCWT) synthesis (modulation) FB.

3.4.1 Dual-Tree Framework

Let the square matrices F_h and F_g are the two real DWTs, then the DTCCWT can be represented by the rectangular matrix

$$F = \begin{bmatrix} F_h \\ F_g \end{bmatrix}. \quad (3.6)$$

For a real signal vector x , the $w_h = F_h x$ represents the real part, $w_g = F_g x$ represents the imaginary part of the DTCCWT, and $(w_h + jw_g)$ represents the complex coefficients. From Eq. (3.6)

$$F^{-1} = \frac{1}{2} \begin{bmatrix} F_h^{-1} & F_g^{-1} \end{bmatrix}. \quad (3.7)$$

$$F^{-1} \cdot F = \frac{1}{2} \begin{bmatrix} F_h^{-1} & F_g^{-1} \end{bmatrix} \cdot \begin{bmatrix} F_h \\ F_g \end{bmatrix} = \frac{1}{2} [2I] = I. \quad (3.8)$$

We can also write F and F^{-1} alternatively in the following form

$$F := \frac{1}{\sqrt{2}} \begin{bmatrix} F_h \\ F_g \end{bmatrix}, \quad F^{-1} = \frac{1}{\sqrt{2}} \begin{bmatrix} F_h^{-1} & F_g^{-1} \end{bmatrix} \quad (3.9)$$

For the two real orthonormal DWTs: $F_h^t \cdot F_h = I$ and $F_g^t \cdot F_g = I$. In this case, the transpose of the F is also a left inverse $F^t \cdot F = I$. This means, the inverse of the DTCWT can be performed using the transpose of the forward DTCWT [116].

The complex coefficients can be computed using the following form:

$$F_c := \frac{1}{2} \begin{bmatrix} I & jI \\ I & -jI \end{bmatrix} \cdot \begin{bmatrix} F_h \\ F_g \end{bmatrix}. \quad (3.10)$$

$$F_c^{-1} := \frac{1}{2} \begin{bmatrix} F_h^{-1} & F_g^{-1} \end{bmatrix} \begin{bmatrix} I & I \\ -jI & jI \end{bmatrix}. \quad (3.11)$$

The matrix in (3.8) is unitary (its conjugate transpose is its inverse)

$$\frac{1}{\sqrt{2}} \begin{bmatrix} I & jI \\ I & -jI \end{bmatrix} \cdot \frac{1}{\sqrt{2}} \begin{bmatrix} I & I \\ -jI & jI \end{bmatrix} = I. \quad (3.12)$$

The DTCWT satisfies $F_c^* \cdot F_c = I$, when the two real DWTs are orthonormal transforms, where $()^*$ denotes conjugate transpose. Let

$$\begin{bmatrix} u \\ v \end{bmatrix} = F_c \cdot x \quad (3.13)$$

For the real input signal x , $v = u^*$. And when the input signal x is complex, then $v \neq u^*$.

For a general complex N -point signal, the form in Eq. (3.10) yields $2N$ general complex coefficients. And it also yields $2N$ complex coefficients, but N of these coefficients are the complex conjugates of the other N coefficients in the case of a real N -point. Therefore, for both real and complex input signals, the complex wavelet transform (CWT) is two times more expensive.

The Parseval's energy theorem (the energy of the input signal is equal to the energy in the wavelet domain) for DTCWT, when the two real DWTs are orthonormal, is given by

$$\sum_{j,n} (|d_h(j,n)|^2 + |d_g(j,n)|^2) = \sum_n |x(n)|^2. \quad (3.14)$$

Since there is no data flow between the two real DWTs, the DTCWT is easy to implement using existing DWT software and hardware. Besides, the transform lends itself for parallelization leading to efficient hardware implementation. Furthermore, DTCWT benefits from the existing theory and practice of real wavelet transforms since it is implemented using two real wavelet transforms.

Note that, existing filters for wavelet transforms should not be used to implement both trees of the DTCWT because they do not satisfy the requirement of the Hilbert

transform pair. This means that, the DTCWT requires the design of new filters. Mainly, it requires a pair of scaling filter-sets such that their corresponding wavelet filter-sets form an approximate Hilbert transform pair. If the dual-tree wavelet transform is implemented with filters not satisfying this condition, the transform will not provide the full advantages of analytic wavelets [106].

3.4.2 Half Sample Delay Condition

The two low pass filters should satisfy the condition that one of them is approximately a half-sample shift of the other [117], i.e.,

$$g_0(n) \approx h_0(n - 0.5) \Rightarrow \psi_g(t) \approx H\{\psi_h(t)\} \quad (3.15)$$

This statement can be written in another form as: if $G_0(e^{j\omega}) = e^{-j0.5\omega}H_0(e^{j\omega})$, then $\psi_g(t) = H\{\psi_h(t)\}$ [118], [119], [120], [121]. The half-sample delay condition can also be stated in terms of magnitude and phase function as given hereunder.

$$|G_0(e^{j\omega})| = |H_0(e^{j\omega})| \quad (3.16)$$

$$\angle G_0(e^{j\omega}) = \angle H_0(e^{j\omega}) - 0.5\omega \quad (3.17)$$

In practical implementation of the DTCWT, the delay condition (3.16) and (3.17) are only approximately satisfied and the wavelets $\psi_h(t)$ and $\psi_g(t)$ are only approximate Hilbert pairs. Thus, the complex wavelet $\psi_h(t) + j\psi_g(t)$ is also only approximately analytic. On the other hand, the FT is based on a complex valued oscillating cosine and sine components that form complete Hilbert transform pairs [106], [122].

3.4.3 Filter Design for DTCWT

One needs to adopt a very different approach to designing filters for the DTCWT as compared to the filters for real DWT. The DTCWT filters should be so designed that they fulfil the following conditions:

- Perfect reconstruction (PR) (orthogonal or biorthogonal).
- Approximate half-sample delay property.
- Vanishing moments/good stopband.
- Finite support (FIR filters).
- Linear phase filters, only the complex filter responses need be linear phase - this can be achieved by taking $g_0(n) = h_0(N - 1 - n)$.

One approach to dual-tree filter design is to let $h_0(n)$ be some existing wavelet filter. After that, given $h_0(n)$, it is required to design $g_0(n)$ that satisfy both $G_0(e^{j\omega}) \approx e^{-j0.5\omega} H_0(e^{j\omega})$ and the PR conditions [123]. This approach generally leads to the filter set $h_0(n)$ and $g_0(n)$, that are of equal (or near-equal) length and also relatively short. However, the DT-CWT filters are generally somewhat longer than the filters in real wavelet transform having similar number of vanishing moments. The reason for this is the additional constraints (3.16) and (3.17) that are required to be approximately satisfied by DT-CWT [106]. Next, we describe two methods of filter design for The DT-CWT.

3.4.3.1 First Method

The first method is linear-phase bi-orthogonal method [105] and [124]. $h_0(n)$ and $g_0(n)$ are selected to be a symmetric odd-length and symmetric even-length FIR filters, respectively, such that for N odd

$$h_0(n) = h_0(N - 1 - n). \quad (3.18)$$

$$g_0(n) = g_0(N - n). \quad (3.19)$$

3.4.3.2 Second Method

The second method is the quarter-shift (q-shift) method [108]. For N even, $h_0(n)$ and $g_0(n)$ are sets as:

$$g_0(n) = h_0(N - 1 - n). \quad (3.20)$$

3.4.4 DT-CWT Filters Choice

If the signal x reconstructed from just one type (wavelet or scaling function) and from just one level of the DT-CWT (for example in Fig. 3.3, from y_{001u} and y_{001l}), and it is free of aliasing then we defined the transform to be shift invariant at that level. Absence of aliasing involve that a given subband has an exclusive z-transform function, thus its impulse response is linear and time (shift) invariant. The simplified analysis and reconstruction part of this case is shown in Fig 3.4.

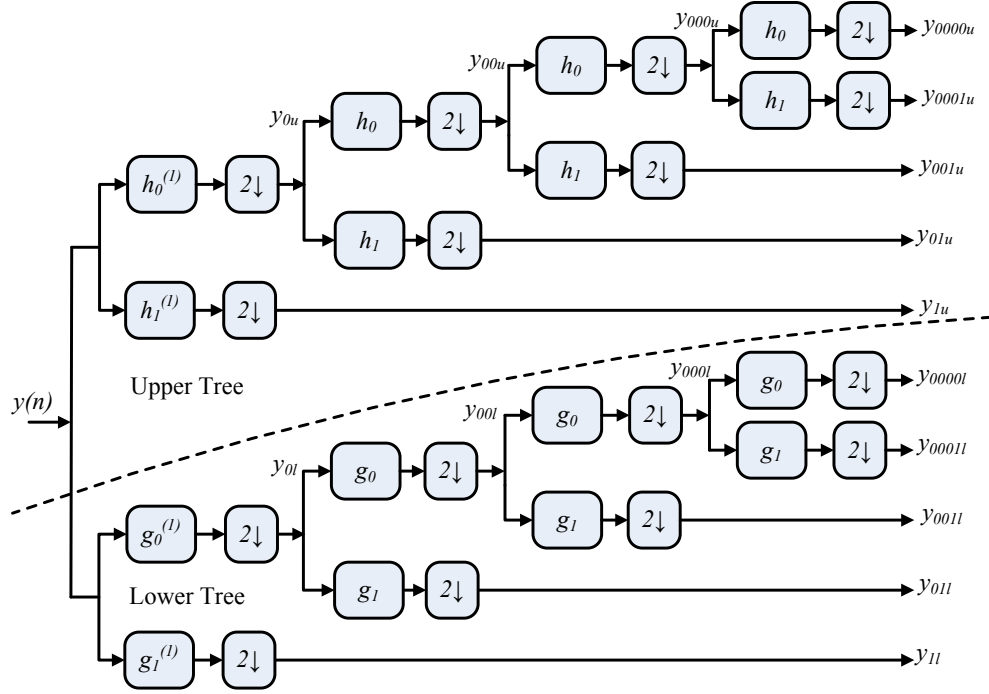


Figure 3.3 Real and imaginary parts of complex coefficients from the upper and lower tree respectively.

$M = 2^m$ is total down up sampling factor, $A = h_0^{(1)} h_0 h_1$, $B = g_0^{(1)} g_0 g_1$. C and D are the inverse function of A and B respectively.

From the result of the multi-rate analysis that a signal $V(z)$, which is down/up-sampled by M , becomes $\frac{1}{M} \sum_{k=0}^{M-1} V(w^k z)$, where $w^k = e^{j2\pi k/M}$. Using this result we can write the following equation from Fig. 3.4.

$$X(z) = X_u(z) + X_l(z) = \frac{1}{M} \sum_{k=0}^{M-1} Y(w^k z) [A(w^k z)C(z) + B(w^k z)D(z)] \quad (3.21)$$

The aliasing terms in the above summation correspond to those for which $k \neq 0$, because only the term in $Y(z)$ (when $k = 0$ and $w^k = 1$) corresponds to a linear time (shift) invariant response.

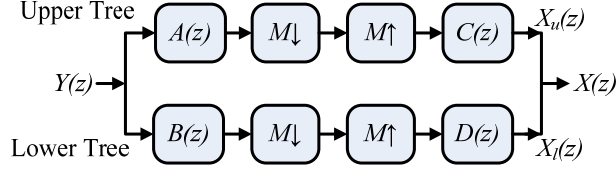


Figure 3.4 DTCWT decomposition and reconstruction.

For shift invariance, the aliasing term must be negligible, so $A(w^k z)C(z)$ and $B(w^k z)D(z)$ must be designed either to be very small or cancel each other when $k \neq 0$. Determine the ratio of the overall energy of the unwanted aliasing transfer functions (the term with $k \neq 0$) to the energy of the wanted transfer functions (when $k = 0$) to quantify the shift dependence of a transform and is given by

$$R_a(z) = \sum_{k=0}^{M-1} \frac{\varepsilon\{A(w^k z)C(z) + B(w^k z)D(z)\}}{\varepsilon\{A(z)C(z) + B(z)D(z)\}} \quad (3.22)$$

where $\varepsilon\{V(z)\}$ calculates the energy $\sum_r |V_r|^2$ of the impulse response of a z-transform function $V(z) = \sum_r V_r z^{-r}$. A range of filters can be designed for the DTCWT and their degree of shift invariance can be investigated based on the aliasing energy ratio (R_a). For any given choice of filters, R_a can be calculated for either wavelet or scaling functions at each level of the transform. The work in [109] deduces that the longer filters provide improved shift invariance.

Typical examples of filters used in this thesis are described in the appendix (E).

3.5 Underlying Structure of the DTCWT-OFDM System

Similar to OFDM and WPM systems, a functional block diagram of DTCWT-OFDM is shown in Fig. 3.5. At the transmitter, an inverse duat-tree discrete CWT (IDTDCWT) block is used in place of the IFFT block in conventional OFDM system or in place of the IDWPT block in WPM system. At the receiver side, a duat-tree discrete CWT (DTDCWT) is used in place of FFT block in conventional OFDM system or in place of DWPT block in WPM system.

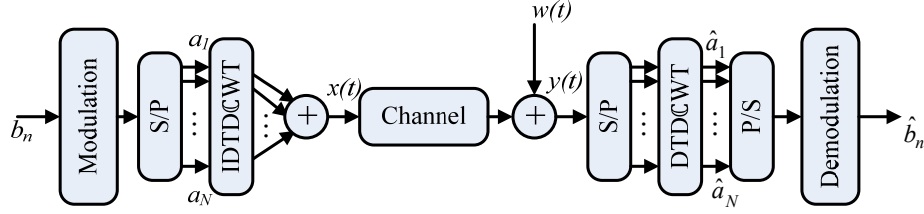


Figure 3.5 Functional block diagram of OFDM based on DTDCWT system.

Data to be transmitted is in general in the form of a serial data stream. PSK or QAM modulation can be implemented in the proposed system and the choice depends on various factors like sensitivity to errors and bit rate. The transmitter accepts modulated data (in this paper we use BPSK and 16QAM). This stream is moved through a serial to parallel (S/P) converter, giving N lower bit rate data stream, and then this stream is modulated through an IDTDCWT matrix realized by an N -band synthesis FB. For the proposed system, a known data interleaved among unknown data are used for channel estimation. Then, the signal is down sampled by 2 and demodulated using elements of the DTDCWT matrix realized by an N -band analysis FB. The signal is equalized after DTDCWT stage.

IDTDCWT works in a similar fashion as IFFT or IDWPT. It takes the input PSK or QAM symbols and outputs them in parallel time-frequency “subcarriers”. Let $\phi(t)$ and $\psi(t)$ be respectively, the complex scaling and wavelet functions and x_i be k^{th} symbol, for $i = 1, 2, \dots, N$. The transmitted signal, $x(t)$, of the DTDCWT-OFDM system can be written in the following form:

$$x(t) = R_e [x(t)] + jI_m [x(t)]. \quad (3.23)$$

$$R_e [x(t)] = \sum_k x_{ar_{1,k}} R_e [\phi_{1,k}(t)] + \sum_k \sum_{j=2}^{N/2} x_{dr_{j,k}} R_e [\psi_{j,k}(t)]. \quad (3.24)$$

$$I_m [x(t)] = \sum_k x_{ai_{N/2+1,k}} I_m [\phi_{1,k}(t)] + \sum_k \sum_{j=N/2+2}^N x_{di_{j,k}} I_m [\psi_{j,k}(t)]. \quad (3.25)$$

From the above equations, we can write the transmitted signal as:

$$x(t) = \sum_k x_{ar_{1,k}} Re[\phi_{1,k}(t)] + \sum_k \sum_{j=2}^{N/2} x_{dr_{j,k}} Re[\psi_{j,k}(t)] \\ + j \left\{ \sum_k x_{ai_{\frac{N}{2}+1,k}} Im[\phi_{1,k}(t)] + \sum_k \sum_{j=\frac{N}{2}+2}^N x_{di_{j,k}} Im[\psi_{j,k}(t)] \right\}. \quad (3.26)$$

In general, we can write the IDTCWT of the signal $x(n)$ as follows:

$$x(t) = \sum_k x_{a_{j_0,k}} \phi_{j_0,k}(t) + \sum_k \sum_j x_{d_{j,k}} \psi_{j,k}(t) \quad (3.27)$$

where $\phi(t)$ and $\psi(t)$ are complex scaling and wavelet function of DTCTWT respectively. The PR condition is satisfied if and only if Eqs. (3.28) and (3.29) are true, i.e.,

$$\langle \phi_{j_0,k}(t), \phi_{j_0',k'}(t) \rangle = \delta(j_0 - j_0') \delta(k - k'). \quad (3.28)$$

$$\langle \psi_{j,k}(t), \psi_{j',k'}(t) \rangle = \delta(j - j') \delta(k - k'). \quad (3.29)$$

The continuous-time transmitted signal is obtained by Eq. (3.26) or Eq. (3.27). And the IDTCWT of the channel impulse response $h(t)$ can be written in the following forms:

$$h(t) = \sum_k h_{ar_{1,k}} Re[\phi_{1,k}(t)] + \sum_k \sum_{j=2}^{N/2} h_{dr_{j,k}} Re[\psi_{j,k}(t)] \\ + j \left\{ \sum_k h_{ai_{\frac{N}{2}+1,k}} Im[\phi_{1,k}(t)] + \sum_k \sum_{j=\frac{N}{2}+2}^N h_{di_{j,k}} Im[\psi_{j,k}(t)] \right\}. \quad (3.30)$$

In general, we can write it as follows:

$$h(t) = \sum_k h_{a_{j_0,k}} \phi_{j_0,k}(t) + \sum_k \sum_j h_{d_{j,k}} \psi_{j,k}(t) \quad (3.31)$$

Now the received signal $y(t)$ is given by:

$$y(t) = x(t) * h(t, \tau) + w(t) = \int_{-\infty}^{\infty} h(\tau) x(t - \tau) d\tau + w(t). \quad (3.32)$$

So far, we have been evaluating the mathematical expressions of the continuous time IDTCWT. Analogous to the relationship between the Fourier series and DFT, DWT and discrete time WT [48] there is also a relationship between the continuous and discrete time IDTCWT. We can evaluate the mathematical expression of the discrete time IDTCWT of the transmitted signal and the channel impulse response i.e., $x(n)$

and $h(n)$ as explained in the following paragraphs.

From dual-tree framework described in (3.9), $F := \frac{1}{\sqrt{2}} \begin{bmatrix} F_h \\ F_g \end{bmatrix}$ and $F^{-1} := \frac{1}{\sqrt{2}} \begin{bmatrix} F_h^{-1} & F_g^{-1} \end{bmatrix}$. The square matrices F_h and F_g represented the two real DWTs (F_h is the upper or the real part of the DTCWT and F_g is the lower or the imaginary part of the DTCWT). If the complex signal representing constellation points of QPSK or x-QAM are given by $X = \begin{bmatrix} X_R \\ X_I \end{bmatrix}$, where X_R is the upper or the real part of X and X_I is the lower or the imaginary part of X , then the IDTCWT of X is given by

$$x = F^{-1}X = \frac{1}{\sqrt{2}} \begin{bmatrix} F_h^{-1} & F_g^{-1} \end{bmatrix} \begin{bmatrix} X_R \\ X_I \end{bmatrix} \quad (3.33)$$

$w_h^{-1} = \frac{1}{\sqrt{2}} F_h^{-1} X_R$ represents the upper or the real part of the IDTCWT and $w_g^{-1} = \frac{1}{\sqrt{2}} F_g^{-1} X_I$ represents the lower or the imaginary part of the IDTCWT. The complex representation of the $F^{-1}X$ is written as:

$$F^{-1}X = (w_h^{-1} + jw_g^{-1}) = \frac{1}{\sqrt{2}} (F_h^{-1} X_R + jF_g^{-1} X_I) \quad (3.34)$$

The received signal $y(n)$ is given by

$$y(n) = x(n) * h'(n) = \sum_k h'(k)x(n-k) \quad (3.35)$$

In the matrices representation the received signal can be written as follows:

$$y = \frac{1}{\sqrt{2}} (hF_h^{-1} X_R + jhF_g^{-1} X_I) \quad (3.36)$$

where the channel matrix h is given by

$$h = \begin{bmatrix} h'(n) & 0 & 0 & \dots & 0 \\ 0 & h'(n) & 0 & \dots & 0 \\ \vdots & \vdots & \vdots & \vdots & \vdots \\ 0 & 0 & \dots & 0 & h'(n) \end{bmatrix} \quad (3.37)$$

The channel h can be estimated from the observation of an a priori known preamble.

Under the assumption of the perfect synchronization, the demodulation i.e., extraction of the constellation symbols (X_R and X_I) obtained by performing DTCWT, i.e.,

$$\begin{aligned} Fy &= \frac{1}{\sqrt{2}} \begin{bmatrix} F_h \\ F_g \end{bmatrix} y = \frac{1}{\sqrt{2}} \begin{bmatrix} F_h \\ F_g \end{bmatrix} \cdot \frac{1}{\sqrt{2}} (F_h h F_h^{-1} X_R + jF_g h F_g^{-1} X_I) \\ &= \frac{1}{2} (H_h X_R + jH_g X_I) \end{aligned} \quad (3.38)$$

where $H_h = F_h h F_h^{-1}$ and $H_g = F_g h F_g^{-1}$. Note that F_h and F_g are both orthogonal matrices. The channel (H_h) and (H_g) are complex thus can be written as: $H_h = H_{h_R} + jH_{h_I}$ and $H_g = H_{g_R} + jH_{g_I}$, respectively. By using

$$y_R = \frac{1}{2} (H_{h_R} X_R - H_{g_I} X_I) \quad (3.39)$$

$$y_I = \frac{1}{2} (H_{h_I} X_R + H_{g_R} X_I) \quad (3.40)$$

We obtain,

$$X_R = 2 \frac{(H_{h_R}^T y_R + H_{h_I}^T y_I)}{(H_{h_R}^T H_{h_R} + H_{h_I}^T H_{h_I})} \quad (3.41)$$

$$X_I = 2 \frac{(H_{g_R}^T y_I - H_{g_I}^T y_R)}{(H_{g_R}^T H_{g_R} + H_{g_I}^T H_{g_I})} \quad (3.42)$$

Assuming the channel is known at the receiver side, it's now possible to recover the transmitted symbols (X_R and X_I) from the received signal y using Eq. (3.41) and Eq. (3.42), respectively.

3.6 Analysis of DTCWT-OFDM System

The DTCWT-OFDM system inherits all the advantages of WPM. In addition to these advantages of WPM systems, namely, higher suppression of sidelobes, good spectral containment between subchannels, better immunity to NBI, more robustness with respect to ICI, avoiding of the CP and pilot tone, higher data rate, lower amount of interference between carriers when the orthogonality between carriers is lost, and better bandwidth efficiency, the DTCWT-OFDM system gives better results of suppression of out-of-band attenuation, better PAPR results and, hence, lesser sensitivity to the nonlinear HPA and lower value of power back-off. It is also seen that the complexity of the DTCWT is lesser than those of FFT and WPT, which means that the proposed system is computationally more efficient.

3.6.1 Power Spectrum Density

The general expression of the PSD of a baseband transmitted signal $x(t) =$

$\sum_{n=-\infty}^{\infty} a_n f(t - nT_{sym})$, where a_n is the signal constellation and $f(t)$ is the impulse response of the transmitting filter, can be written as [125], [126], [127], and [128]

$$P_s(f) = \frac{\sigma_a^2}{T_{sym}} |F(f)|^2 \quad (3.43)$$

where $F(f)$ is the Fourier transform of $f(t)$ and σ_a^2 is the variance of an information symbol a_n . The PSD of the MCM signal can be described the summation of the spectra of the individual subcarriers.

3.6.2 Peak-to-Average Power Ratio

3.6.2.1 Effect of the Nonlinear HPA

From Eq. (2.42), Eq. (2.43) and Eq. (3.27), it can be seen that the construction of the discrete versions of transmitted waveforms in OFDM, WPM, and DTCWT-OFDM is quite similar. For any time index n , all waveforms are the sum of random symbols a_i or x_i . By using the central limit theorem (CLT), we conclude that all the three signals are Gaussian processes, and their envelopes are Rayleigh distributed, resulting in, sometimes, large PAPR. This, therefore, demands that the HPA operates in its linear region. When the input signal goes out of its linear operational region, it results in the generation of unwanted spectral energy, both in-band and out-of-band (OOB). The first phenomenon causes ISI and deteriorates the system's BER performance, while the second causes an increase in the sidelobes of the PSD of the MCM signal, a phenomenon recognized as spectral re-growth.

By operating the amplifier with its input power backed-off (IBO), the spectral re-growth can be alleviated. The IBO is defined as the ratio of the maximum instantaneous power to the average power of the input signal.

$$IBO_{dB} = 10 \log_{10} \left(\frac{P_{s,in}}{P_i} \right) \quad (3.44)$$

where $P_{s,in}$ and P_i are respectively, the power when the input voltage is equal to saturation voltage ($V_i = V_s$) and the average power of an input signal. Another term which is proportionally related to IBO is output power back-off (OBO).

$$OBO_{dB} = 10 \log_{10} \left(\frac{P_{s,out}}{P_{out}} \right) \quad (3.45)$$

where $P_{s,out}$ and P_{out} are respectively, the power when the output voltage is equal to saturation voltage ($V_{out} = V_s$) and the average power of an output signal.

The nonlinear behavior of HPA can be characterized by its amplitude modulation-amplitude modulation (AM/AM) and amplitude modulation-phase modulation (AM/PM) responses. Fig. 3.6 shows a typical AM/AM response for an HPA, with the associated IBO and OBO regions labeled appropriately.

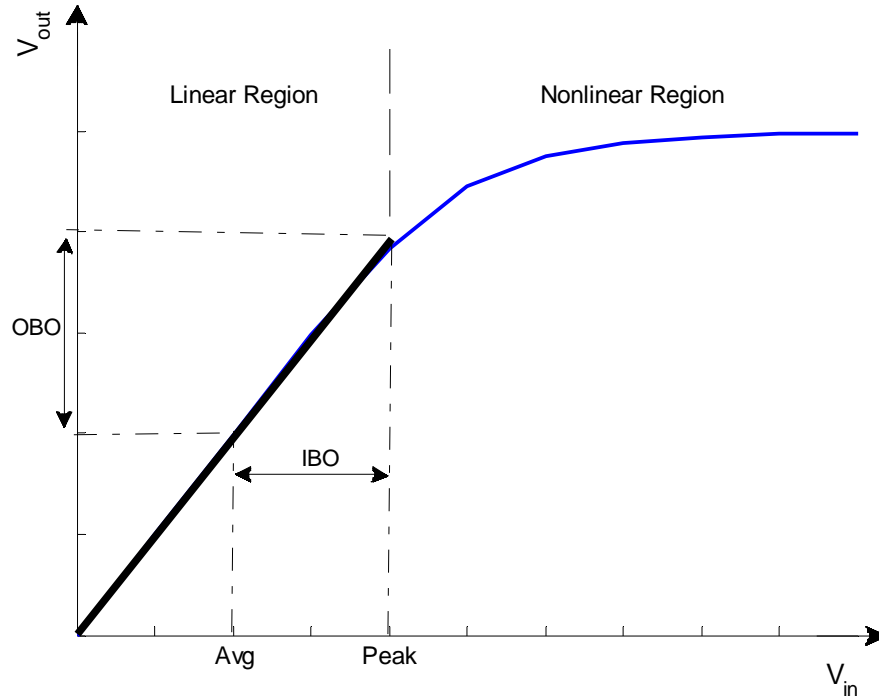


Figure 3.6 A typical power amplifier response.

A typical solid state high power amplifier (SSPA) is mostly realized with gallium arsenide field effect transistors (GaAs-FET's) [129]. The Rapp's nonlinear amplifier mode is usually utilized [130] where its AM/PM function ($\Phi(A)$) is assumed to be sufficiently small, so that it can be neglected. Then, its AM/AM conversion function ($g(A)$) is given as in Eq. (3.47).

$$\frac{AM}{PM} : \Phi(A) \cong 0 \quad (3.46)$$

$$\frac{AM}{AM} : g(A) = \frac{vA}{\left(1 + \left(\frac{vA}{A_0}\right)^{2p}\right)^{\frac{1}{2p}}} \quad (3.47)$$

where v is the small signal amplification, p is a positive number (also called ‘knee parameter’) to control the nonlinear characteristic of the power amplifier model, and A_0 is the saturation output amplitude. The resulting amplitude transfer function for different values of p is shown in Fig. 3.7.

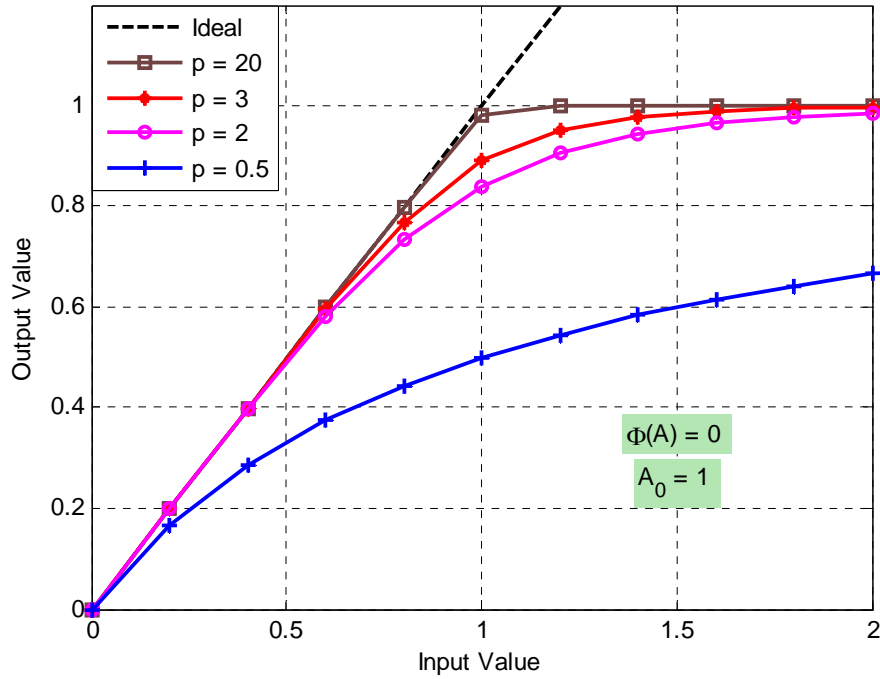


Figure 3.7 AM/AM characteristic of the SSPA.

Similarly, the AM/AM and AM/PM conversions functions of a travelling-wave-tube amplifier (TWTA) are shown in Fig. 3.8. By using an approximation with the two-parameter formulas, the transfer characteristic are obtained [131] as hereunder:

$$\frac{AM}{AM} : g(A) = \frac{\alpha_A A}{(1 + \beta_A A^2)} \quad (3.48)$$

$$\frac{AM}{PM} : \Phi(A) = \frac{\alpha_\Phi A^2}{(1 + \beta_\Phi A^2)} \quad (3.49)$$

where $\alpha_A, \beta_A, \alpha_\Phi, \beta_\Phi$ are constants to be determined in order to fit with the TWTA measured data. These four constants can be determined from the actual TWTA tube measurements via a least-square fit. Typical values of these parameters, used in many simulations [130], are given as follows:

$$\alpha_A = 1 \quad \beta_A = 0.25 \quad \alpha_\Phi = 0.26 \quad \beta_\Phi = 0.25.$$

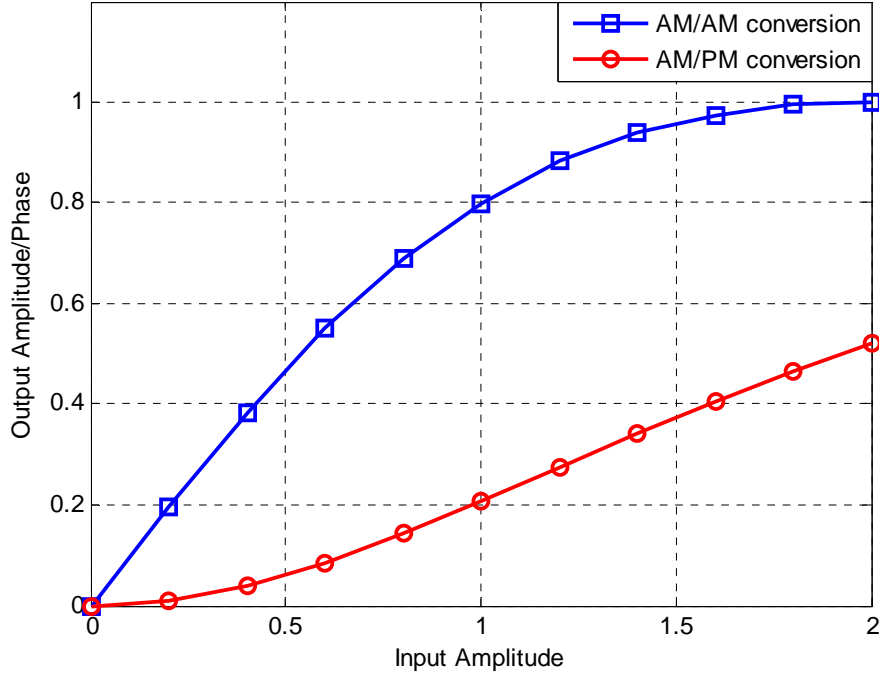


Figure 3.8 AM/AM and AM/PM characteristic of the TWTA.

The PAPR of the transmitted signals (2.42), (2.43) and (3.27) is defined as the maximum instantaneous power of the over average power [132], [133].

$$PAPR = \frac{\max\{|x[n]|^2\}}{E\{|x[n]|^2\}} \quad (3.50)$$

where $E\{\cdot\}$ denotes the ensemble average calculated over the duration of the OFDM or WPM or DTCWT-OFDM symbol.

Given a specified PAPR threshold, $PAPR_0 = \lambda_0$, the complementary cumulative distribution function (CCDF) of the PAPR is given as [39]:

$$CCDF(PAPR\{x(t)\}) = P_r(PAPR\{x(t)\} \geq \lambda_0) = 1 - (1 - e^{-\lambda_0})^N \quad (3.51)$$

There have been several attempts to determine the closed-form approximation for the distribution of PAPR. Some of the approximations are listed in Table 3.1.

Table 3.1 Approximations to CCDF of PAPR.

CCDF	Remarks
$Pr[\lambda > \lambda_0] \approx 1 - \left(1 - e^{-\frac{\lambda_0}{\sigma^2}}\right)^{\alpha N}$	$\alpha = 2.8$ and $N \geq 64$ [117]
$Pr[\lambda > \lambda_0] \approx 1 - \exp\left(-\sqrt{\frac{\pi\lambda_0}{3}} N e^{-\lambda_0}\right)$	[119]
$Pr[\lambda > \lambda_0] \approx 1 - \exp\left(-\sqrt{\frac{\pi \log N}{3}} N e^{-\lambda_0}\right)$	[120]
$Pr[\lambda > \lambda_0] \approx 1 - \exp\left(-\frac{2N}{\sqrt{3}} e^{-\lambda_0/2}\right)$	N and λ are large [121]
$Pr[\lambda > \lambda_0] \approx 1 - \left(1 - \operatorname{erfc}(\sqrt{\lambda_0}/2)\right)^2 (1 - e^{-\lambda_0})^{\frac{N-2}{2}}$	[134]

The parameter α in [117] is empirically determined $\alpha = 2.8$ and this approximation is quite accurate for $N \geq 64$. And [119] assumed that the OFDM signal is a band-limited complex Gaussian process with statistically uncorrelated peaks. However, in [120] the approximation of PAPR has been derived under the presumption that the signal is feebly converges to the Gaussian random process. The approximation in [121] is suitable for circularly modulated signals with large values of N . And the approximation in [134] is suitable for non-circular constellation.

3.6.2.2 DT-CWT-OFDM and nonlinear HPA

Fig. 3.9 is the functional block diagram of the proposed system with nonlinear HPA. The memoryless envelope model is used to described the bandpass nonlinearity modeling the HPA [135]. Let the input bandpass signal to the HPA and the signal at the output of the HPA have the form of Eq. (3.52) and Eq. (3.53) respectively.

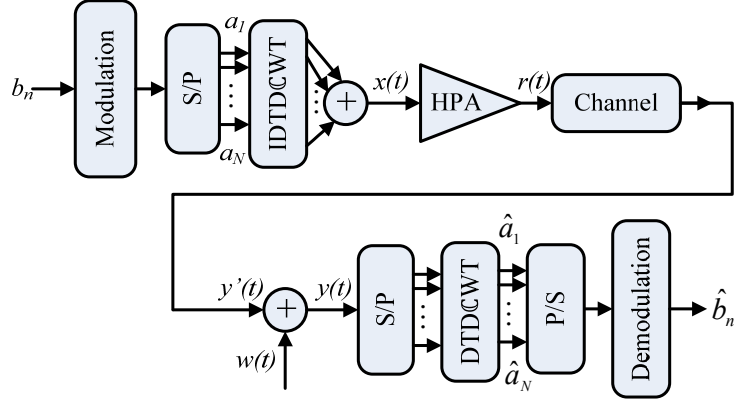


Figure 3.9 Functional block diagram of OFDM based on DTCWT system with HPA.

$$x_{BP}(t) = A(t)\cos[2\pi f_c t + \theta(t)] \quad (3.52)$$

$$r_{BP}(t) = g(A(t))\cos[2\pi f_c t + \theta(t) + \Phi(A(t))] \quad (3.53)$$

The complex envelope of the above two signals can be written as

$$x(t) = A(t)e^{-j\theta(t)} \text{ \& } r(t) = g(A(t))e^{-j\theta(t) + \Phi(A(t))} \quad (3.54)$$

where $g(A)$ and $\Phi(A)$ are the AM/AM and AM/PM conversion respectively. The known distortions when amplifying a modulated signal with constant envelope are

- Spectral spreading of the transmitted signal, which can cause adjacent channel interference (ACI).
- Additional nonlinear interference in the receiver.
- Intermodulation effects, which occur when several channels are amplified in the same HPA.
- Interference between the in-phase and quadrature components due to AM/PM conversion.

It is the endeavor of this work to obtain, among others, PAPR of DTCWT transmission and evaluate its performance in the presence of HPA. When comparing the PAPR of the considered systems, DTCWT-OFDM system achieves better results of PAPR than OFDM and WPM systems.

3.6.3 Bit Error Rate

BER reduction is another key issue in wireless communication. To measure the noise robustness of DTCWT-OFDM scheme, the relationship of the BER as a function of E_b/N_o for different levels of noise is a useful performance tool.

The BER performance of the considered systems in the absence of the nonlinearity HPA, matches the theoretical BER performance of BPSK modulation given as

$$P_e = Q\left(\sqrt{2\frac{E_b}{N_o}}\right) \quad (3.55)$$

This essentially confirms the model performed for the simulation and verifies previous results [74], [136], and [137].

3.6.4 Computational Complexity

Computational complexity is an important issue. Due to the high data rates required in modern applications, low complexity is imperative. Both Fourier and WPT, have a computational complexity of $O(N\log_2 N)$, where N is the rank of the transform, or the number of subchannels [54]. While the computational complexity for DWT is $O(N)$. Since the DTCWT use two DWT (upper and lower parts), the computational complexity for DTCWT is $O(2N)$. The complexity of the DTCWT is of less order as compared to the complexity of FFT and WPT.

3.6.5 Channel Estimation and Synchronization

Perfect channel estimation can greatly improve the performance of system in wireless transmission. Pilot symbol assisted modulation (PSAM) with pilot interpolation in time-domain or frequency-domain is one of the channel estimation methods in conventional OFDM system. Since more bandwidth will be possessed with more pilots inserted, the pilot density should be decided by jointly considering estimation accuracy and system complexity. However, the channel estimation in WPM system has received little attention. Although channel estimation is used to investigate the best basis in WPM system in [138], pilot interpolation algorithm is not provided during channel estimation. In [139], a blind identification method for channel

estimation in WPM system is proposed with impulse redundancy pilot inserted into each frame head after IDWPT process.

However, the inherent properties of wavelet packet decomposition and reconstruction are not considered when designing the pilot interpolation strategy in [139]. In [140] the pilot arrangement is carefully designed based on wavelet packet theory for WPM system. This method utilizes the frequency selective properties of wireless channel to decide the pilot interval during pilot arrangement design, which can achieve high-speed transmission with lower bit rates error guaranteed. In this work, a transform based design method is used, where the distorted channel is transformed to the frequency-domain by using the DFT as explained in section 3.5.

CHAPTER 4

RESEARCH METHODOLOGY AND RESULTS

This chapter describes the performance metric parameters of the proposed DTCCWT-OFDM system, explains the research methodology to obtain them and presents the results obtained. The system model is proposed and simulation experiments are detailed out, both for the performance metric of the proposed system as well as of the conventional OFDM system and WPM system which are used as the benchmark for comparison. The results of the proposed simulation experiments are then systematically presented.

This chapter is organized, accordingly, into six sections. Section 4.1 defines the performance metric parameters of OFDM, WPM and DTCCWT-OFDM systems. Within the scope of the research undertaken herein, it proposes the simulation experiments to be conducted for evaluating the performance of the system. Towards that end, it develops the system model, the assumptions made and the related simulation parameters. As mentioned before, the performance-metric parameters chosen for the purpose are the PSD, PAPR, BER and average BER and computational complexity. The PAPR simulation outcomes of the proposed system are presented in section 4.2 using different numbers of subcarriers and different types of filters. The DTCCWT-OFDM PAPR results are compared also with those for the conventional OFDM and WPM systems under different scenario.

Section 4.3 presents the PSD simulation results for OFDM, WPM and DTCCWT-OFDM systems using 16 QAM with 64 subcarriers with and without insertion of the nonlinear HPA. This section is also discussed the amount of required power back-off and spectral re-growth. Section 4.4 presents the BER simulation results in AWGN. It also includes average BER results of a 10-tap Rayleigh channel when used with the considered systems using both BPSK and 16 QAM with Haar wavelets (db1, db3, db9

and db13 in MATLAB[®]) to construct the wavelet packet trees and different type of filters to construct the DTCWT. Also in this section the results of the BER simulation in AWGN channel of the considered systems using both BPSK and 16 QAM in the presence of nonlinear HPA (SSPA and TWTA) are presented. This is to capture the resulting BER degradation when HPA is present. BER in the presence of frequency-selective wireless channels is expected to capture the impact of the shift-invariance property thus; section 4.5 studies this property in term of the average BER. Finally, section 4.6 concludes this chapter by explaining the computational complexity of the proposed system.

4.1 Performance Metric Parameters and Research Methodology

Among the performance metric parameters of the considered systems such as, PAPR, PSD, accuracy of channel estimation, computational complexity, data rate, and sensitivity to synchronization, the focus in this work will be on PAPR, PSD, BER and average BER, and computational complexity because, as explained in the scope of the work, these parameters reflect the true nature of wavelet filters and their impact on the system performance. Other parameters, although important, do not directly relate to the wavelet filters used in the design of the system, and hence, are outside the scope of the thesis.

(a) The peak-to average power ratio:

The PAPR study is conducted using only the low-pass equivalent system model. To calculate the PAPR of the transmitted signals for the considered systems, the system model consists of only the transmitter side of the flow chain shown in the Figs. 2.16, 2.17 and Fig. 3.5 without the HPA. These blocks of the system model are developed under a MATLAB[®] environment. The blocks are implemented by using MATLAB[®] functions. The following is an overview of procedures to simulate the considered systems:

- A binary random data vector is generated for transmission using the random bit generator.
- The random data are BPSK or 16-QAM modulated.

- The baseband modulated data vector is reshaped into parallel column vectors using the serial-to-parallel (S/P) conversion.
- The subcarrier mapping for the OFDM, WPM and DTCWT-OFDM systems are accomplished by using the IFFT, IDWPT and IDTCWT respectively. For the considered systems, sufficiently large, but identical, number of random data bits are generated and used for the system simulation and analysis. For example, for clipping probability of 10^{-4} at least 10^6 symbols are generated and errors are averaged over 100 errors.
- CP duration, as stipulated in WiMAX standard, is taken to be of $0.8 \mu\text{s}$ duration (16 samples at 20 MHz), and is inserted only in the conventional OFDM system while the WPM and DTCWT-OFDM system are transmitted without any guard interval insertion.
- Parallel-to-serial (P/S) conversion is performed to make the signals ready for transmission.
- The PAPR analysis is carried out using the time-domain peak envelope and CCDF. The time-domain peak envelope gives a heuristic understanding of which waveform is likely to have more PAPR than others, while CCDF gives an accurate estimate of PAPR of the system under consideration.

(b) The power spectrum density:

The PSD of the transmitted signals for the considered systems is investigated both before and after the nonlinear HPA. For a given HPA, the amount of power back-off and the spectral re-growth are also studied and the performance is compared with each other for the considered systems. To perform the simulations for the transmitter side with the HPA (as shown in Fig. 3.9), an HPA (Rapp's model for SSPA with $p = 3$ and TWTA with $\alpha_A = 1$, $\beta_A = 0.25$, $\alpha_\phi = 0.26$ and $\beta_\phi = 0.25$) block is added to the above simulation procedures. The PSD is obtained from the low-pass equivalent transmitted signal before and after HPA.

(c) The bit error rate:

The BER of the considered systems is calculated by comparing the transmitted and the received data in AWGN channel, while the average BER is calculated using the

Rayleigh channel (the specifications given in Table 4.1 later), both results are investigated in the presence of the HPA and also in its absence.

The system model includes transmitter and the receiver side of the flow chain shown in the Figs. 2.16, 2.17 and Fig. 3.5 together with an AWGN block in between. The simulations are carried out under MATLAB® environment. The procedures to simulate the considered systems are as follows:

- The OFDM signal passes through nonlinear HPA using the SSPA and TWTA models.
- Two scenarios are employed. In first case, the transmitted signal is added with AWGN, and in the second case, it passes through a Rayleigh channel first before AWGN adds on to it – the case when the multipath wireless channel is present. A complex low-pass equivalent model for both the channel and the white Gaussian noise is assumed.
- The received signal is reshaped again into a parallel column vector by performing the S/P conversion.
- Multiplexing the signal using wavelet filters is achieved via both DWPT and DTCWT, while the FFT is used to multiplex the signal in conventional OFDM system.
- The P/S conversion is performed to reshape the signal back to serial format for baseband demodulation.
- Then, the BPSK and 16-QAM symbols are ready for demodulation.

(d) The computational complexity:

Finally, the computational complexity of the considered systems is evaluated and also compared with each other.

The simulation procedures to achieve the objective of this research are summarized in the flowchart shown in Fig. 4.1.

All the simulation mentioned above are carried out using MATLAB® (7.6) R2008a program, a personal computer running Windows XP service pack 3 on Intel® Pentium® 4 2.8GHz processor, 2GB of RAM.

In order to achieve fair comparisons, identical simulation parameters are used. The simulations are carried in MATLAB[®] using FFT/IFFT, WPT/IWPT using wavelet toolbox, and DTCWT/IDTCWT functions [141]. These blocks are utilized in the simulation of the OFDM, WPM and DTCWT-OFDM systems, respectively. The SSPA (Rapp's model) and TWTA are used as the nonlinear HPA and they are utilized in the simulation of the PSD and BER carried out in this work. An AWGN and a Rayleigh channel (as described in Table 4.1) are assumed for the BER and average BER performance evaluation respectively. The simulation parameters are documented as follows:

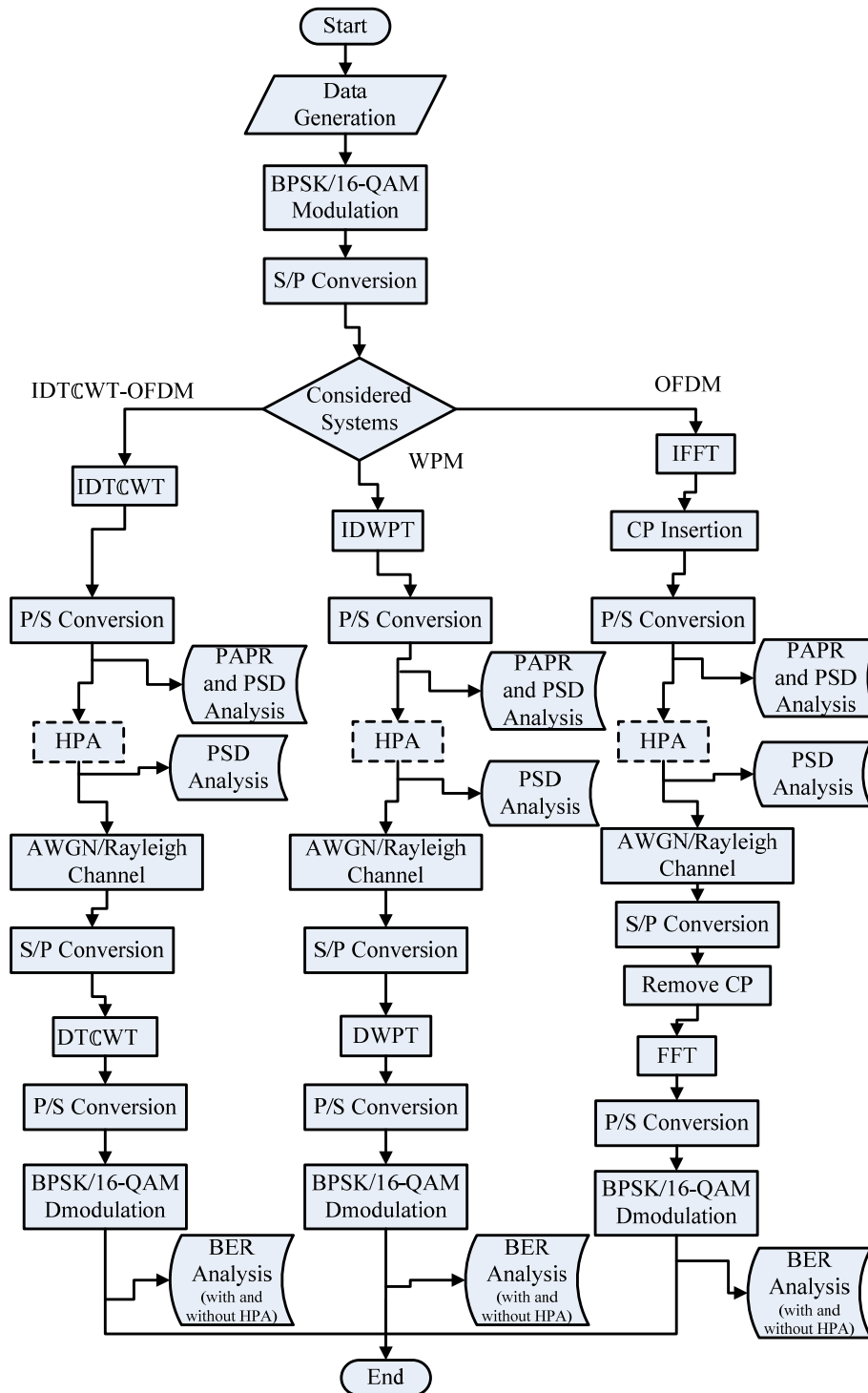


Figure 4.1 Flow charts of the simulation procedures of the considered systems.

4.1.1 For the OFDM System

To simulate the OFDM system, BPSK and 16-QAM modulations are used; subcarriers numbering 64, 128, 256, 512, and 1024 are utilized with PAPR threshold of 2dB; an AWGN and a 10-tap Rayleigh channel scenarios are assumed in the simulation of the BER; SSPA Rapp's model with knee-parameter $p = 3$ and TWTA models of $\alpha_A = 1$, $\beta_A = 0.25$, $\alpha_\phi = 0.26$, and $\beta_\phi = 0.25$ are used to characterize HPA nonlinearity. As the defined CP duration is $0.8 \mu\text{s}$, the 10-tap Rayleigh channel is selected to be of maximum duration $0.26 \mu\text{s}$. The real and imaginary parts of each 10-tap is independent Gaussian random variable with zero mean and 0.5 variance. Table 4.1 shows the main properties of the 10-tap Rayleigh channel models, which were used for simulation. This channel model was described in [142] and [143].

Table 4.1 Main channel properties of the 10-tap model.

Tap Index	Delay (ns)	Power (dB)
1	0	-0.39
2	10	-20.6
3	20	-26.8
4	50	-24.2
5	90	-15.3
6	95	-20.5
7	100	-28.0
8	180	-18.8
9	205	-21.6
10	260	-19.9

4.1.2 For the WPM System

In addition to the simulation parameters of OFDM system mentioned in the above section, the wavelet packets using Haar wavelets (db1), db3, db9 and db13 are selected and maximum tree depth of 7 (i.e., $D = 7$) is used for the tree nodes of WPT.

Different Daubechies wavelets are used as they are claimed to provide best BER performance for the WPM systems [144].

4.1.3 For the DT-CWT-OFDM System

Also, in addition to the simulation parameters of OFDM system mentioned in the above section of OFDM simulation parameters, the construction of the DT-CWT is made using different filters like, LeGall 5,3 tap filters (LEG), Antonini 9,7 tap filters (ANTO), Near Symmetric 5,7 tap filters (n -SYM- a), and Near Symmetric 13,19 tap filters (n -SYM- b) in the first stage of the FB. Moreover, Quarter-Sample-Shift Orthogonal 10,10 tap filters (q -SH-06) with only 6,6 non-zero taps, Quarter-Sample-Shift Orthogonal 10,10 tap filters (q -SH- a) with 10,10 non-zero taps, Quarter-Sample-Shift Orthogonal 14,14 tap filters (q -SH- b), Quarter-Sample-Shift Orthogonal 16,16 tap filters (q -SH- c), and Quarter-Sample-Shift Orthogonal 18,18 tap filters (q -SH- d) were utilized in the succeeding stages of the FB.

4.2 Peak-to-Average Power Ratio

In this section, the performance of the PAPR of the considered systems is quantified through the simulation. The PAPR results are obtained using the peak time-domain envelopes and the CCDF. As explained in section 3.6.2, the PAPR performance can be illustrated by plotting the peak time-domain envelope or the CCDF of the PAPR. The system model contains only the transmitter section of the considered systems without the HPA as shown in Fig. 2.16, Fig. 2.17, and Fig. 3.5. The simulation parameters used in the evaluation of the performance of PAPR based on the CCDF are documented in Table 4.2.

It should be mentioned that the PAPR performance analysis results, shown in this work, are obtained without using any PAPR reduction technique.

The PAPR value of the proposed system is investigated and compared with the OFDM and WPM systems in terms of time-domain peak envelope and CCDF.

Table 4.2 Simulation parameters.

Modulation	BPSK and 16-QAM
Channel	AWGN and a 10-tap Rayleigh
Number of Subcarriers (N)	64, 128, 256, 512, and 1024
Wavelet Packet Bases ($\phi_j[t]$)	Haar (db1), db3, db9 and db13
PAPR Threshold	2 dB
First stage FB of DT-CWT	Near Symmetric Filters
Succeeding stages FB of DT-CWT	Quarter Sample Shift Orthogonal Filters
SSPA Model	Rapp's model, $p = 3$ and $A_0 = 1$
TWTA Model	$\alpha_A = 1, \beta_A = 0.25, \alpha_\Phi = 0.26, \beta_\Phi = 0.25$

4.2.1 Peak Envelope

In order to analyze PAPR, we present the time-domain peak envelope waveforms. To do so, we generate the transmitted waveforms using 16 QAM modulation with 64 subcarriers. WPM systems employ, as mentioned before, db13 based wavelet packet bases, and n -SYM- b and q -SH- b filters for DT-CWT based OFDM system. Fig. 4.2 shows, in the time-domain, the envelope of the proposed system over a span of time.

For the purpose of comparison, we also plot the envelope of the OFDM and WPM waveforms corresponding to the same information symbol pattern.

The transmitted envelopes for the conventional OFDM and WPM systems illustrate approximately similar behavior, where the peak is about 2.25, while the transmitted envelope for the proposed system demonstrates better behavior than the other two systems, where the peak is only about 1.25. This indicates that the proposed system is likely to give better result for PAPR than the other two systems in terms of the range of variations of PAPR [145], [146], [147].

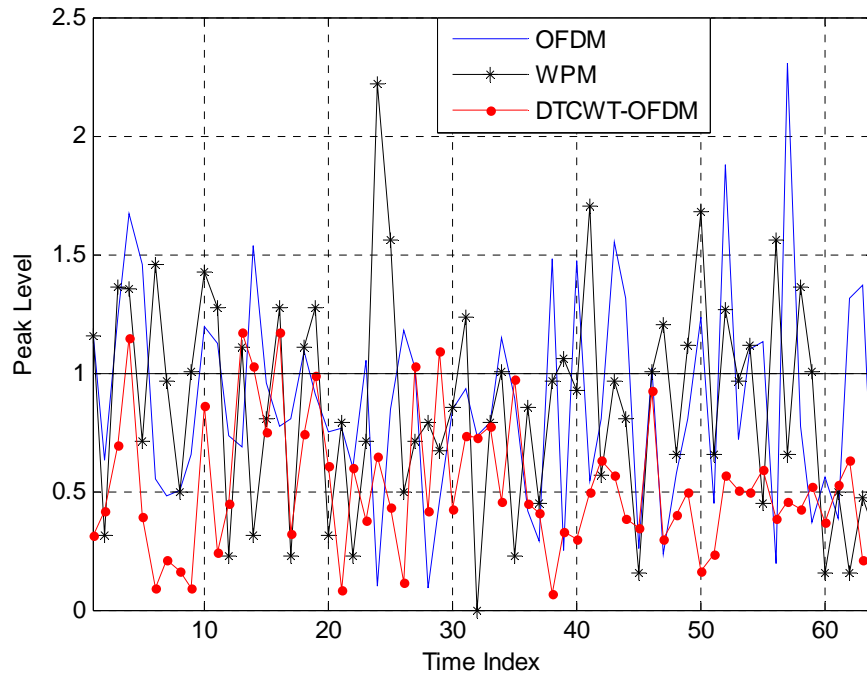


Figure 4.2 Envelope of the OFDM, WPM and DTCWT-OFDM systems.

To limit PAPR, one popular method is to clip [148] the waveform above a threshold. If we set the threshold (also called clipping level) at $|Amplitude| = 1.0$ in Fig. 4.2, we can see that the number of peaks above this threshold is higher for both OFDM and WPM transmitted signals than for DTCWT-OFDM transmitted signal. Therefore, for same clipping level, DTCWT-OFDM system is less sensitive to nonlinear HPA than OFDM and WPM systems.

In order to illustrate the superior peak and average values of the envelope for WT modulated subcarriers, Figs. 4.3 and 4.4 show the envelope of 16 subcarriers using FT and WT, respectively. The summation of these subcarriers shows a peak of 16 using FT and 3.2 when using WT.

This result shows good performance of WT modulated subcarrier in terms of peak and average values for the envelope. This results leads to better results of PAPR for WT over FT modulated subcarrier as would be demonstrated now.

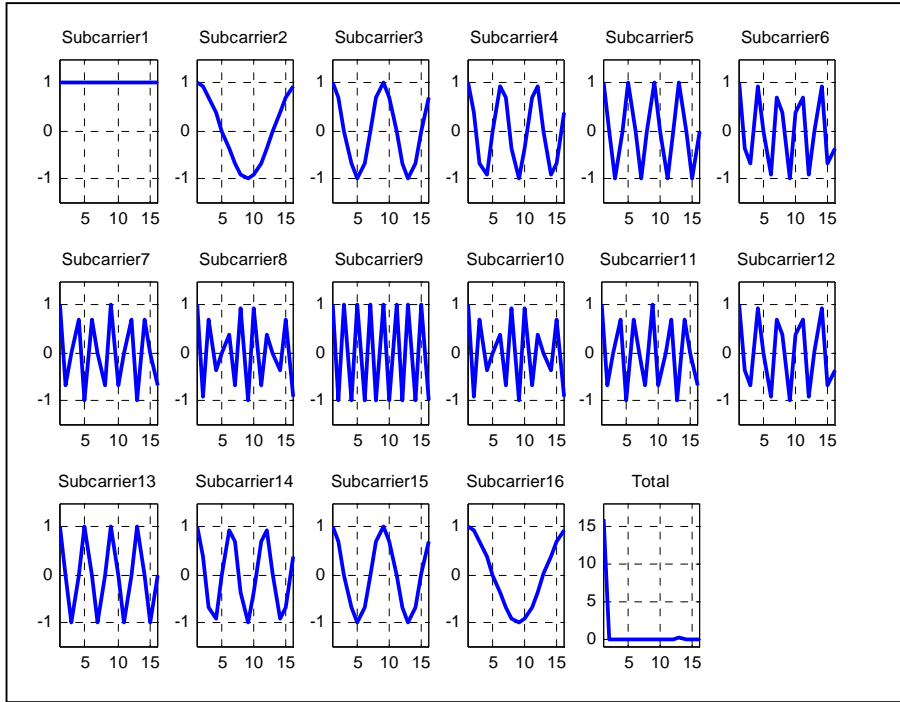


Figure 4.3 Envelope of the 16 subcarriers using FT.

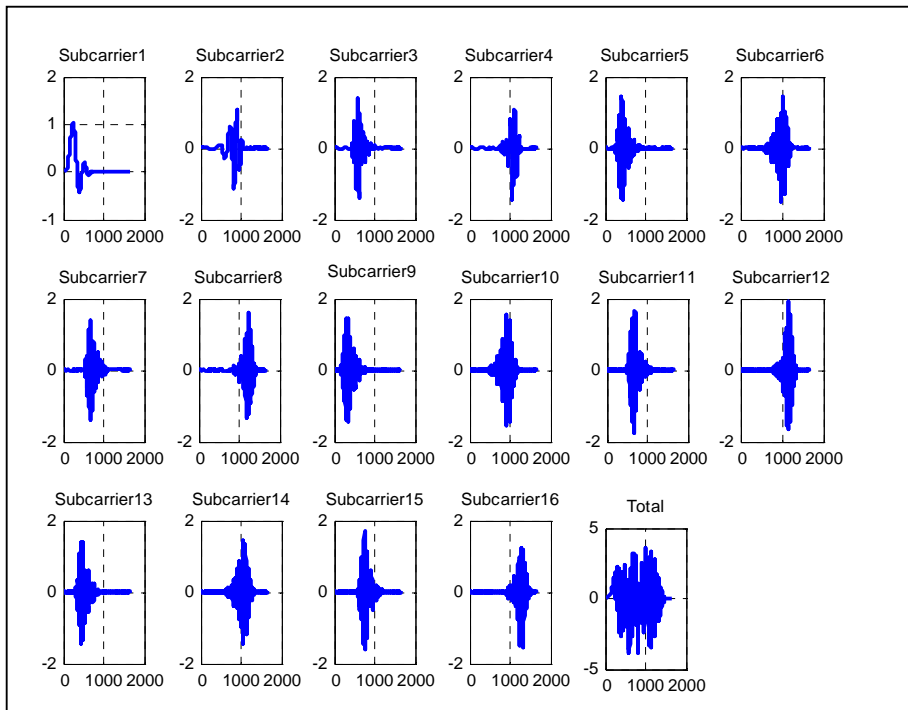


Figure 4.4 Envelope of the 16 subcarriers using WT.

4.2.2 CCDF

Now, to quantify the PAPR values of the considered systems, the CCDF as mentioned in section 3.6.2 is obtained for each system.

4.2.2.1 Typical Comparison

The CCDF of the transmitted signals for the considered systems is quantified in this section using same simulation parameters of the above section and the results are shown in Fig. 4.5. The first curve (solid red line) represents the CCDF of the proposed system while the other two curves (dashed blue line and dotted black line) represent the conventional OFDM and WPM systems respectively. The proposed system has a PAPR approximately 7.3 dB for 0.01% of CCDF and WPM and OFDM has a PAPR approximately 8.4 dB and 10.7 dB respectively at 0.01% of CCDF. The figure shows that the DTϕWT-OFDM system achieves 3.4 dB improvements over the OFDM and 1.1 dB improvements over the WPM systems at 0.01% of CCDF.

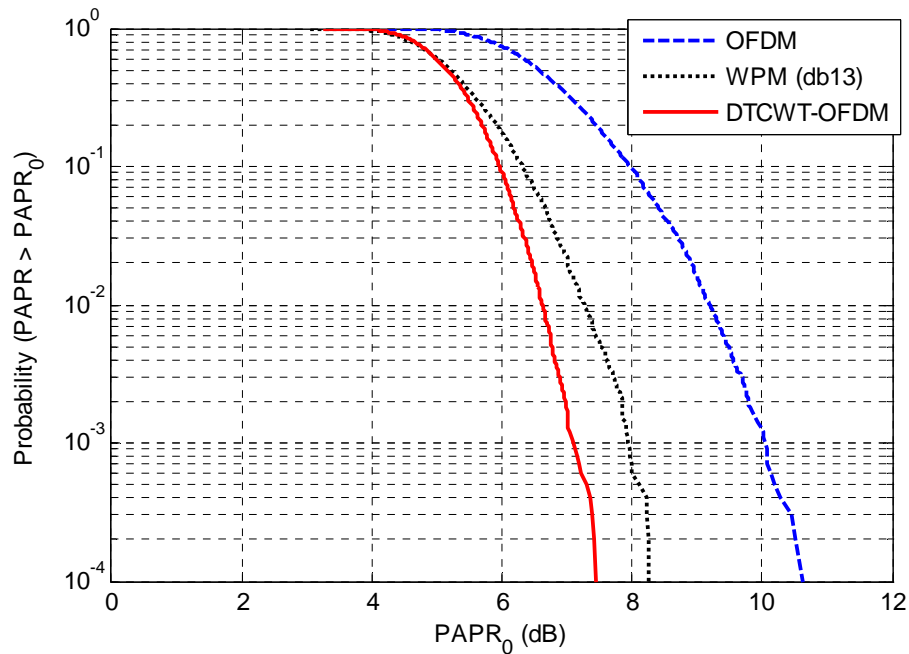


Figure 4.5 CCDF for the OFDM, WPM and DTϕWT-OFDM systems.

4.2.2.2 Study of use of different filters in DTCCWT

Next, the above experiment is repeated with different sets of filters. These filters are used to construct the DTCCWT and WPT in the DTCCWT-OFDM and WPM systems, respectively. DTCCWT-OFDM1 represents the proposed system when using n -SYM- b in the first stage of the FB with q -SH- d in the succeeding stages. DTCCWT-OFDM2 represents the proposed system when using n -SYM- b with q -SH- c filters. DTCCWT-OFDM3 represents the proposed system when using ANTO with q -SH- b filters. DTCCWT-OFDM4 represents the proposed system when using ANTO with q -SH- a filters. DTCCWT-OFDM5 represents the proposed system when using n -SYM- a with q -SH-06 filters. DTCCWT-OFDM6 represents the proposed system when using LEG with q -SH-06 filters. These results are shown in Fig. 4.6. While the results for the WPM system for different Daubechies wavelets are shown in Fig. 4.7. WPM1, WPM2, WPM3 and WPM4 represent the WPM system when using db13, db9, db3 and db1 respectively.

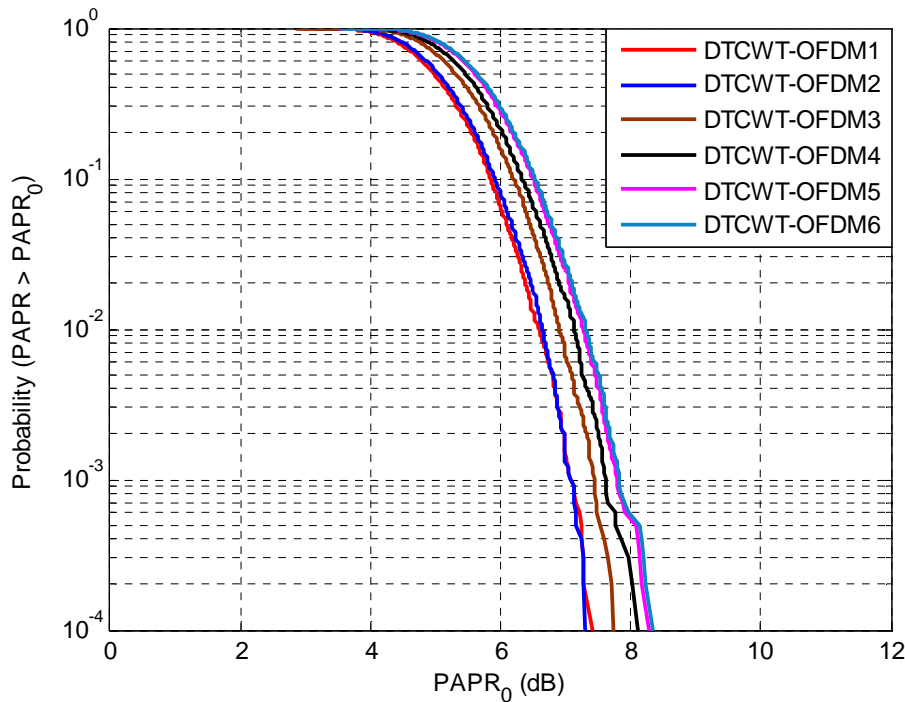


Figure 4.6 Effect of using different set of filters in design of the DTCCWT-OFDM.

The results in Fig. 4.6 show that the proposed system using n -SYM- b with q -SH- d filters has a PAPR of 7.3 dB at 0.01% of CCDF and has a PAPR of 7.4 dB when using n -SYM- b with q -SH- c filters, approximately same. The 0.01% PAPR of the proposed system is 7.7 dB when ANTO with q -SH- b filters are used, 8.1 dB when using ANTO with q -SH- a filters, and 8.4 when n -SYM- a with q -SH-06 filters and LEG with q -SH-06 filters; these results prove that increasing the filter length give better result of PAPR. As discussed in section 2.6, the problem of the lack of shift invariance related to the DWT and DWPT has been solved by utilizing the DTCWT [109]. The DTCWT can design using a range of filters. The work in [109] investigate the degree of shift invariance for the filters used to construct the DTCWT and prove that the longer filters provide improved shift invariance.

The results in Fig. 4.6 confirm the results in [109]. In term of complexity, the longer filters are more complex but not same complexity order as the longer filters for DWPT as it will be discussed in see section 4.5.

From the results in Fig. 4.7 we can deduce that the higher order of Daubechies wavelets give better CCDF results. However, for the higher order of Daubechies wavelets the complexity of system will be very high compare to complexity of OFDM and DTCWT-OFDM [20], [149].

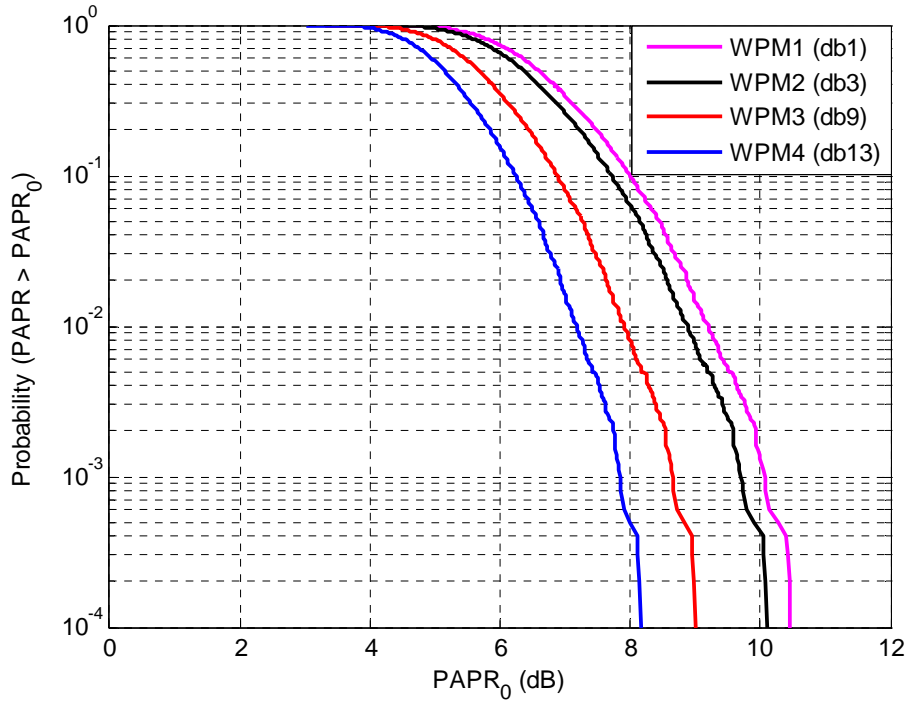


Figure 4.7 Effect of using different set of filters in design of the WPM system.

4.2.2.3 Study on use of different number of subcarriers

Next, the above experiments are repeated for the considered systems using different numbers of subcarriers N (64, 128, 256, 512, and 1024). n -SYM- b with q -SH- d are used in the proposed system and db13 is used in the WPM system. The results are shown in Figs. 4.8, 4.9, and 4.10 for the conventional OFDM, WPM, and the DTCCWT-OFDM systems, respectively.

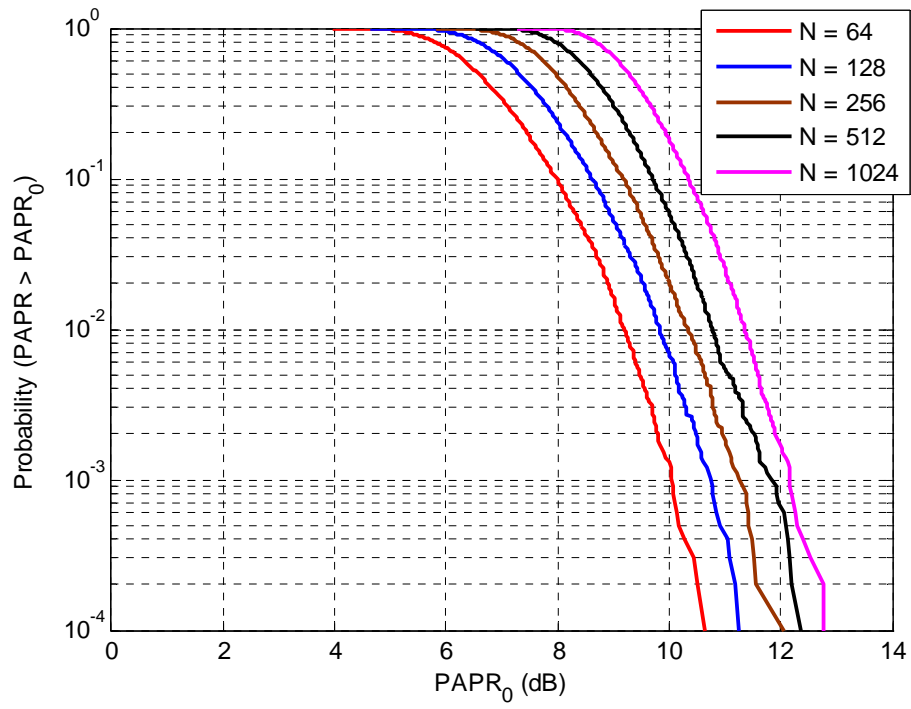


Figure 4.8 CCDF results for the OFDM using different subcarriers (N).

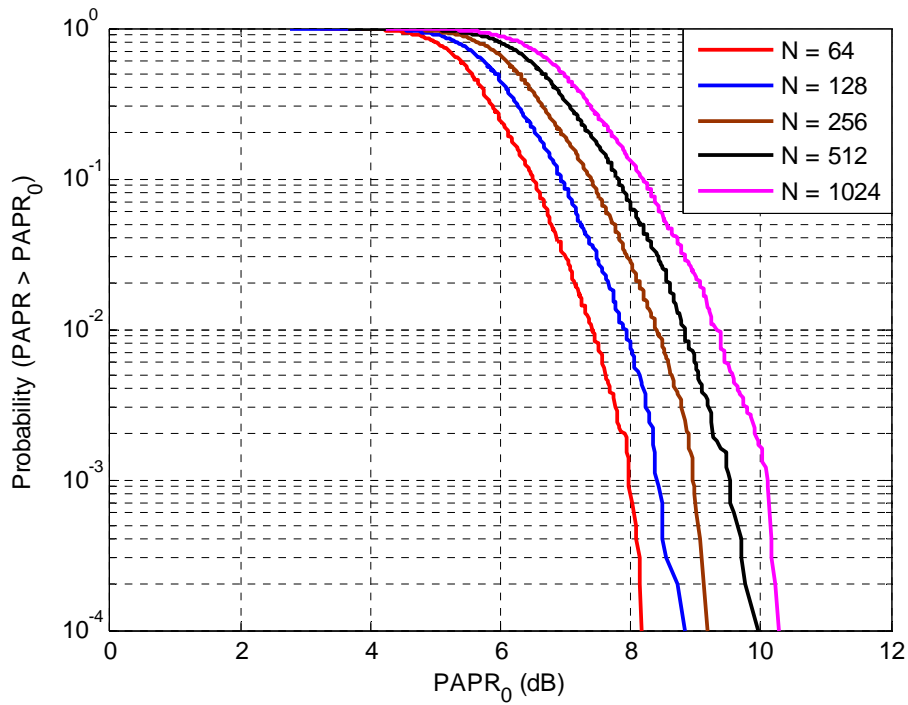


Figure 4.9 CCDF results for the WPM using different subcarriers (N).

It is quite clear from Fig. 4.8, Fig. 4.9 and Fig. 4.10 that the PAPR increases with the number of the subcarriers as do the other two systems. But, as the figures indicate, the DTCWT system gives better PAPR results than the other systems. It achieves 3.4 dB improvement over the conventional OFDM system and 1.1 dB improvement over the WPM system at 10^{-4} of the CCDF.

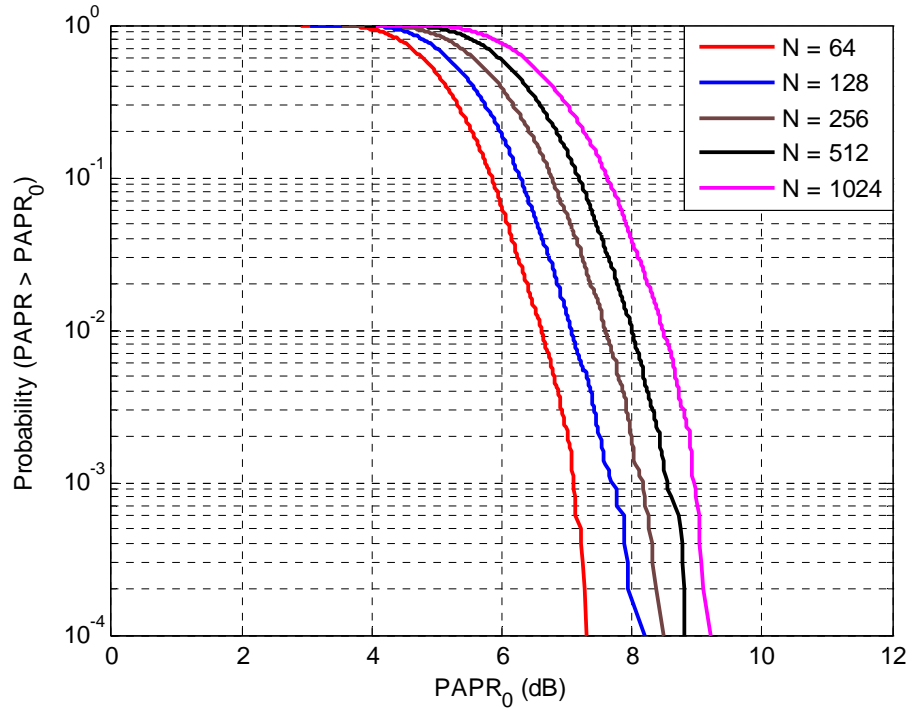


Figure 4.10 CCDF results for the DTCWT-OFDM using different subcarriers (N).

4.3 Power Spectrum Density

Now we present the results of PSD with and without the nonlinear HPA.

4.3.1 Power Spectrum Density without the HPA

To demonstrate the similarities and dissimilarities between the OFDM, WPM and DTCWT-OFDM systems, as it mentioned in section 3.6.1 their PSD characteristics are shown in Fig. 4.11, when signaling with 16-ary QAM using 64 subcarriers. The db13 wavelet packet bases were used to construct the wavelet packet trees in WPM system. For the DTCWT-OFDM, n -SYM- b and q -SH- d were used to construct the real and the imaginary part of DTCWT respectively.

The PSD characteristics of the considered systems are presented in Fig. 4.11. The solid blue, dotted black and dashed red curves represent the conventional OFDM, WPM and the DTCWT-OFDM systems, respectively.

For the OFDM system the simulation results show that the spectral re-growth begins below 25 dB, 33 dB and 38 dB from the main signal level of 0 dB for conventional OFDM, WPM and DTCWT-OFDM systems, respectively. We can deduce that the proposed system is relatively showing better spectrum characteristics in terms of more low out of band attenuation (more suppression of out of band attenuation), than the conventional OFDM and the WPM systems [150], [151].

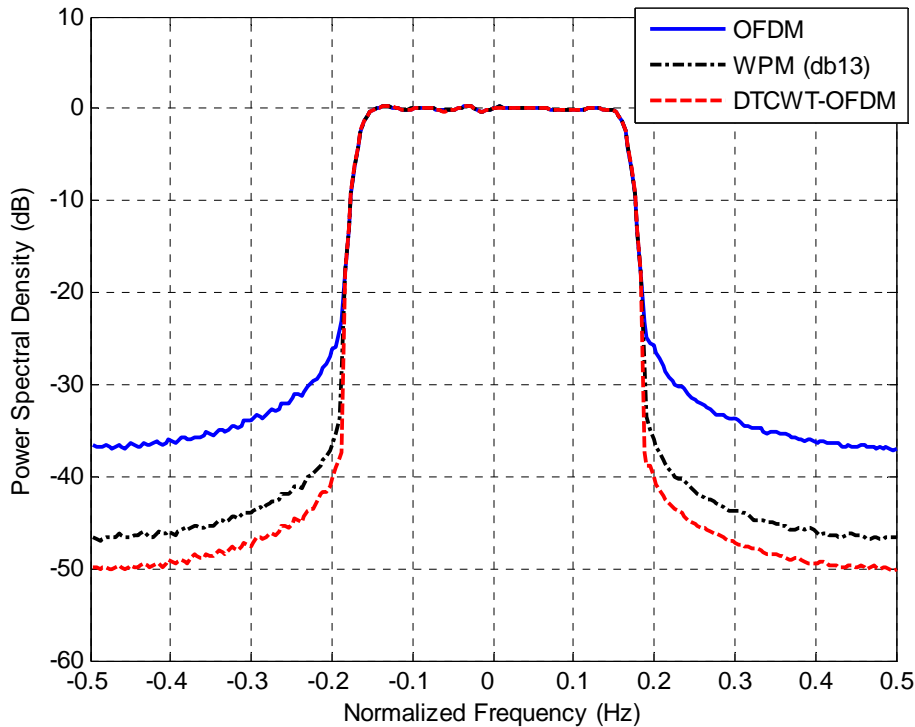


Figure 4.11 PSD for the OFDM, WPM and DTCWT-OFDM systems.

4.3.2 Power Spectrum Density with the HPA

Section 3.6.2 concluded that the two influences of the nonlinear HPA on the transmitted signals are the out-of-band distortion that causes the power spectrum distortion (the spectral spreading of the amplified signal and ACI) and the in-band distortion that disturbs the signal constellations and results in BER performance degradation.

4.3.2.1 Spectrum Re-growth

Because the transmitter's power amplifier gain is generally adjusted to provide a fixed average power, high peak can cause the power amplifier to move toward saturation. This causes inter-modulation distortion which generates spectral re-growth. Spectral re-growth is the generation of new range of frequencies that develops on each side of the carrier (similar to sidebands) and extends into the adjacent frequency bands. Consequently, spectral re-growth interferes with communication in the adjacent bands. Reducing the PAPR leads to reducing the spectral re-growth.

4.3.2.2 Input Power Back-off

As defined in section 3.6.2.1, the time-domain waveforms of the considered systems are passed through the Rapp's nonlinear amplifier model (Eqs. (3.46) and (3.47)) with ($p = 3$ and $A_0 = 1$) and TWTA (Eq. (3.48) and Eq. (3.49)) with ($\alpha_A = 1$, $\beta_A = 0.25$, $\alpha_\phi = 0.26$, $\beta_\phi = 0.25$). The PSD results are shown respectively in Fig. 4.12 and Fig. 4.13.

As the nonlinearities of the HPA cause the spectrum re-growth, we evaluate the influence of the nonlinear HPA on the PSD. We generate the transmitted waveforms using 16 QAM modulation with 64 subcarriers. WPM systems employ, as mentioned before, db13 based wavelet packet bases, and n -SYM- b and q -SH- b filters for DTCWT based OFDM system. The simulation results in Fig. 4.12 show that spectral re-growth begins below 26 dB, 35 dB and 39 dB from the main signal level of 0 dB for conventional OFDM, WPM, and DTCWT-OFDM systems, respectively. In Fig 4.13, the spectral re-growth begins below 28 dB, 37 dB and 41 dB from the main signal level of 0 dB for conventional OFDM, WPM, and DTCWT-OFDM systems, respectively. These figures show the PSD of the considered systems in the linear case and at the output of the nonlinear HPA with back-off value of 6 dB. Hence, the required power back-off can be compared. From the simulation results we can deduce that the proposed system required lesser amount of the IBO comparing with WPM and OFDM systems when the considered systems are adjust to produce spectral re-growth of the PSD as close to each other as possible.

From the study, it can be seen that the SSPA has a smaller out of band distortion and hence less spectral re-growth than the TWTA. This is true for all the three cases.

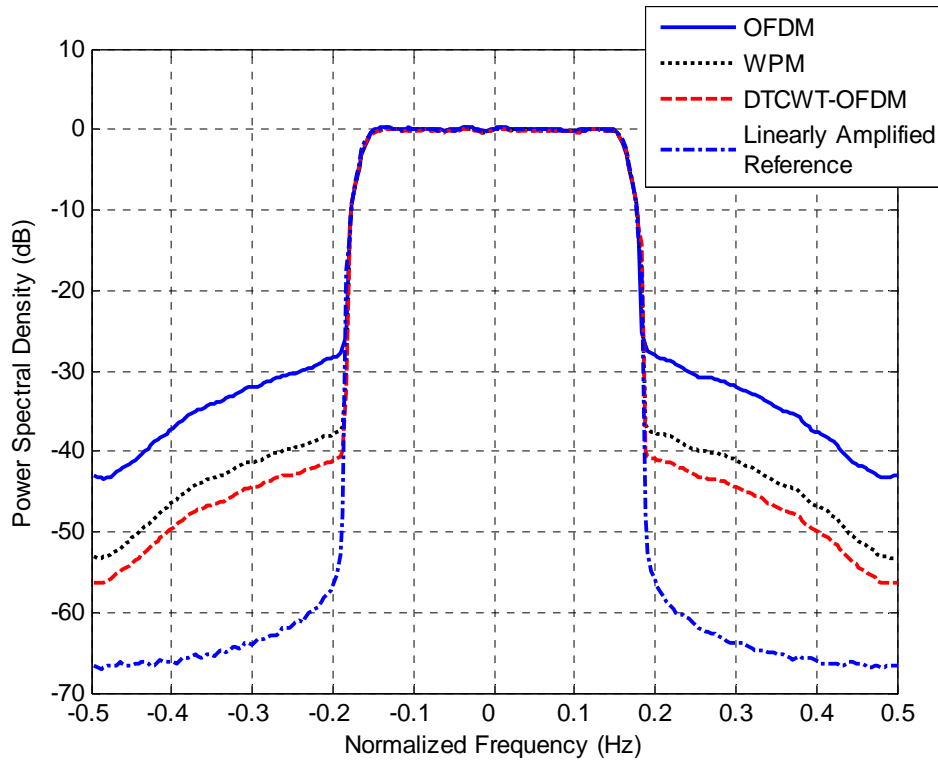


Figure 4.12 PSD for the OFDM, WPM and DTCWT-OFDM systems in presence of nonlinear SSPA.

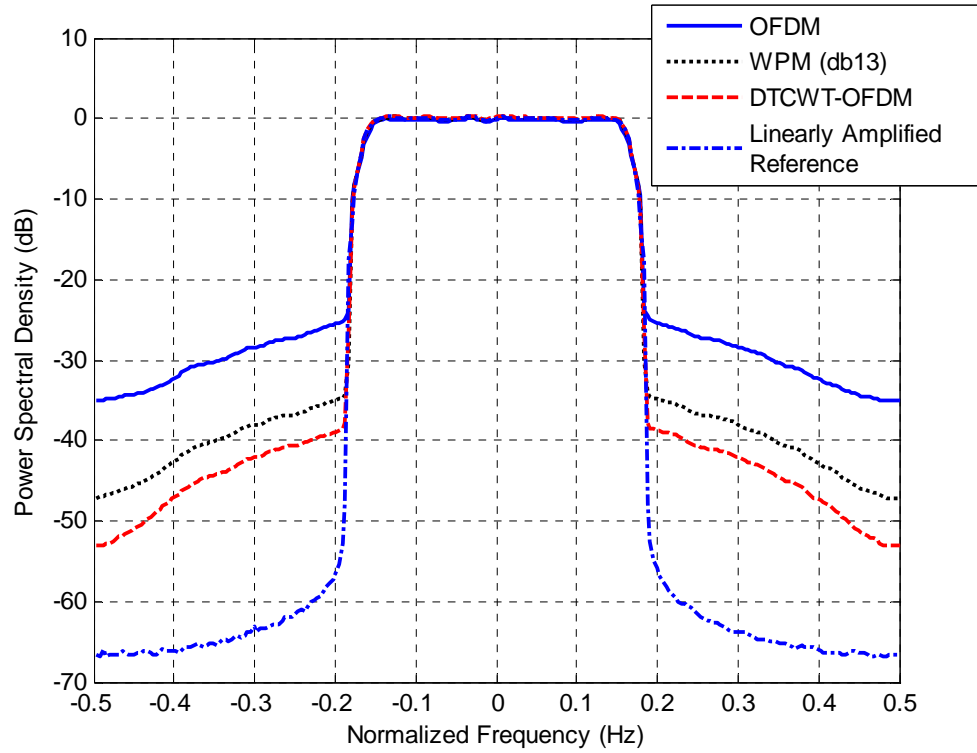


Figure 4.13 PSD for the OFDM, WPM and DTCWT-OFDM systems in presence of nonlinear TWTA.

To further compare the SSPA and the TWTA effects in the PSD of the considered systems transmitted signals, Fig. 4.12 and Fig. 4.13 are combined together in Fig. 4.14 where OFDM1, WPM1 and the DTCWT-OFDM1 represent the consider systems in the present of SSPA and OFDM2, WPM2 and the DTCWT-OFDM2 represent the consider systems in the present of TWTA.

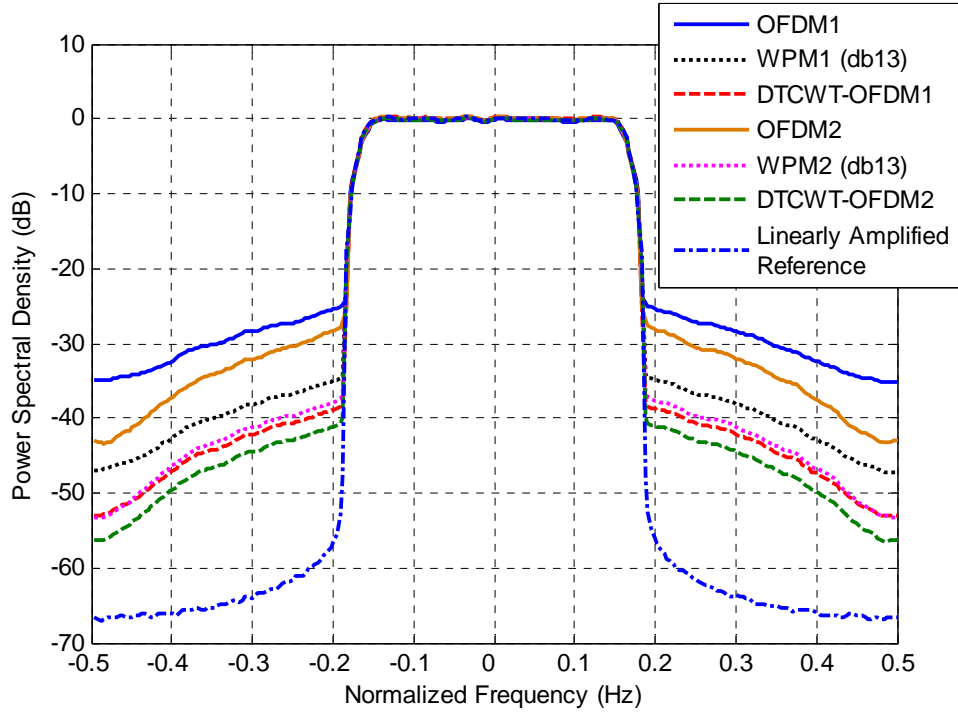


Figure 4.14 PSD for the OFDM, WPM and DTCWT-OFDM systems in presence of nonlinear SSPA and TWTA.

The results in Fig. 4.15 and Fig. 4.16 show the PSD of the considered systems in the linear case and at the output of the nonlinear SSPA and TWTA respectively. It has to be emphasized that the different back-off values are used so as to adjust the considered systems to achieve nearly same spectral performance as possible.

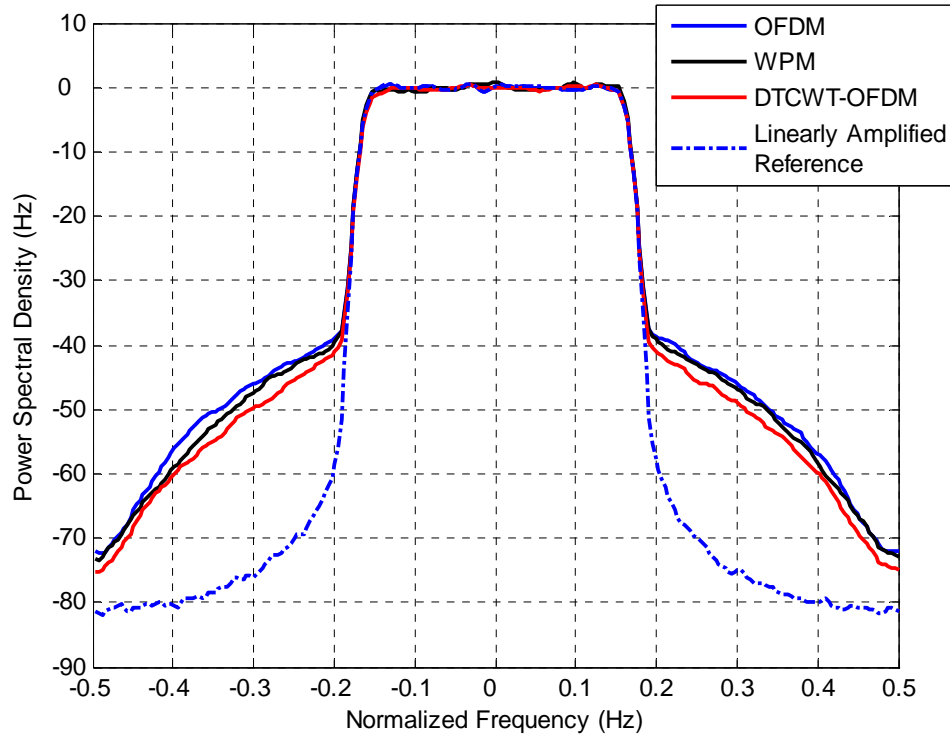


Figure 4.15 PSD of the considered systems. OFDM (IBO = 10.9 dB), WPM (IBO = 6.8 dB), DTCWT-OFDM (IBO = 5.5 dB).

The conventional OFDM system required 10.9 dB of IBO and the WPM system required 6.8 dB of IBO, where the proposed system required only 5.5 dB of IBO. From these results we conclude that the proposed system required lesser amount of IBO comparing by the conventional OFDM and WPM systems, at the same time the proposed system produced lesser amount of spectral re-growth comparing to the other two systems. From the results we saw that the TWTA produced more spectral re-growth than the SSPA. This is true for all the three cases.

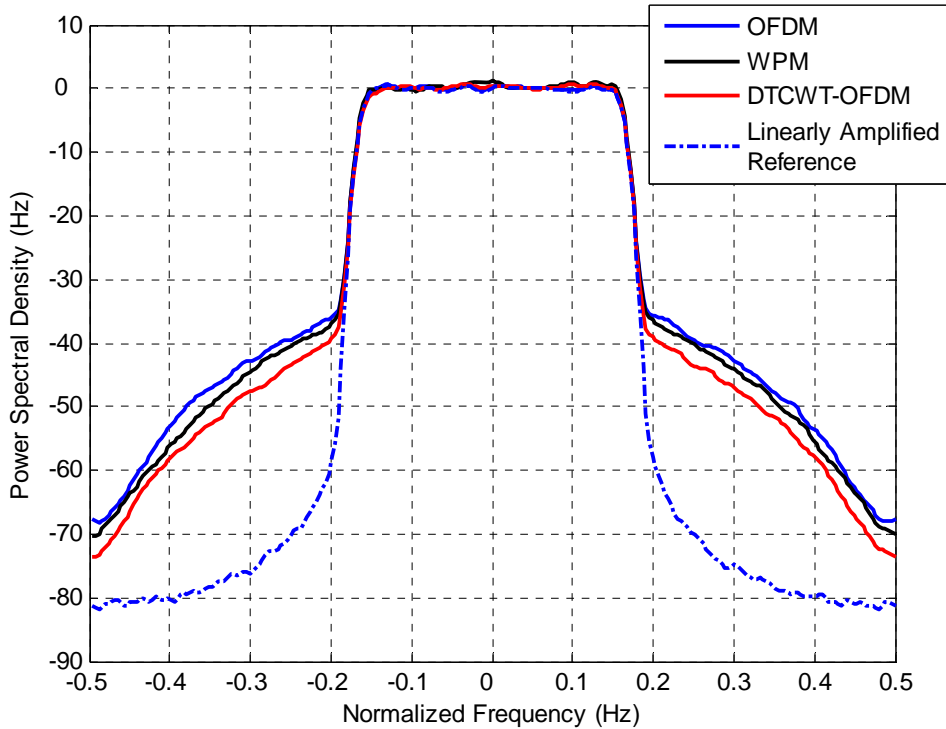


Figure 4.16 PSD of the considered systems. OFDM (IBO = 10.9 dB), WPM (IBO = 6.8 dB), DTϕWT-OFDM (IBO = 5.5 dB).

4.4 Bit Error Rate

Now we present the results of BER with and without the HPA.

4.4.1 Bit Error Rate without the HPA

In all communication systems, the BER represents a very important performance metric of the system that captures the probability of error in demodulating the information sent. To measure the noise robustness of DTϕWT-OFDM communication scheme the relationship of the BER as a function of the energy per bit to noise power spectral density ratio (E_b/N_0) performance is a useful performance tool.

4.4.1.1 BER in AWGN

To further demonstrate the similarities and dissimilarities between the OFDM, WPM and DTϕWT-OFDM systems, the BER performances are shown in Fig. 4.17 when signaling with BPSK and 16-QAM along with 64 subcarriers in AWGN channel. n -

SYM- b with q -SH- d filters are used to construct FB of DTCWT and db13 wavelet packet bases are used to construct the wavelet packet trees.

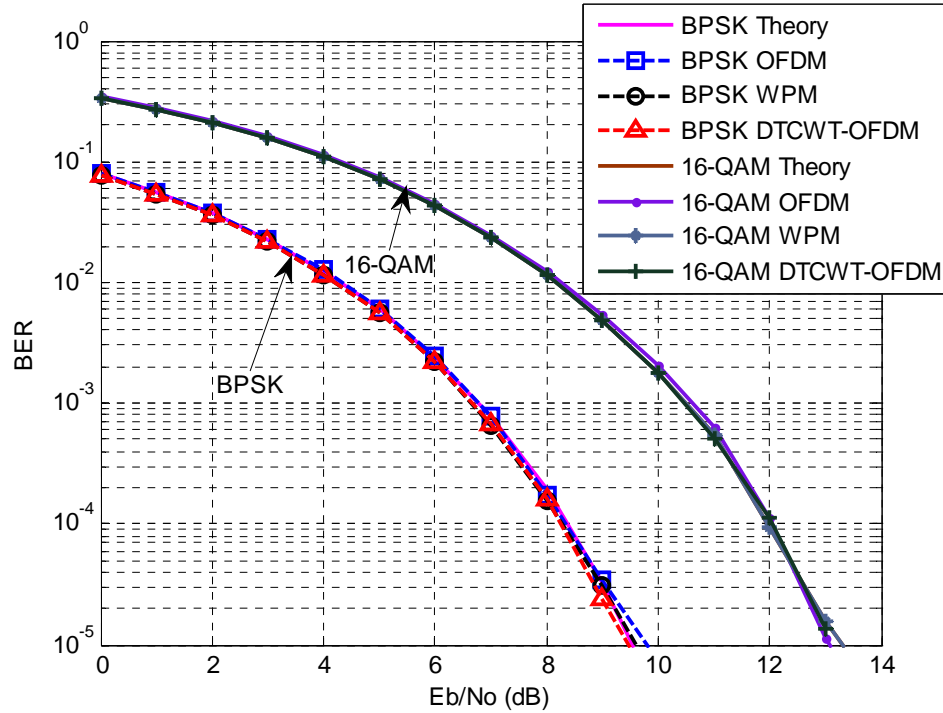


Figure 4.17 BER performance of DTCW-OFDM using BPSK and 16-QAM in AWGN channel.

In Fig 4.17, the first four curves represent theoretical BPSK and the conventional OFDM, WPM, and DTCWT-OFDM systems using BPSK modulation. While the others four curves are representing the theoretical 16-QAM and the conventional OFDM, WPM, and DTCWT-OFDM systems using 16-QAM modulation.

This figure indicates that the BER performance of the considered system nearly matches the theoretical BPSK and 16-QAM modulation BER performance in an AWGN channel.

4.4.1.2 BER in Rayleigh Flat Fading Channel

The above experiment is repeated again using a 10-tap Rayleigh channel while the other parameters are kept as above. This result is shown in Fig. 4.18.

This figure indicates that the average BER performance of the considered system nearly matches the theoretical BPSK and 16-QAM modulation BER performance in the Rayleigh channel.

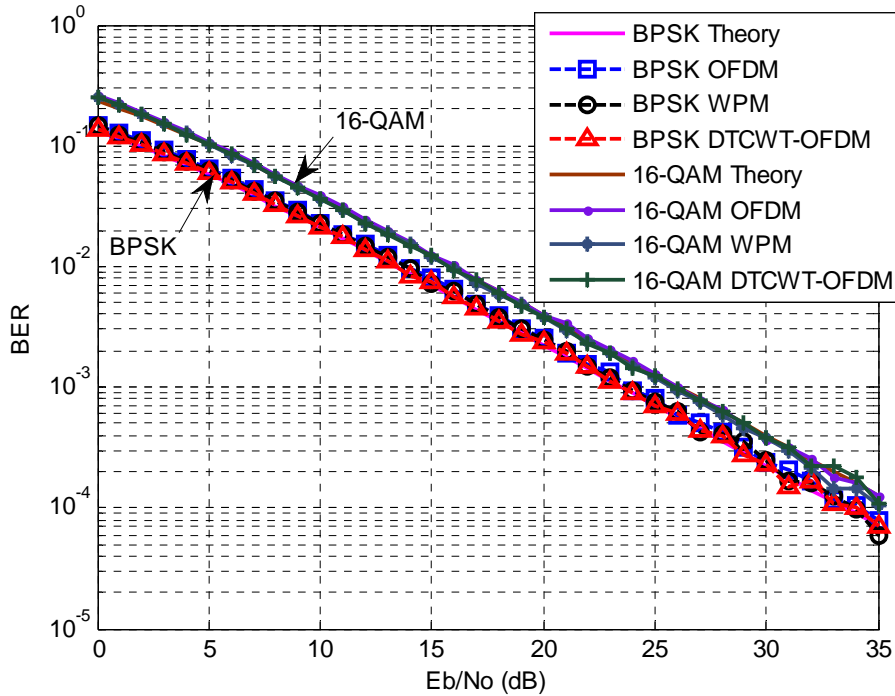


Figure 4.18 BER performance of DTCW-OFDM using BPSK and 16-QAM in a 10-tap Rayleigh channel.

4.4.1.3 Study of BER with different wavelet filters

The above experiments are repeated for the DTCWT-OFDM and WPM systems in AWGN channel using BPSK with different set of filters and the results are shown in Fig. 4.19 and Fig. 4.20, respectively.

In Fig. 4.19, when using BPSK, DTCWT-OFDM1 represents the proposed system when using n -SYM- b in the first stage of the FB with q -SH- d in the succeeding stages. DTCWT-OFDM2 represents the proposed system when using n -SYM- b with q -SH- c filters. DTCWT-OFDM3 represents the proposed system when using ANTO with q -SH- b filters. DTCWT-OFDM4 represents the proposed system when using ANTO with q -SH- a filters. DTCWT-OFDM5 represents the proposed system when

using n -SYM- a with q -SH-06 filters. DTCWT-OFDM6 represents the proposed system when using LEG with q -SH-06 filters.

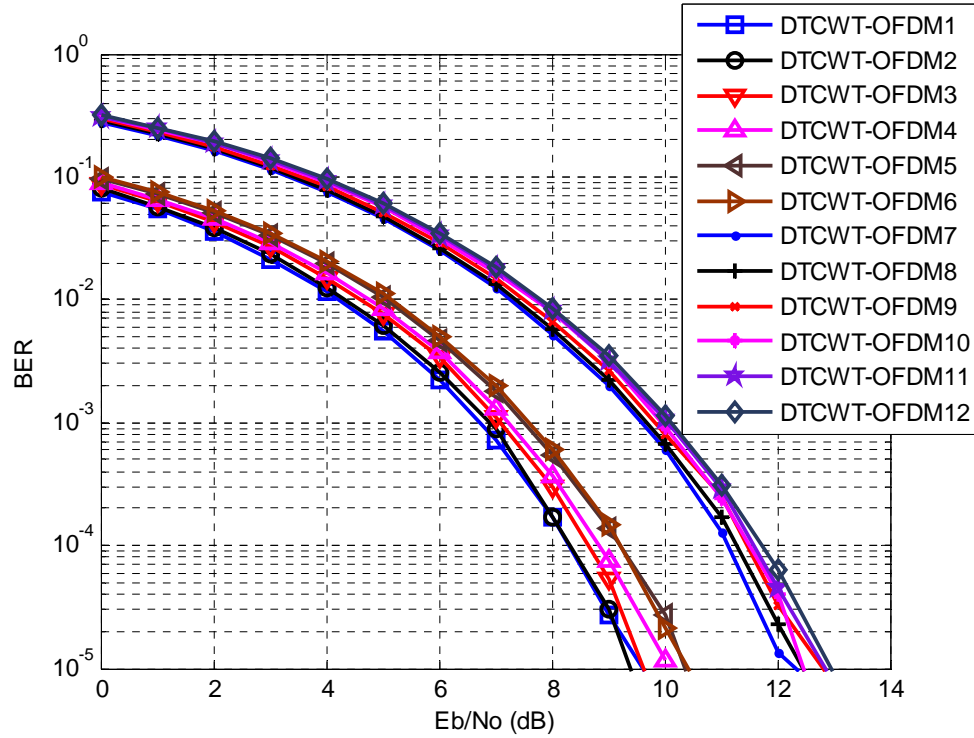


Figure 4.19 BER performance of DTCWT-OFDM using BPSK and 16-QAM in AWGN channel for different type of filters.

In Fig. 4.19, the systems that are labeled from 7 to 12 represent the proposed system when signaling with 16 QAM, DTCWT-OFDM7 represents the proposed system when using n -SYM- b with q -SH- d filters. DTCWT-OFDM8 represents the proposed system when using n -SYM- b with q -SH- c filters. DTCWT-OFDM9 represents the proposed system when using ANTO with q -SH- b filters. DTCWT-OFDM10 represents the proposed system when using ANTO with q -SH- a filters. DTCWT-OFDM11 represents the proposed system when using n -SYM- a with q -SH-06 filters. DTCWT-OFDM12 represents the proposed system when using LEG with q -SH-06 filters.

In Fig. 4.20 WPM1, WPM2, WPM3 and WPM4 represent the WPM system when using db13, db9, db3 and db1 respectively.

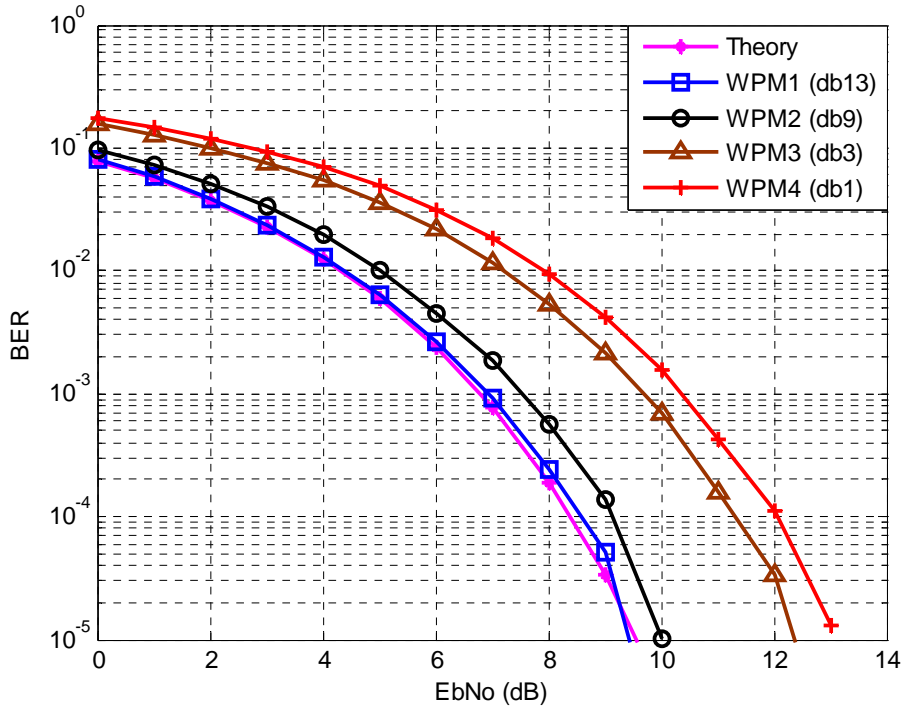


Figure 4.20 BER performance of WPM using BPSK in AWGN channel for different type of filters.

The results in Fig. 4.19 and Fig. 4.20 show that the BER performance is getting better and better with increasing the length of filters for both systems. That's because with increasing the filter length the spectral containment is higher, therefore, ICI reduction is much greater. However, this leads to increasing the system computational complexity especially for the WPM system. Hence a tradeoff should be made between BER performance and filter length. But, in the case of the proposed system, the computational complexity, in general, is very low as compared to that of the WPM system [146], [151], [152], [153] as will be shown in section 4.6.

4.4.2 Bit Error Rate with HPA

Now, we evaluate the influence of the nonlinear HPA on the BER. As the nonlinearities of HPA cause spectrum re-growth, the BER performance is expected to degrade. This study is to capture the relative amount of BER degradation for all considered systems.

To approximate the effect of nonlinear HPA, we adopt SSPA Rapp's and TWTA

models. The AM/AM and AM/PM characteristic of these amplifiers were given in chapter 3 in Eqs. (3.46), (3.47), (3.48) and Eq. (3.49).

Figure 4.21 shows the BER curve for the considered systems. They are compared to the BER curve of the theoretical BPSK and 16-QAM modulation without distortion. To evaluate the effect of the nonlinear HPA on the BER of the considered systems, Rapp's model ($p = 3$ and $A_0 = 1$) for AM/PM Eq. (3.46) and AM/AM Eq. (3.47) conversions has been adopted with 64 subcarriers and BPSK and 16-QAM modulation in AWGN channel. And figure 4.22 shows the case when the TWTA model has been adopted (AM/AM Eq. (3.48) and AM/PM Eq. (3.49)).

In Fig 4.21 when signaling with BPSK and 16-QAM along with 64 subcarriers in AWGN channel. n -SYM- b with q -SH- d filters are used to construct FB of DTCWT and db13 wavelet packet bases are used to construct the wavelet packet trees. OFDM1, WPM1, and DTCWT-OFDM1 are respectively conventional OFDM, WPM, and DTCWT-OFDM system using BPSK modulation while OFDM2, WPM2, and DTCWT-OFDM2 are the considered system when using 16-QAM modulation. This figure shows that the DTCWT-OFDM system is less sensitive to the nonlinear HPA than OFDM and WPM systems.

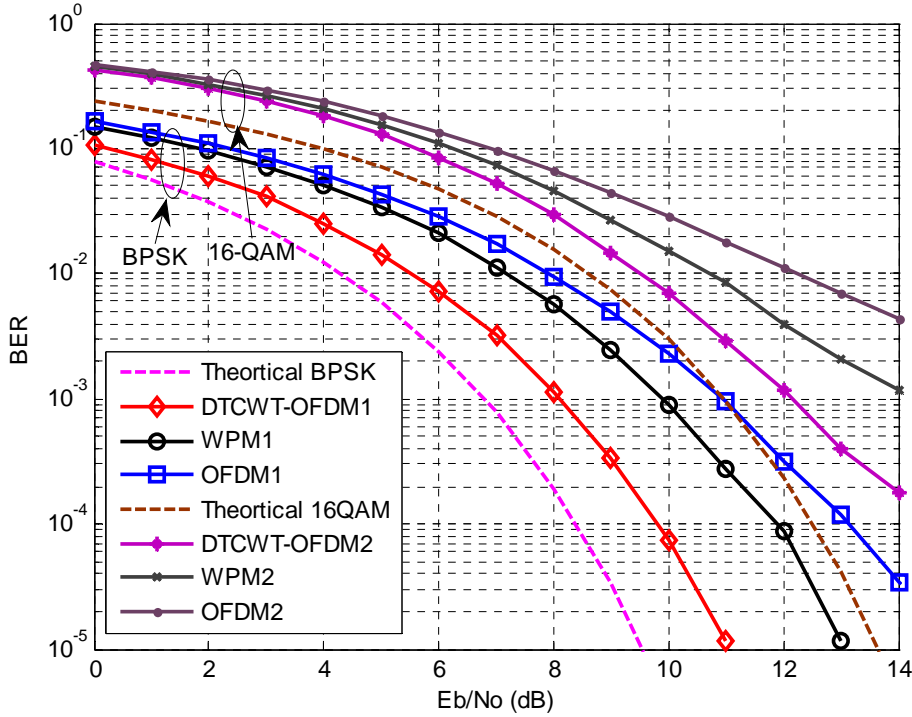


Figure 4.21 BER performance of DTCWT-OFDM using BPSK and 16-QAM in the presence of SSPA.

Moreover, the effect of the nonlinear HPA on the BER of the considered systems is examined again using the TWTA model ($\alpha_A = 1$, $\beta_A = 0.25$, $\alpha_\phi = 0.26$, $\beta_\phi = 0.25$) for AM/AM Eq. (3.42) and AM/PM Eq. (3.43) conversions with other simulation parameters as same as for the above experiment. Fig. 4.22 shows the BER curve of the considered systems using BPSK and 16-QAM along with the BER curve of the theoretical BPSK and 16-QAM modulation. Again, OFDM1, WPM1, DTCWT-OFDM1, OFDM2, WPM2, and DTCWT-OFDM2 are defined same as above. Also these results confirm that the proposed system is less sensitive to the nonlinear HPA than OFDM and WPM systems.

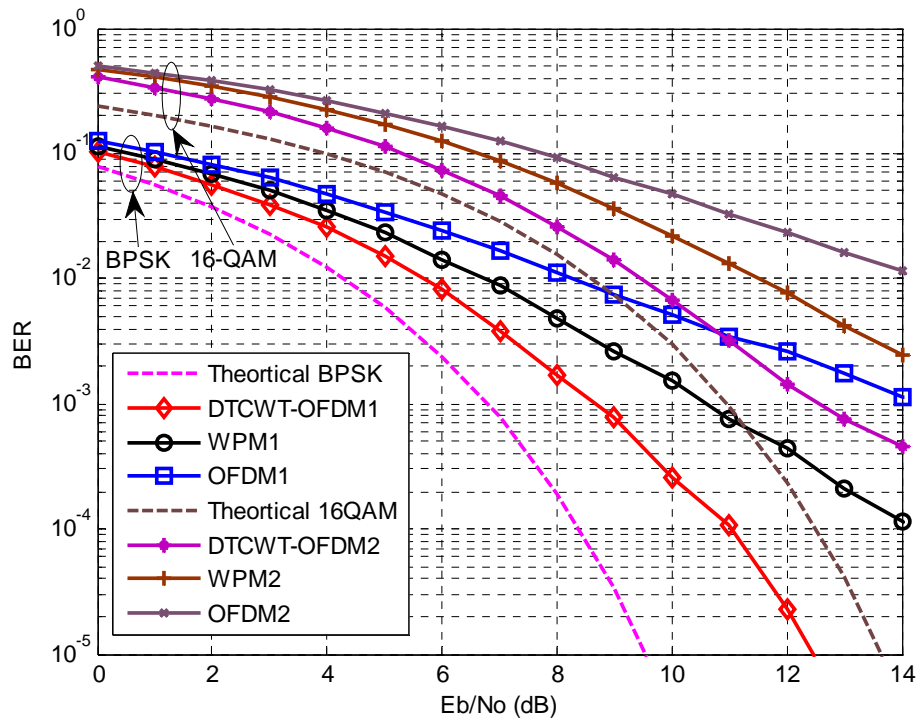


Figure 4.22 BER performance of DTCWT-OFDM using BPSK and 16-QAM in the presence of TWTA.

From the study above on BER performance, it can be seen that without using HPA the BER results of the considered systems are similar and close to the theoretical case. However, when using the HPA the degradation of BER happens. Also it's clear that the SSPA has a smaller in band distortion and hence less BER performance degradation than the TWTA.

The results in Fig. 4.23 show the BER performance of the considered systems when different IBO values are used so as to adjust the considered systems to achieve nearly same spectral performance as possible. The conventional OFDM, the WPM and the DTCWT-OFDM systems are required 10.9 dB, 6.8 dB and 5.5 dB respectively. From this results we see that the proposed system produced better BER results with lesser amount of IBO than the WPM and conventional OFDM systems. At the same time the WPM system outperform the conventional OFDM system in term of better BER results with lesser IBO value.

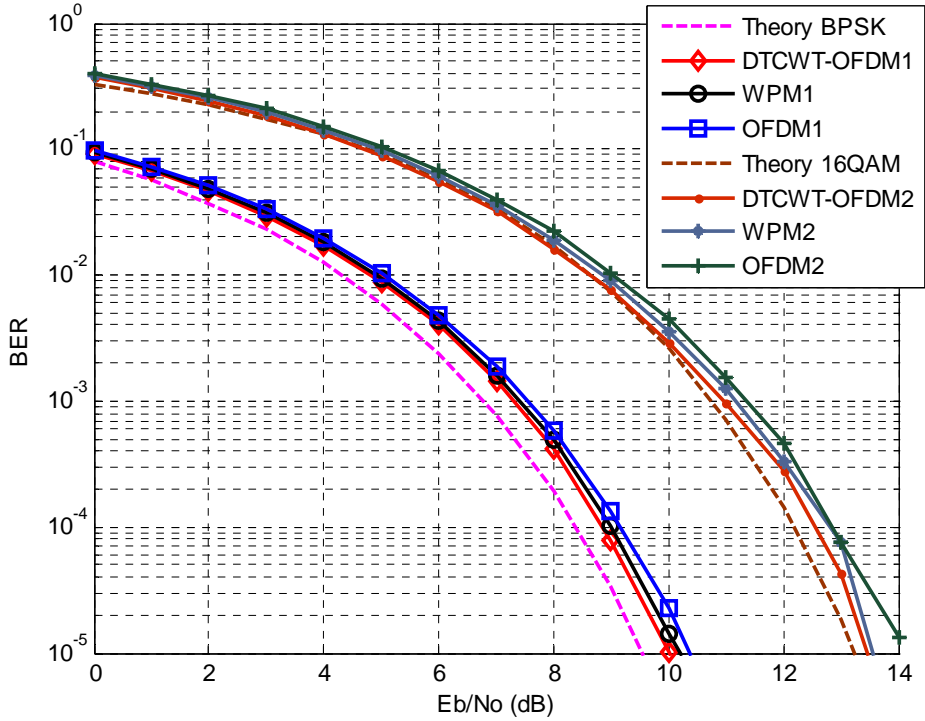


Figure 4.23 BER performances of the OFDM, WPM and DTCWT-OFDM systems using 10.9 dB, 6.8 dB and 5.5 dB of IBO respectively.

4.5 Study of the Shift Invariance Property

This study is motivated by the fact that OFDM systems based on wavelets ought to suffer from lack of shift-invariance property while that based on DTCWT should not. Among various performance metrics, BER in the presence of frequency-selective wireless channels is expected to capture the impact of this property. In frequency selective channels, copies of the signal arrive at the receiver at different times. If each copy produces wavelet coefficients differing both in magnitude and their number, their sum would vary for each transmission. Averaged over several symbols, the BER value so obtained will be different and more than the case where each copy produces same coefficients maybe with different phase. Accordingly, it is suggested to study the average BER of WPM system and DTCWT based OFDM system in the presence of 2-path frequency-selective wireless channel where the second path has varying amount of delay relative to first path.

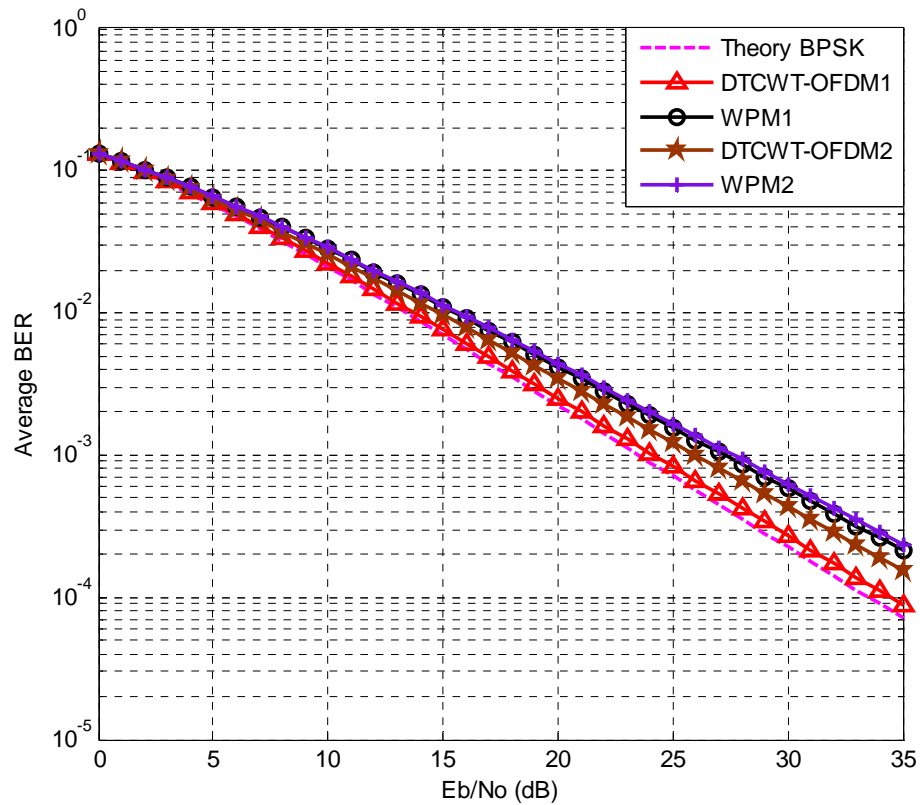


Figure 4.24 BER performance of the DTCWT-OFDM using BPSK in frequency selective channel.

The advantages of the shift-invariance property can be seen from the results of the average BER performance of the proposed system under different filters length. The average BER performances are shown in this experiment when signaling with BPSK and 16-QAM along with 64 subcarriers and different tap delay variation; less than and greater than 13 tap delay (2 and 26 tap delay). Fig. 4.24 shows the BER curves for the considered systems in the frequency selective channel using BPSK with 2 and 26 tap delays, DTCWT-OFDM using n -SYM- b with q -SH- d filters and 13th Daubechies wavelets is used in the WPM system. DTCWT-OFDM1 and WPM1 represent the DTCWT based OFDM and WPM systems respectively, in the present of the 2-tap delay. DTCWT-OFDM2 and WPM2 represent the DTCWT based OFDM and WPM systems respectively in the present of the 26-tap delay. The considered systems are using BPSK modulation.

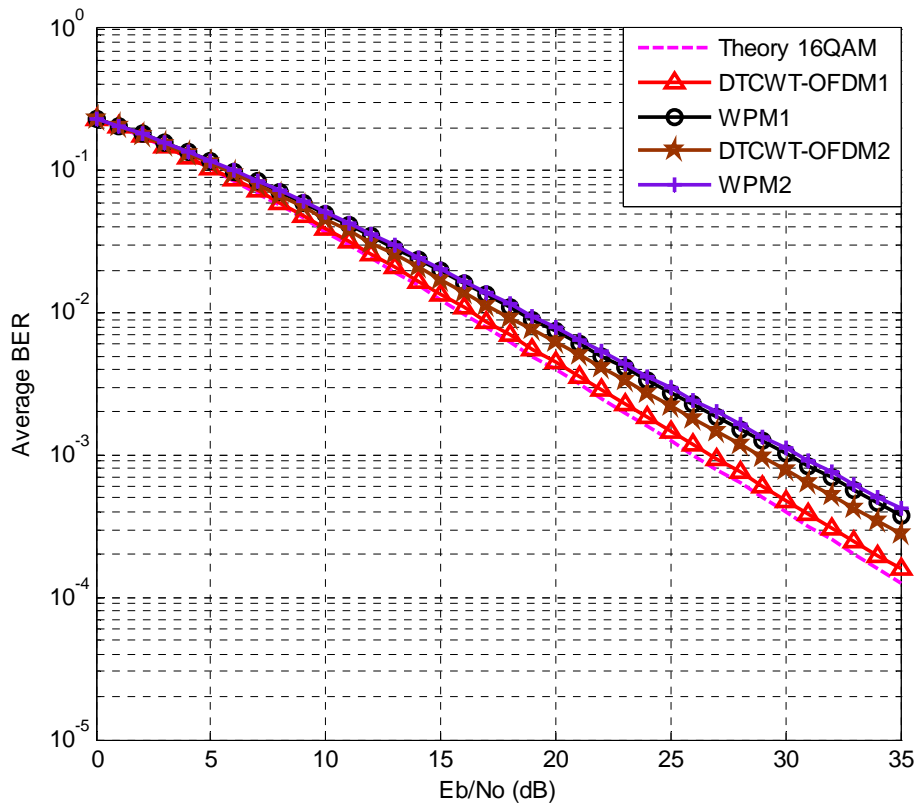


Figure 4.25 BER performance of the DTCWT-OFDM using 16-QAM in frequency selective channel.

This experiment is repeating again using 16-QAM and the results are shown in Fig. 4.25. Again DTCWT-OFDM1 and WPM1 represent the DTCWT based OFDM and WPM systems respectively, in the presence of the 2-tap delay. DTCWT-OFDM2 and WPM2 represent the DTCWT based OFDM and WPM systems respectively, in the presence of the 26-tap delay.

The above results are compared to the BER curves of the theoretical BPSK and 16-QAM in Fig 4.24 and Fig. 4.25 respectively. From the results in Fig. 4.24 and Fig. 4.25 when using 2 tap delay, the BER performance of the DTCWT-OFDM system is close to the theoretical BPSK and 16-QAM respectively. Because when we used tap delay less than filter length the system will be shift-invariance. However, when using 26-tap delay, the DTCWT-OFDM system is no longer shift-invariance systems and this implies the degradation to the BER performance.

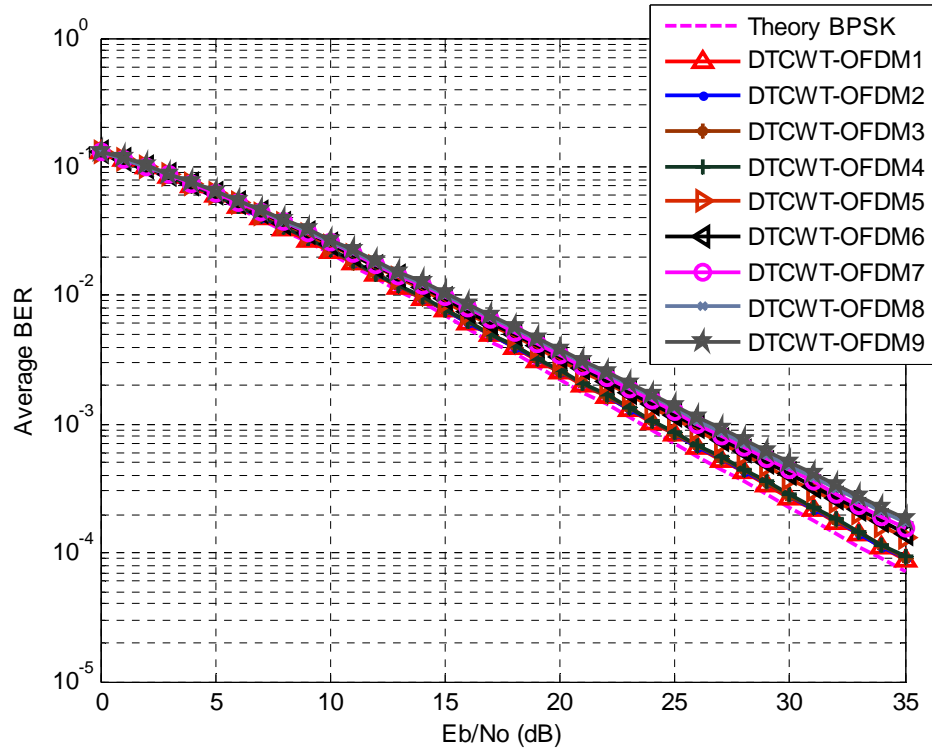


Figure 4.26 BER performance of the DTCWT-OFDM using BPSK with different values of the tap delay.

Finally, the above experiment is repeated again using n -SYM- b with q -SH- d filters with different values of tap delay (2, 5, 7, 10, 13, 17, 20, 23 and 26) and the results are shown in Fig. 4.26 when signaling with BPSK and in Fig. 4.27 when signaling with 16-QAM. In these figures, DTCWT-OFDM label from 1-9 represent the proposed system when using 2, 5, 7, 10, 13, 17, 20, 23 and 26 tap delay, respectively. From these results we can deduced that, when using tap delay less than or equal to the length of filter i.e., 2, 5, 7, 10 and 13 the BER performance of the system is close to theoretical BPSK. However, when using tap delay longer than the filter length i.e., 17, 20, 23 and 26 the BER performance is degrade.

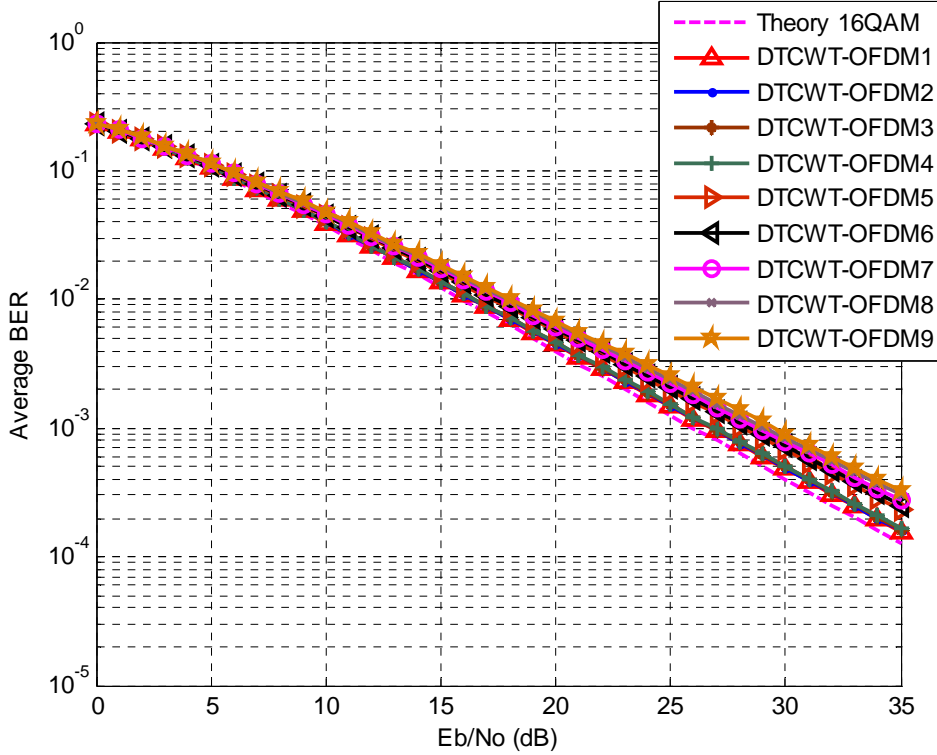


Figure 4.27 BER performance of the DTCWT-OFDM using 16-QAM with different values of the tap delay.

4.6 Complexity Analysis

Computational complexity is an important design issue for multicarrier systems. Due to the high data rates required in modern applications, low complexity is imperative. From the computational burden point of view, this section reports the implementation complexity of the FFT, DWT, WPT, and DTCWT. In fact, the structure of a DTCWT based OFDM system is very similar to that of FFT and WPT based OFDM system.

As the complexity measure, the total number of complex multiplication is considered. For the DFT based multicarrier system, efficient implementation can be developed using FFT, i.e., the FFT is an algorithm that takes advantage of special form of the matrix to reduce the N^2 computational complexity that required by DFT to $N \log_2 N$, where N is the rank of the transform, or the number of subcarriers. i.e., the complexity of FFT is given by

$$C_{FFT} = O(N \log_2 N) \quad (4.1)$$

where $O(N)$ denotes linear complexity. A rough estimate of the WPT gives a complexity of order $O(N \log_2 N)$ thus of similar order to what is required for FFT. Hence, the complexity of WPT is

$$C_{WPT} = O(N \log_2 N) \quad (4.2)$$

While the computational complexity for DWT is given by

$$C_{DWT} = O(N) \quad (4.3)$$

Since the DT-CWT use two DWT (upper and lower parts), the computational complexity for DT-CWT is given by

$$C_{DT-CWT} = O(2N) \quad (4.4)$$

In general, the computational complexity of the WPT is on the same order of that required by the FFT. The complexity of the DT-CWT is in less order comparing by the complexity of FFT and WPT, which means that, the proposed system is more efficient time wise.

We note that the complexity of the considered systems increases according to the number of subcarriers N .

Therefore, it can be concluded that the proposed system is computationally more efficient comparing with the conventional OFDM and WPM systems.

CHAPTER 5

CONCLUSION AND FUTURE WORK

The main focus of this dissertation has been to design a novel OFDM system based on dual-tree complex wavelet transform (DTCWT). The contributions of this dissertation are summarized in section 5.1, and possible future work based on the results from this research is suggested in section 5.2.

5.1 Dissertation Summary and Contributions

This work has used the dual-tree complex wavelet transform (DTCWT) to design a new OFDM system. The feasibility of the proposed OFDM system is theoretically examined and then different performance-metrics have been investigated to prove the usefulness of the proposed system. Specifically, the following performance-metrics are studied. First, the PAPR of the proposed system is studied. It was demonstrated via the peak envelop and the CCDF of the transmitted signal that the proposed system gives better PAPR results than the conventional OFDM and WPM systems. The PAPR of the proposed system increases with the number of the subcarriers as do the other two systems. The PAPR results also show that the best PAPR results are obtained by using longer filters in both the WPM and DTCWT-OFDM systems.

Next, the PSD results were obtained and it is shown that the proposed system has better spectrum characteristics in terms of lower out-of-band (OOB) attenuation (more suppression of OOB attenuation), than the conventional OFDM and the WPM systems. In the presence of the nonlinear HPA, the proposed system requires lesser amount of input power back-off (IBO) as compared to those needed in the conventional OFDM and WPM systems, while, at the same time, the proposed system produces lesser amount of spectral re-growth compared to the other two systems.

Next, the BER performance in AWGN was investigated followed by average BER

performance in 10-tap Rayleigh channels as well. The simulation results of the BER and the average BER of the considered systems indicate that the performance of the considered system nearly matches the theoretical BER performance of both BPSK and 16-QAM modulation in the absence of the nonlinear HPA. This is particularly true when longer filters are used in the design of the WPM and DTCWT-OFDM systems. However, in the presence of the nonlinear HPA, the results show that the proposed system performs better than the OFDM and WPM systems.

Further, a study was conducted to investigate the usefulness of the shift-invariance property of the DTCWT. Since WPT is not shift-invariant, it was proposed to use a 2-path frequency-selective wireless channel through which the transmitted signal and its copy reach the receiver. WPT based WPM was expected to produce different WPT coefficients and hence the average BER was expected higher than that of DTCWT based system where magnitude of DTCWT coefficients do not change for different delay spreads. The DTCWT based OFDM system indeed has better average BER performance than WPM system. Table 5.1 gives the comparison of DTCWT-OFDM, WPM and the conventional OFDM systems.

Finally, it was shown that the proposed system is computationally more efficient compared to the conventional OFDM and WPM systems as far as number of operations are involved. However, the disadvantages of the proposed system can be seen in the frequency-selective channel specially when using tap delay longer than the filters length. In this case the proposed system is no longer shift-invariance and this implies the degradation to the BER performance.

To overcome this problem, the one possible way is to use filter length less than or equal to the tap delay of the frequency-selective channel. This implies increasing the computational complexity of the proposed system. Since the computational complexity of the proposed system is increase with increasing the length of filters, thus; for high values of the tap delay the computational complexity of the proposed system will increase accordingly.

Table 5.1 Comparison of DTCWT-OFDM, WPM and the conventional OFDM systems.

System Case	DTCWT-OFDM	WPM	OFDM
Peak envelope	Low	High	High
PAPR	Low	High	Very high
Side lobes suppression	Very high	High	Low
Out of band attenuation	Very high	High	Less
Spectrum re-growth	Low	Very low	High
Required amount of IBO	Low	Average	High
BER as comparing to theoretical	Confirm	Confirm	Confirm
BER (in HPA)	Better	Bad	Very bad
Computational Complexity	Low	High	High

Over all, the performance results of the DTCWT based OFDM over the conventional OFDM and WPM systems lead us to conclude that the proposed system is a viable alternative to conventional OFDM and WPM systems and it should be considered in future wireless communication systems.

5.2 Future Work

There are many possibilities of the future work in this area. Some of these suggestions for future works are listed as follows:

- The study of the proposed system can be extended to develop an end-to-end air interface design for the proposed system.
- The synchronization techniques, both the timing and frequency synchronization in the proposed system based on DTCWT could also be an area that should be addressed.
- Channel estimation technique in the proposed system based on DTCWT needs to be more thoroughly investigated.

- ❏ The effects of the multiple transmit and receive antennas on the DTCWT-OFDM can also be explored.
- ❏ The PAPR reduction techniques can also be tested in this system in order to give still better PAPR reduction results.

Clearly, there are many possibilities for the future work in proposed system, and the OFDM based on wavelet open many research possibilities for the further improving OFDM system performance.

PUBLICATIONS

So far, based on this work we have the following publications:

Conference Papers

1. Mohamed H. M. Nerma, Nidal S. Kamel and Varun Jeoti, “OFDM Based on Complex wavelet Transform” in National Postgraduate Conference on Engineering, Science & Technology (NPC 2008), Postgraduate Studies Office, Universiti Teknologi PETRONAS, Bandar Seri Iskandar, 31750 Tronoh, Perak, Malaysia. March 31, 2008.
2. Mohamed H. M. Nerma, Nidal S. Kamel and Varun Jeoti, “PAPR Analysis for OFDM Based on DTCWT” in Student Conference on Research and Development (SCORED 2008), Johor, Malaysia: 26-27 Nov. 2008.
3. Mohamed H. M. Nerma, Nidal S. Kamel and Varun Jeoti, “On DTCWT Based OFDM: PAPR Analysis” in proceeding of 7th International work shop on Multi-Carrier Systems & Solutions MC-SS 2009, vol. 41, Herrsching, Germany: pp. 207-217, May 2009.
4. Mohamed H. M. Nerma, Nidal S. Kamel and Varun Jeoti, “BER Performance Analysis of OFDM System Based on Dual-Tree Complex Wavelet Transform in AWGN Channel” in 8th WSEAS International Conference on SIGNAL PROCESSING (SIP '09), Istanbul, Turkey: May 30 - June 1, 2009.
5. Mohamed H. M. Nerma, Varun Jeoti and Nidal S. Kamel, “The Effects of HPA on OFDM System Based on Dual – Tree Complex Wavelet Transform (DTCWT)” submitted to the in International Conference on Intelligent & Advance Systems (ICIAS 2010).

Journal Papers

1. Mohamed H. M. Nerma, Nidal S. Kamel and Varun Jeoti, “An OFDM System Based on Dual-Tree Complex Wavelet Transform (DTCWT)” Journal: Signal Processing: An International Journal, Volume: 3, Issue: 2, Pages: 14-21, May 2009.

2. Mohamed H. M. Nerma, Nidal S. Kamel and Varun Jeoti, “Performance Analysis of a Novel OFDM System Based on Dual-Tree Complex Wavelet Transform” Ubicc Journal, Volume 4 No. 4, 15 August 2009.
3. The WSEAS paper “BER Performance Analysis of OFDM System Based on Dual-Tree Complex Wavelet Transform in AWGN Channel” is also chosen to be published in journals of the WSEAS or NAUN

Book Chapters

1. Mohamed H. M. Nerma, Nidal S. Kamel and Varun Jeoti, “On DTCWT Based OFDM: PAPR Analysis” Book Chapter, Lecture Notes Electrical Engineering, Multi-Carrier Systems & Solutions 2009, vol. 41, pp. 207-217, Springer Netherlands, April 2009.

BIBLIOGRAPHY

1. B. Li, Y. Qin, C. P. Low, and C. L. Gwee, *A survey on mobile wimax wireless broadband acces*]. Communication Magazine, IEEE. 45(12): p. 70-75, December 2007.
2. O. Ileri and N. Mandayam, *Dynamic spectrum access models: toward an engineering perspective in the spectrum debate*. Communication Magazine, IEEE. 46(1): p. 153-160, January 2008.
3. D. Estrin, D. Culler, K. Pister, and G. Sukhatme, *Connecting the physical world with pervasive networks*. IEEE Pervasive Computing. 1: p. 59-69, 2002.
4. D. Cox, *Wireless Personal Communications: A Perspective*. S. Suthersan, Ed. Boca Raton: CRC Press LLC, 1999.
5. D. Hatfield. *Perspectives on the next generation of communications*. [Online]. Available: http://www.fcc.gov/oet/speeches/perspec_next_generation.doc. remarks before the Vehicular Technology Conference Fall 2000, (Accessed October 2007).
6. J. Burns, *Measuring spectrum efficiency – the art of spectrum utilization metrics*, in *IEEE Two Day Conference. Getting the Most Out of the Radio Spectrum*: London, UK. 1: Oct. 2002.
7. M. K. Lakshmanan and H. Nikookar, *A review of wavelets for digital wireless communications*. Wireless Personal Communications. 37, No. 3-4: p. 387-420, May 2006.
8. IEEE, *Proceedings of the IEEE, Special Issue on Wavelets*, . Apr. 1996.
9. P. Addison, *The Illustrated Wavelet Transform Handbook*, ed. London: Institute of Physical Publishing. 2002.
10. S. Haykin, *Cognitive Radio: Brain-empowered wireless communications*. IEEE J. Select. Area Commun. 23(2): p. 201-220, Feb. 2005.
11. M. Gautier, and J. Lienard. *Performance of Complex Wavelet Packet Based Multicarrier Transmission through Double Dispersive channel*. in *Proceedings of the 7th IEEE Nordic Signal Processing Symposium NORSIG'06*. 2006.
12. M. Wickerhauser, *Adapted Wavelet Analysis from Theory to Software*. 1994: Wellesley Massachusetts: A K Peters, 1994.
13. A. Jamin and P. Mahonen, *Wavelet Packet Modulation for wireless communications*. Wireless Comm. and Mobile Journal. 5, Issue 2(2): p. 123-137, March 2005.
14. S. B. Weinstein, and P. M. Ebert, *Data transmission by frequency division multiplexing using discrete Fourier transform*. IEEE Transactions on Communication Technology. Com-19: p. 628-634, October 1971.
15. A. Peled, and A. Ruiz, *Frequency domain data transmission using reduced complexity algorithms*, in *IEEE International Conference Acoustics, Speech, Signal Processing ICASSP '80,(Denver, CO)*. p. 964-967, 1980.
16. L. J. Cimini, Jr., , *Analysis and Simulation of a Digital Mobile Channel Using*

- Orthogonal Frequency Division Multiplexing*. IEEE Transactions on Communication. COM-33, No.7: p. 665-675, July 1985.
17. Selesnick, I.W., *The Double Density Dual Tree DWT*. IEEE Transactions on Signal Processing. 52, No. 5(5): p. 1304-1315, Mai 2004.
 18. Lina, J.M., *Complex Daubechies Wavelets: Filter Design and Applications*, in *ISAAC Conference*: June 1997.
 19. Mohamed H. M. Nerma, Nidal S. Kamel and varun Jeoti, *OFDM Based on Complex wavelet Transform*, in *National Postgraduate Conference on Engineering, Science & Technology (NPC 2008)*,: Postgraduate Studies Office, Universiti Teknologi PETRONAS, Bandar Seri Iskandar, 31750 Tronoh, Perak, Malaysia. March 31, 2008.
 20. R.V. Nee, and R. Prasad, *OFDM for Wireless Multimedia Communications*: House Publishers, 2000.
 21. M. Baro, and J. Ilow, *PAPR Reduction in Wavelet Packet Modulation Using Tree Pruning*, in *IEEE 65th Vehicular Technology Conference, VTC'07-Spring*. p. 1756-1760. April 2007.
 22. M. Baro, and J. Ilow, *Improved PAPR Reduction for Wavelet Packet Modulation Using Multipass Tree Pruning*, in *IEEE 18th International Symposium on Personal, Indoor and Mobile Radio Communication. PIMRC 2007*. p. 1-5, Sept. 2007.
 23. M. Baro, and J. Ilow, *PAPR Reduction in OFDM Using Wavelet Packet pre-processing*, in *5th IEEE Consumer Communications and Networking Conference, CCNC 2008*. p. 195-199, Jan. 2008.
 24. J.W. Cooley, and J.W. Tukey, *An Algorithm for the Machine Calculation of Complex Fourier Series*. Math. Computation. 19: p. 297-301, 1965.
 25. IEEE Std 802.16-2004, *Air interface for fixed broadband wireless access systems*. June 2004.
 26. A. Bahai, and B. Saltzberg, *Multi-Carrier Digital Communication, Theory and Applications of OFDM*, New York: Kluwer Academic, 1999.
 27. B. L. Floch, M. Alard, and C. Berrou, *Coded orthogonal frequency division multiplex*, in *Proc. IEEE*. p. 982-996, June 1995.
 28. M. Ardakani, T. Esmailian, and F. R. Kschischang, *Near-capacity coding in multicarrier modulation systems*, in *IEEE Trans. Commun.*, . p. 1880-1889, Nov. 2004.
 29. M. Rahman, S. Das, and F. Fitzek, *OFDM based WLAN systems*: Technical Report, Aalborg University, Denmark, February 2005.
 30. Rohling M., May T., Bruninghaus K., and Grunheid R., *Broadband OFDM radio transmission for multimedia applications*, in *proceedings of the IEEE*. p. 1778-1789, Oct 1999.
 31. John A. C. Bingham, *Multicarrier Modulation for Data Transmission: An Idea Whose Time Has Come*, in *IEEE Communications Magazine*. p. 5-14, May 1990.
 32. H. Sari, G. Karam, and I. Jeanclaude, *Transmission techniques for digital terrestrial TV broadcasting*, in *IEEE Communications Magazine*. p. 100-109,

- Feb. 1995.
33. Cioffi, J.M., *A multicarrier primer*: “<http://www.stanford.edu/group/cioffi/documents/multicarrier.pdf>”, last accessed on 15 May 2007.
 34. IEEE Std 802.11a-1999 (R2003), *Part 11: Wireless LAN Medium Access Control (MAC) and Physical Layer (PHY) specifications: High speed Physical Layer in the 5 GHz Band*. June 2003.
 35. IEEE Std 802.11g, *Part 11: Wireless LAN Medium Access Control (MAC) and Physical Layer (PHY) specifications Amendment 4: Further Higher Data Rate Extension in the 2.4 GHz Band*. June 2003.
 36. ETSI TS 101 475, *Broadband Radio Access Networks (BRAN); HIPERLAN Type 2; Physical (PHY) layer*. April 2000.
 37. Amara Graps, *An Introduction to Wavelets*. IEEE Computational Science and Engineering 2, No. 2(2): p. 50-61, Summer 1995.
 38. Martin Vetterli and Jelena Kovacevic, *Wavelets and Subband Coding*. 1995: Prentice-Hall PTR, New Jersey. 1995.
 39. Ramjee Prasad, *OFDM for Wireless Communication Systems*, Artech House: Boston, USA. p. 117-147, 2004.
 40. Proakis, J.G., *Digital Communications*: 4th Ed., McGraw-Hill, New York, USA, 2003.
 41. Y. J. Guo, *Advances in Mobile Radio Access Networks*. Artech House Publishers, 2004.
 42. Prasad, H.N.A.R. *Wave shaping of Multicarrier Signal for data Transmission over Wireless Channels*. in *IEEE 6th International Conference on Universal Personal Communications Record (ICUPC)*. October 1997.
 43. Prasad, H.N.A.R., *Optimal Waveform Design for Multicarrier Transmission through a Multipath Channel*, in *Proceedings of the IEEE Vehi. Tech. Conf. (VTC)*. May 1997.
 44. . IEEE Broadband Wireless Standard 802.16.3.
 45. S. Mallat, *Multiresolution approximations and wavelet orthonormal bases of L^2* . Transactions on American Math. Society. 315: p. 69-87, June 1989.
 46. Y. Meyer. *Wavelet and applications*. in *Proceeding of the International Conference Marseille*. France, springer Verlag 1992, May 1989.
 47. I. Daubechies, *Ten lectures on wavelets*. SIAM, CBMS Series, April 1992.
 48. C. S. Burrus, R. A. Gopinath, and H. Guo *Introduction to Wavelet and Wavelet Transform: A Primer*, New Jersey: Prentice Hall, 1998.
 49. Mallat, S., *A Wavelet Tour of Signal Processing*, Massachusetts: Academic Press, 1997.
 50. A. R. Lindsey, and J. C. Dill. *Wavelet Packet Modulation: A Generalized Method for Orthogonal Multiplexed Communication*. in *Proceedings of IEEE the 27th Southeastern Symposium*. pp. 392-396. Mar 1995.
 51. D. Daly, C. Heneghan, A. Fagan and M. vetterli. *Optimal Wavelet Packet Modulation under Finite Complexity Constraint*. in *proceeding of IEEE ICASSP'02*. vol. 3, pp. III-2789-III-2792, 2002
 52. R. Polikar, *The engineer's ultimate guide to wavelet analysis*, available at

- [http:// users.rowan.edu/polikar/WAVELETS/WTtutorial.html](http://users.rowan.edu/polikar/WAVELETS/WTtutorial.html).
53. S. D. Sandberg, and M. A. Tzannes, *Overlapped Discrete Multitone Modulation for High Speed Copper Wire Communications*. IEEE Journal on selected Areas in Communications. 13, No. 9: p. 1571-1585, December 1995.
 54. Anthony Teolis, *Computational Signal Processing with Wavelets*, Birkhauser, Boston, USA, 1998.
 55. M. L. Doelz, E. T. Heald, D. L. Martin,. *Binary Data Transmission Technique for Linear systems*. in *Proceeding of IRE*. Vol. 45, pp. 656 - 661, May 1957.
 56. P. A. Bello, *Selective fading limitations of the Kathryn modem and some system design considerations*, in *IEEE Transactions on Communications Technology*: Vol. con-13, pp. 320-333, Sept. 1965.
 57. R. W. Chang, *Synthesis of Band-limited Orthogonal Signals for Multichannel Data Transmission*. Bell Systems Technology Journal. 45: p. 1775-1796, Dec. 1966.
 58. M. Zimmerman, and A. Kirsch, *the AN/GSC-10 (Kathryn) variable rate data modem for HF radio*, in *IEEE Transactions on Communications Technology*: Vol. com-16, pp. 197-205, April 1967.
 59. J. A. C. Bingham, *Multicarrier Modulation for Data Transmission: An Idea Whose Time Has Come*, in *IEEE Communications Magazine*: pp. 5-14, May 1990.
 60. B. R. Saltzberg, *Performance of an efficient parallel data transmission system*, in *IEEE Transactions on Communications*: vol. COMM-15, pp. 805-811, Dec. 1967.
 61. H. Steendam, and M. Moeneclaey, *Analysis and optimization of the Performance of OFDM on Frequency-selective Time-selective Fading Channels*. IEEE Transactions on Communication. 51(12): p. 1811-1819, December 1999.
 62. Y. H. Kim, I. Song, and H. G. Kim, *Performance Analysis of a Coded OFDM System in Time-Varying Multipath rayleigh Channels*. IEEE Transactions on Vehicular Technology. 48(5): p. 1610-1615, sep. 1999.
 63. N. Erdol, F. Bao, and Z. Chen, *Wavelet modulation: a prototype for digital communication systems*, in *IEEE Southcon Conference*. p. 168-171, 1995.
 64. Lindsey, A.R., *Wavelet Packet Modulation for Orthogonally Multiplexed communication*, in *IEEE Transactions on Signal Processing*. May 1997.
 65. G. W. Wornell. *Emerging Applications of Multirate signal Processing and Wavelets in Digital Communications*. in *Proceeding of the IEEE*. Vol. 84, No. 4, pp. 586-603, April 1996.
 66. M. Vettereli, and C. Herley, *Wavelets and Filter Banks: Theory and Design*, in *IEEE Transactions on Signal Processing*: Vol. 40, No. 9, pp. 2207 - 2232, Sept. 1992.
 67. H. W. Newlin. *Developments in the use of wavelets in communication systems*. in *Proceeding of IEEE Millennium Commun. Conf. MILCOM '98*. Bedford, Massachusetts, USA, vol. 1, pp. 343-349, October 1998
 68. M. A. Tzannes, M. C. Tzannes, J. Proakis and P. N. Heller. *DMT Systems*,

- DWMT Systems and Digital Filter Banks*. in *proceeding of IEEE ICC'94*. pp. 311-315, 1994.
69. W. Yang, G. Bi and T. P. Yum *A Multirate Wireless Transmission System Using Wavelet Packet Modulation*. Vehicular Technology Conference, IEEE 47th Volume, 368-372, Mar 1997
 70. M. Sablatash, T. Cooklev and J. Lodge. *Design and Implementation of Wavelet Packet Based Filter Bank Trees for Multiple Access communications*. in *IEEE International Conference on Communications, ICC '97*. vol. 1, Issue 8-12, pp. 176-181, June 1997.
 71. A. N. Akansu, and X. Lin, *A Comparative Performance Evaluation of DMT (OFDM) and DWMT (DSBMT) Based DSL Communications Systems for Single and Multitone interference*, in *Proceeding of the IEEE ICASSP*. p. 3269-3272. May 1998.
 72. K. M. wong, J. Wu, T. N. Davidson, Q. Jin and P. C. Ching, *Performance of Wavelet Packet Division Multiplexing in Impulsive and Gaussian Noise*, in *IEEE Transactions on Communications*. p. 1083-1086, June 2000.
 73. C. V. Bouwel, J. Potemans, S. Schepers, B. Nauwelaers and A. V. Capelle, *Wavelet Packet Based Multicarrier Modulation*, in *IEEE Symposium on Communications and Vehicular Technology, SCVT-200*. p. 131-138, 19 Oct. 2000.
 74. M. J. Manglani, and A. E. Bell. *Wavelet Modulation Performance in Gaussian and Rayleigh Fading Channel*. in *IEEE MILCOM 2001*. vol. 2, pp. 845-849, 2001
 75. W. Kozek, G. Pfander, J. ungermann, and G. zimmermann, *A comparison of Various MCM Schemes*, in *5th International OFDM-Workshop Hamburg*, Germany, 2000.
 76. H. Zhang, D. Yuan, M. Jiang and D. Wu,. *Research of DFT-OFDM and DWT-OFDM on Different Transmission scenarios*. in *Proceedings of 2nd Interenational Conference on Infromation Technology and Applications ICITA, 2004*
 77. M. C. Sun and D. P. K. Lun. *Power-Line Communications Using DWMT Modulation*. in *IEEE International Symposium on Circuits and Systems, ISCAS 2002*.
 78. V. C. Doux, J. Lienard, B. Conq and P. Gallay. *Efficient Implementation of Discrete Wavelet Multitone in DSL Communications*. in *IEEE EC-VIP-MC2003, 4th EURASIP Conference focused on Video/Image Processing and Multimedia Communications*. vol. 1, Issue 2-5, pp. 393-398, July 2003
 79. Z. Feng, Y. Dongfeng and Z. Haixia, *Research of Wavelet Based Multicarrier Modulation System with Woven Convolutional Codes*, in *IEEE International Conference on Communication Technology, ICCT '06*. p. 1-4, Nov. 2006.
 80. H. Zhang, D. Yuan, M. Jiang and D. Wu, . *Performance Comparison of WOFDM with Different Coding Schemes*. in *Proceedings of IEEE Radio and Wireless Conference, RAWCON'03*. pp. 59-62, Aug. 2003.
 81. E. Okamoto, Y. Iwanami and T. Ikegami, *Multimode Transmission Using*

- Wavelet Packet Modulation and OFDM*, in *IEEE 58th Vehicular Technology Conference, VTC 2003-Fall*. p. 1458-1462, Oct. 2003.
82. M. Charina, K. Jetter, A. Kehrein, G. E. Pfander and G. Zimmermann, *ISI/ICI Comparison of DMT and Wavelet Based MCM Schemes for Time-Invariant Channels*, in *J. Speidel (ed.), Neue Kommunikationsanwendungen in modernen Netzen ITG-Fachbericht*,. p. 109-115, Berlin 2002.
 83. H. Koga, N. Kodama and T. Konishi, *High-speed Power Line Communication System Based on wavelet OFDM*. in *proceeding of 7th International Symposium on PLC and its Applications*, Kyoto, Japan, March 2003.
 84. M. You and J. Ilow, *A Multi-Wavelet Packet Modulation in Wireless Communications*, in *Canadian Conference on Electrical and Computer Engineering*. p. 2367-2370, May 2004
 85. M. You and J. Ilow, *An Application of Multi-Wavelet Packet in Digital communications*, in *Proceedings of the 2nd Annual Conference on Communication Network and Services research CNSR'04*. p. 10-18, May 2004.
 86. F. Zhao, H. Zhang and D. Yuan, , *Performance of COFDM with Different Orthogonal Bases on AWGN and Frequency selective channel*, in *Proceedings of the IEEE 6th CAS Symp. on Emerging Technologies: IEEE 6th CAS Symp. on Emerging Technologies: Mobile and Wireless Comm*. p. 473- 475, June 2004.
 87. K. Anwar, A. U. Priantoro, M. Saito, T. Hara, M. Okada and H. Yamamoto, , *On the PAPR Reduction for Wavelet Based transmultiplexer*, in *Proceeding of the IEEE International Symp., on Comm. and Information Technology, ISCIT'04*. p. 812-815, Oct. 2004.
 88. A. B. Aicha, F. Tlili and S. B. Jebara. *PAPR analysis and reduction in WPDM Systems*. in *1st International Symposium on Control, Communications and Signal Processing*. pp. 315- 318, 2004.
 89. S. Baig, F. Rehman and M. J. Mughal. *Performance Comparison of DFT, Discrete Wavelet Packet and Wavelet Transforms in an OFDM Transceiver for Multipath Fading Channel*. in *9th International Multitopic Conference, IEEE INMIC'05*. pp. 1-6, Dec. 2005.
 90. H. Sakakibara, E. Okamoto and Y. Iwanami. *A wavelet Packet Modulation Method for Satellite communications*. in *IEEE Region 10 TENCON'05*. pp. 1-5, Nov. 2005.
 91. J. Abad, L. M. Torres and J. C. Riveiro, *OFDM and Wavelets Performance Comparison in Power Line Channels*, in *IEEE International Symposium on Power Line Communications and Its Applications*. p. 341-345, April 2005.
 92. S. Y. Ameen, and W. A. H. Hadi, *Investigation of using Turbo code to improve the Performance of DWT-OFDM System over Selective Fading Channel*, in *Proceeding of IEEE 2nd Information and Communication Technologies, ICTTA '06*. p. 2365-2369, 2006.
 93. M. Gautier, M. Arndt and J. Lienard, *Efficient wavelet Packet Modulation for Wireless communication*. in *The Third Advanced International Conference on*

- Telecommunications, AICT 2007.*
94. K. Izumi, D. Umehara and S. Denno, *Performance Evaluation of Wavelet OFDM Using ASCET*. in *IEEE International Symposium on Power Line Communications and Its Applications. ISPLC'07*. pp. 246-251, March 2007.
 95. S. Maki, E. Okamoto and Y. Iwanami. *Performance Improvement of Haar-based Wavelet Packet Modulation in Multipath fading Environment*. in *IEEE International Symposium on Communications and Information Technologies, ISCIT*. pp. 1021-1026, Oct. 2007.
 96. S. Xu, R. Luo, H. Yang and H. Wang, *The Spectral Efficiency and Anti-interference of Multiwavelet Packet-based OFDM*, in *ISAST Transactions on Comm. And Networking*: vol. 1, No. 1, 2007.
 97. S. Galli, H. Koga and N. Kodama, *Advanced Signal Processing for PLCs: Wavelet-OFDM*, in *IEEE International Symposium on Power Line Communications and Its Applications, ISPLC'08*. p. 187-192, April 2008.
 98. D. Gupta, V. B. Vats and K. K. Garg, *Performance Analysis of DFT-OFDM, DCT-OFDM, and DWT-OFDM Systems in AWGN Channel*, in *The Fourth International Conference on Wireless and Mobile Communications, ICWMC'08*. p. 214-216, Aug. 2008.
 99. V. Kumbasar, and O. Kucur, *Better Wavelet Packet Tree structures for PAPR reduction in WOFDM Systems*. *Digital signal Processing*. 18, Issue 6(6): p. 885-891, Nov. 2008.
 100. T. K. Adhikary, and V. U. Reddy, *Complex Wavelet Packets for Multicarrier Modulation*, in *Proceeding of the IEEE ICASSP*. p. 1821-1824, May 1998.
 101. X. Zhang and G. Bi, *OFDM Based on Complex Orthogonal Wavelet Packet*, in *12th IEEE International Symposium on Personal Indoor and Mobile Radio Communications*. p. E-99-E-104, 2001.
 102. Y. Wang and X. Zhang. *Design of M-band complex-valued filter banks for multicarrier transmission over multipath wireless channels*. in *IEEE International Conference on Acoustics, Speech, and Signal Processing (ICASSP'03)*. Vol. 4, PP. IV-556 - IV-559, April 2003
 103. X. Yu, and G. Bi. *Performance of Complex Orthogonal Wavelet Packet Based MC-CDMA System with Space-time Coding over Rayleigh Fading Channel*. in *IITA International Conference on Control, Automation and System Engineering*. 11 -12 July 2009. pp. 136-139, 2009.
 104. C. J. Mtika, and R. Nunna, , *A wavelet-based multicarrier modulation scheme*, in *Proceedings of the 40th Midwest Symposium on Circuits and Systems*. p. 869-872, August 1997.
 105. N.G. Kingsbury, *The dual-tree complex wavelet transform: A new technique for shift invariance and directional filters*, in *Proc. 8th IEEE DSP Workshop: Utah*, paper no. 86, Aug. 9–12, 1998
 106. Ivan W. Selesnick, Richard G. Baraniuk, and Nick G. Kingsbury, *The Dual-Tree Complex Wavelet Transform*, in *IEEE Signal Processing Mag.* p. 1053-5888, Nov. 2005.
 107. N.G. Kingsbury, *Image processing with complex wavelets*. *Philos. Trans. R.*

- Soc. London A, Math. Phys. Sci. 357, No. 1760: p. 2543-2560, Sept. 1999.
108. N.G. Kingsbury, *A dual-tree complex wavelet transform with improved orthogonality and symmetry properties*, in *Proc. IEEE Int. Conf. Image Processing, Vancouver, BC, Canada*. p. 375-378, Sept. 10-13, 2000.
 109. N.G. Kingsbury, *Complex wavelets for shift invariant analysis and filtering of signals*. Appl. Comput. Harmon. Anal. 10, No. 3: p. 234-253, May 2001.
 110. P.L. Dragotti, and M. Vetterli, *Wavelet footprints: Theory, algorithms, and applications*. IEEE Trans. Signal Processing. 51, No. 5: p. 1306-1323, May 2003.
 111. N.G. Kingsbury, and J.F.A. Magarey, *Wavelet transforms in image processing*, in *Proc. 1st European Conf. Signal Anal. Prediction*,: Prague. p. 23-34, June 24-27, 1997.
 112. J. Romberg, H. Choi, R.G. Baraniuk, and N.G. Kingbury, *Multiscale classification using complex wavelets and hidden Markov tree models*, in *Proc. IEEE Int. Conf. Image Processing*,: Vancouver, BC, Canada. p. 371-374, Sept. 10-13, 2000.
 113. J.K. Romberg, M. Wakin, H. Choi, N.G. Kingsbury, and R.G. Baraniuk, *A hidden Markov tree model for the complex wavelet transform*: Rice ECE, Tech. Rep., Sept. 2002
 114. H. Choi, J. Romberg, R.G. Baraniuk, and N. Kingsbury *Hidden Markov tree modeling of complex wavelet transforms*, in *Proc. IEEE Int. Conf. Acoust., Speech, Signal Processing (ICASSP)*. p. 133-136, June 5-9, 2000.
 115. M. Lang, H. Guo, J.E. Odegard, C.S. Burrus, and R.O. Wells, Jr., *Noise reduction using an undecimated discrete wavelet transform*. IEEE Signal Processing Lett. 3, No. 1: p. 10-12, Jan. 1996.
 116. E.P. Simoncelli, W.T. Freeman, E.H. Adelson, and D.J. Heeger, *Shiftable multi-scale transforms*, in *IEEE Trans. Inform. Theory*. p. 587-607, Mar. 1992.
 117. R. Van Nee and A. De Wild, *reduction the peak-to average power ratio of OFDM*, in *48th IEEE Vehicular Technology Conference*, IEEE New York, USA: Ottawa, Canada. p. 2072-2076, May 18-21, 1998.
 118. I W. Selenick, *Hilbert transform pairs of wavelet bases*, in *IEEE Signal Processing Lett*. p. 170-173, June 2001.
 119. H. Ochiai and H. Imai, *On the distribution of the peak-to-average power ratio in OFDM signals*, in *IEEE Trans. Commun*. p. 282-289, 2001.
 120. S. wei, D. L. Goeckel, and P. E. Kelly *A modern extreme value theory approach to calculate the distribution of the peak-to-average power ratio in OFDM systems*, in *IEEE International Conference on Communications*, IEEE New York, USA: New York. p. 1686-1690, Apr. 28- May 2, 2002.
 121. H. Yu, M. Chen and G. wei *Distribution of PAPR in DMT systems*, in *Electron. Lett*. p. 799-801, 2003.
 122. R. Yu and H. Ozkaramanli, *Hilbert transform pairs of orthogonal wavelet bases: Necessary and sufficient conditions*. IEEE Trans. Signal Processing IEEE Transactions on Signal Processing. 53, No. 12: p. (82- 87), Dec. 2005.
 123. J.O. Chapa and R.M. Rao, *Algorithms for designing wavelets to match a*

- specified signal*. IEEE Trans. Signal Processing IEEE Transactions on Signal Processing. 48, No. 122: p. 3395-3406, Dec. 2000.
124. N. G. Kingsbury. *The dual-tree complex wavelet transform: a new efficient tool for image restoration and enhancement*. in *Proc. European Signal Processing Conf.* Rhodes: pp. 319 - 322, Sept. 1998.
 125. J. G. Proakis and M. Salehi, *Communication Systems Engineering*: 2nd ed. Upper Saddle River, NJ: Prentice-Hall, 2002.
 126. M. Pauli and H. P. Kuchenbecker. *On the reduction of the out-of-band radiation of OFDM signals*. in *ICC*. pp. 1304-1308, 1998.
 127. A. D. S. Jayalath and C. Tellambura. *Reducing the out-of-band radiation of OFDM using an extended guard interval*. in *Proc. VTC'01*. pp. 829-833, 2001.
 128. C. Liu and F. Li. *On spectrum modeling of OFDM signals for digital broadcasting*. in *Proc. ICSP'04*. pp. 1886-1889, 2004.
 129. H. Balshem, B.H., and H. J. Thaler. *Advanced RF Power Amplifiers for High Capacity digital Radio Systems*. in *Conf. Rec. GLOBECOM, Global Communication Conference*. pp. 28-33, 1987.
 130. Rapp, C. *Effects of HPA-nonlinearity on 4-DPSK-OFDM Signal, for Digital Sound Broadcasting Systems*. in *in Proc. ECSC'91, Liege, Belgium*. Oct. 1991.
 131. A. A. M. Saleh, *Frequency-independent and frequency-dependent nonlinear models of TWT amplifiers*, in *IEEE Trans. Commun.*: vol. COM-29, pp. 1715-1720, Nov. 1981.
 132. S. H. Han, and J. H. Lee, *An overview of peak-to-average power ratio reduction techniques for multicarrier transmission*. IEEE Wireless Communications. 12, No. 2: p. 56-65, 2005.
 133. C. Schurgers, and M. B. Srivastava, , *A systematic approach to peak-to-average power ratio n OFDM*, in *SPIE's 47th Annual Meeting*,: San Diego, CA. p. 454-464, July 2001.
 134. R. Rajbanshi, A. M. Wyglinski and G. J. Minden, . *Multicarrier Transceivers: Peak-to-average power ratio reduction*. in *WCNC08 proceedings*, IEEE Commun. Society, 2008.
 135. Blachman, N.M., *Bandpass nonlinearities*, in *IEEE Trans. Inform. Theory*. Apr. 1964.
 136. G. W. Wornell, and A. V. Oppenheim, *Wavelet-based representations for a class os self-similar signals with application to fractal modulation*, in *IEEE Transactions on Infromation theory*: vol. 38, no. 2, pp. 785-800, 1992.
 137. H. S. Ptasiniski, and R. D. Fellman. *Implementation and simulation of a fractal modulation communication system*. in *Proceeding of the IEEE SUPERCOMM/ICC*. vol. 3, pp. 1551-1555, 1994.
 138. H. Y. Dou, and G. G. Bi, *Optimal wavelet packet multicarrier modem technique*. Journal of China Institute of Communications: p. (95 -100), Vol. 21, No. 6, 2006.
 139. L. Zhou, J. Li, F. Li, and C. Chen, *OWDM system based on ML algorithm and blind identification in multipath fading channel*, in *IEEE Electronics Letters*. p. (66 - 69), 2004.

140. M. Yang, Z. Liu, and J. Dai,. *Frequency Selective Pilot Arrangement for Orthogonal Wavelet Packet Modulation Systems*. in *IEEE ICCSIT'08*. pp. 499 - 503, 2008.
141. <http://www-sigproc.eng.cam.ac.uk/~ngk/>.
142. Joint Technical Committee on Wireless Access, *Final Report on RF Channel Characterization*. JTC(AIR)/93.09.23-238R2, September 1993.
143. “Final Report on Link Level and System Level Channel Model”, IST-2003-507581 WINNER, D5.4 v 1.4, <https://www.ist-winner.org/>.
144. S. L. Linfoot, *A Study of Different Wavelets in Orthogonal Wavelet Division Multiplex for DVB-T*, in *IEEE Transaction on Consumer Electronics*, Vol. 54, No. 3, August 2008.
145. Mohamed H. M. Nerma, Nidal S. Kamel and varun Jeoti, *PAPR Analysis for OFDM Based on DT-CWT*, in *Student Conference on Research and Development (SCORED 2008)*,: Johor, Malaysia: 26-27 Nov. 2008.
146. Mohamed H. M. Nerma, Nidal S. Kamel and varun Jeoti, *An OFDM System Based on Dual Tree Complex Wavelet Transform (DT-CWT)*. Journal: *Signal Processing: An International Journal*. 3, Issue: 2: p. 14-21, May 2009.
147. Mohamed H. M. Nerma, Nidal S. Kamel and varun Jeoti, *On DT-CWT Based OFDM: PAPR Analysis*, in *Multi-Carrier Systems & Solutions 2009*, Springer Netherlands: Lecture Notes Electrical Engineering. p. 207-217, April 2009.
148. S. C. Thompson, J.G.P., and J. R. Zeidler. *The Effectiveness of Signal Clipping for PAPR and Total Degradation Reduction in OFDM Systems*. in *Global Telecommunication Conference (GLOBECOM '05)*. December 2005.
149. M. Gautier, C. Lereau, M. Arndt and J. Lienard, *PAPR analysis in wavelet packet modulation*, in *3rd International Symposium on Communications, Control and Signal Processing, ISCCSP08*. p. 799-803, 12-14 March 2008.
150. Mohamed H. M. Nerma, Nidal S. Kamel and varun Jeoti, *On DT-CWT Based OFDM: PAPR Analysis*, in *proceeding of 7th International workshop on Multi-Carrier Systems & Solutions MC-SS 2009*: Herrsching, Germany. p. 207-217, 05-06 May 2009.
151. Mohamed H. M. Nerma, Nidal S. Kamel and varun Jeoti, *BER Performance Analysis of OFDM System Based on Dual – Tree Complex Wavelet Transform in AWGN Channel*, in *8th WSEAS International Conference on SIGNAL PROCESSING (SIP '09)*, Istanbul, Turkey: May 30 - June 1, 2009.
152. Mohamed H. M. Nerma, Nidal S. Kamel and varun Jeoti, *Performance Analysis of a Novel OFDM System Based on Dual Tree Complex Wavelet Transform*. *Ubicc Journal* 4(No. 3): p. (813 - 822), August 2009.
153. Mohamed H. M. Nerma, Nidal S. Kamel and varun Jeoti, “BER Performance Analysis of OFDM System Based on Dual – Tree Complex Wavelet Transform in AWGN Channel” accepted in journals of the WSEAS.

APPENDIX A

MATLAB Function to Perform IDTCWT (1-D):

```
function Z = dtwaveifm(Yl,Yh,biort,qshift,gain_mask);

% Function to perform an n-level dual-tree complex wavelet (DTCWT)
% 1-D reconstruction.
%
% Z = dtwaveifm(Yl,Yh,biort,qshift,gain_mask);
%
% Yl -> The real lowpass subband from the final level
% Yh -> A cell array containing the complex highpass subband for
each level.
%
% biort -> 'antonini' => Antonini 9,7 tap filters.
%         'legall'   => LeGall 5,3 tap filters.
%         'near_sym_a' => Near-Symmetric 5,7 tap filters.
%         'near_sym_b' => Near-Symmetric 13,19 tap filters.
%
% qshift -> 'qshift_06' => Quarter Sample Shift Orthogonal (Q-
Shift) 10,10 tap filters,
%
%                 (only 6,6 non-zero taps).
%         'qshift_a' => Q-shift 10,10 tap filters,
%
%                 (with 10,10 non-zero taps, unlike
qshift_06).
%         'qshift_b' => Q-Shift 14,14 tap filters.
%         'qshift_c' => Q-Shift 16,16 tap filters.
%         'qshift_d' => Q-Shift 18,18 tap filters.
%
% gain_mask -> Gain to be applied to each subband.
%             gain_mask(l) is gain for wavelet subband at level
l.
%             If gain_mask(l) == 0, no computation is performed
for band (l).
%             Default gain_mask = ones(1,length(Yh)).
%
% Z -> Reconstructed real signal vector (or matrix).
%
%
% For example: Z = dtwaveifm(Yl,Yh,'near_sym_b','qshift_b');
% performs a reconstruction from Yl,Yh using the 13,19-tap filters
% for level 1 and the Q-shift 14-tap filters for levels >= 2.
%

a = length(Yh); % No of levels.
if nargin < 5, gain_mask = ones(1,a); end % Default gain_mask.

if isstr(biort) & isstr(qshift) %Check if the inputs are strings
    biort_exist = exist([biort '.mat']);
```

```

    qshift_exist = exist([qshift '.mat']);
    if biort_exist == 2 & qshift_exist == 2;           %Check to see
if the inputs exist as .mat files
        load (biort);
        load (qshift);
    else
        error('Please enter the correct names of the Biorthogonal or Q-
Shift Filters, see help DTWAVEIFM for details.');
```

```

    end
else
    error('Please enter the names of the Biorthogonal or Q-Shift
Filters as shown in help DTWAVEIFM.');
```

```

end

level = a; % No of levels = no of rows in L.

Lo = Yl;
while level >= 2; % Reconstruct levels 2 and above in reverse order.
    Hi = c2qld(Yh{level}*gain_mask(level));
    Lo = colifilt(Lo, g0b, g0a) + colifilt(Hi, glb, gla);

    if size(Lo,1) ~= 2*size(Yh{level-1},1) % If Lo is not the same
length as the next Yh => t1 was extended.
        Lo = Lo(2:size(Lo,1)-1,:); % Therefore we have to clip
Lo so it is the same height as the next Yh.
    end
    if any(size(Lo) ~= size(Yh{level-1}).*[2 1]),
        error('Yh sizes are not valid for DTWAVEIFM');
```

```

    end

    level = level - 1;
end

if level == 1; % Reconstruct level 1.
    Hi = c2qld(Yh{level}*gain_mask(level));
    Z = colfilter(Lo,g0o) + colfilter(Hi,glo);
end

return

%=====
%***** INTERNAL FUNCTION *****
%=====
%=====

function z = c2qld(x)

% An internal function to convert a 1D Complex vector back to a real
array,
```

```
% which is twice the height of x.  
[a b] = size(x);  
z = zeros(a*2,b);  
skip = 1:2:(a*2);  
z(skip,:) = real(x);  
z(skip+1,:) = imag(x);  
  
return
```

APPENDIX B

MATLAB Function to Perform IDTCWT (2-D):

```
function Z = dtwaveifm2(Yl,Yh,biort,qshift,gain_mask);

% Function to perform an n-level dual-tree complex wavelet (DTCWT)
% 2-D reconstruction.
%
% Z = dtwaveifm2(Yl,Yh,biort,qshift,gain_mask);
%
% Yl -> The real lowpass image from the final level
% Yh -> A cell array containing the 6 complex highpass subimages
for each level.
%
% biort -> 'antonini' => Antonini 9,7 tap filters.
%         'legall'   => LeGall 5,3 tap filters.
%         'near_sym_a' => Near-Symmetric 5,7 tap filters.
%         'near_sym_b' => Near-Symmetric 13,19 tap filters.
%
% qshift -> 'qshift_06' => Quarter Sample Shift Orthogonal (Q-
Shift) 10,10 tap filters,
%
%         (only 6,6 non-zero taps).
%         'qshift_a' => Q-shift 10,10 tap filters,
%         (with 10,10 non-zero taps, unlike
qshift_06).
%         'qshift_b' => Q-Shift 14,14 tap filters.
%         'qshift_c' => Q-Shift 16,16 tap filters.
%         'qshift_d' => Q-Shift 18,18 tap filters.
%
% gain_mask -> Gain to be applied to each subband.
%             gain_mask(d,l) is gain for subband with direction
d at level l.
%             If gain_mask(d,l) == 0, no computation is
performed for band (d,l).
%             Default gain_mask = ones(6,length(Yh)).
%
% Z -> Reconstructed real image matrix
%
%
% For example: Z = dtwaveifm2(Yl,Yh,'near_sym_b','qshift_b');
% performs a 3-level reconstruction from Yl,Yh using the 13,19-tap
filters
% for level 1 and the Q-shift 14-tap filters for levels >= 2.
%
a = length(Yh); % No of levels.
if nargin < 5, gain_mask = ones(6,a); end % Default gain_mask.

if isstr(biort) & isstr(qshift) %Check if the inputs are strings
```

```

biort_exist = exist([biort '.mat']);
qshift_exist = exist([qshift '.mat']);
if biort_exist == 2 & qshift_exist == 2;      %Check to see if the
inputs exist as .mat files
    load (biort);
    load (qshift);
else
    error('Please enter the correct names of the Biorthogonal or Q-
Shift Filters, see help DTWAVEIFM2 for details.');
```

```

end
else
    error('Please enter the names of the Biorthogonal or Q-Shift
Filters as shown in help DTWAVEIFM2.');
```

```

end

current_level = a;
Z = Y1;

while current_level >= 2; ; %this ensures that for level -1 we never
do the following
    lh = c2q(Yh{current_level}(:, :, [1 6]), gain_mask([1
6], current_level));
    hl = c2q(Yh{current_level}(:, :, [3 4]), gain_mask([3
4], current_level));
    hh = c2q(Yh{current_level}(:, :, [2 5]), gain_mask([2
5], current_level));

    % Do even Qshift filters on columns.
    y1 = colifilt(Z, g0b, g0a) + colifilt(lh, glb, gla);
    y2 = colifilt(hl, g0b, g0a) + colifilt(hh, glb, gla);
    % Do even Qshift filters on rows.
    Z = (colifilt(y1.', g0b, g0a) + colifilt(y2.', glb, gla)).';

    % Check size of Z and crop as required
    [row_size col_size] = size(Z);
    S = 2*size(Yh{current_level-1});
    if row_size ~= S(1)      %check to see if this result needs to be
cropped for the rows
        Z = Z(2:row_size-1,:);
    end
    if col_size ~= S(2)      %check to see if this result needs to be
cropped for the cols
        Z = Z(:, 2:col_size-1);
    end
    if any(size(Z) ~= S(1:2)),
        error('Sizes of subbands are not valid for DTWAVEIFM2');
```

```

    end

    current_level = current_level - 1;
end

if current_level == 1;
```

```

    lh = c2q(Yh{current_level}(:, :, [1 6]), gain_mask([1
6], current_level));
    hl = c2q(Yh{current_level}(:, :, [3 4]), gain_mask([3
4], current_level));
    hh = c2q(Yh{current_level}(:, :, [2 5]), gain_mask([2
5], current_level));

    % Do odd top-level filters on columns.
    y1 = colfilter(Z, g0o) + colfilter(lh, g1o);
    y2 = colfilter(hl, g0o) + colfilter(hh, g1o);
    % Do odd top-level filters on rows.
    Z = (colfilter(y1.', g0o) + colfilter(y2.', g1o)).';

end

return

%=====
%***** INTERNAL FUNCTION
%*****
%=====

function x = c2q(w, gain)

% function z = c2q(w, gain)
% Scale by gain and convert from complex w(:, :, 1:2) to real quad-
numbers in z.
%
% Arrange pixels from the real and imag parts of the 2 subbands
% into 4 separate subimages .
% A----B      Re   Im of w(:, :, 1)
% |      |
% |      |
% C----D      Re   Im of w(:, :, 2)

sw = size(w);
x = zeros(2*sw(1:2));

if any(w(:)) & any(gain)
    sc = sqrt(0.5) * gain;
    P = w(:, :, 1)*sc(1) + w(:, :, 2)*sc(2);
    Q = w(:, :, 1)*sc(1) - w(:, :, 2)*sc(2);

    t1 = 1:2:size(x, 1);
    t2 = 1:2:size(x, 2);

    % Recover each of the 4 corners of the quads.
    x(t1, t2) = real(P); % a = (A+C)*sc;

```

```
x(t1,t2+1) = imag(P); % b = (B+D)*sc;  
x(t1+1,t2) = imag(Q); % c = (B-D)*sc;  
x(t1+1,t2+1) = -real(Q); % d = (C-A)*sc;  
end  
  
return
```

APPENDIX C

MATLAB Function to Perform DTCWT (1-D):

```
function [Yl,Yh,Yscale] = dtwavexfm(X,nlevels,biort,qshift);

% Function to perform a n-level DTCWT decomposition on a 1-D column
vector X
% (or on the columns of a matrix X).
%
% [Yl,Yh,Yscale] = dtwavexfm(X,nlevels,biort,qshift);
%
% X -> real 1-D signal column vector (or matrix of vectors)
%
% nlevels -> No. of levels of wavelet decomposition
%
% biort -> 'antonini'   => Antonini 9,7 tap filters.
%          'legall'     => LeGall 5,3 tap filters.
%          'near_sym_a' => Near-Symmetric 5,7 tap filters.
%          'near_sym_b' => Near-Symmetric 13,19 tap filters.
%
% qshift -> 'qshift_06' => Quarter Sample Shift Orthogonal (Q-
Shift) 10,10 tap filters,
%                               (only 6,6 non-zero taps).
%          'qshift_a' => Q-shift 10,10 tap filters,
%                               (with 10,10 non-zero taps, unlike
qshift_06).
%          'qshift_b' => Q-Shift 14,14 tap filters.
%          'qshift_c' => Q-Shift 16,16 tap filters.
%          'qshift_d' => Q-Shift 18,18 tap filters.
%
%
% Yl    -> The real lowpass subband from the final level.
% Yh    -> A cell array containing the complex highpass subband
for each level.
% Yscale -> This is an OPTIONAL output argument, that is a cell
array containing
%          the real lowpass coefficients at every scale.
%
%
% Example: [Yl,Yh] = dtwavexfm(X,5,'near_sym_b','qshift_b');
% performs a 5-level transform on the real image X using the 13,19-
tap filters
% for level 1 and the Q-shift 14-tap filters for levels >= 2.
%
%
if isstr(biort) & isstr(qshift) %Check if the inputs are strings
    biort_exist = exist([biort '.mat']);
    qshift_exist = exist([qshift '.mat']);
```

```

    if biort_exist == 2 & qshift_exist == 2; %Check to see if the
filters exist as .mat files
    load (biort);
    load (qshift);
    else
    error('Please enter the correct names of the Biorthogonal or Q-
Shift Filters, see help DTWAVEXFM for details.');
```

```

    end
else
    error('Please enter the names of the Biorthogonal or Q-Shift
Filters as shown in help DTWAVEXFM.');
```

```

end

L = size(X);

if any(rem(L(1),2)), % ensure that X is an even length, thus
enabling it to be extended if needs be.
    error('Size of X must be a multiple of 2');
```

```

end

if nlevels == 0, return; end

%initialise
Yh=cell(nlevels,1);
if nargout == 3
    Yscale=cell(nlevels,1); % This is only required if the user
specifies a third output component.
end

j = sqrt(-1);

% Level 1.
Hi = colfilter(X, h1o);
Lo = colfilter(X, h0o);
t = 1:2:size(Hi,1);
Yh{1} = Hi(t,:) + j*Hi(t+1,:); % Convert Hi to complex form.
if nargout == 3
    Yscale{1} = Lo;
end

if nlevels >= 2; % Levels 2 and above.
    for level = 2:nlevels;
        if rem(size(Lo,1),4), % Check to see if height of Lo is
divisible by 4, if not extend.
            Lo = [Lo(1,:); Lo; Lo(end,:)];
        end
        Hi = coldfilt(Lo,h1b,h1a);
        Lo = coldfilt(Lo,h0b,h0a);
        t = 1:2:size(Hi,1);
        Yh{level} = Hi(t,:) + j*Hi(t+1,:); % Convert Hi to complex form.
        if nargout == 3
            Yscale{level} = Lo;
        end
    end
end

```

```
        end
    end
end

Yl = Lo;

return
```

APPENDIX D

MATLAB Function to Perform DTCWT (2-D):

```
function [Yl,Yh,Yscale] = dtwavexfm2(X,nlevels,biort,qshift);

% Function to perform a n-level DTCWT-2D decomposition on a 2D matrix
X
%
% [Yl,Yh,Yscale] = dtwavexfm2(X,nlevels,biort,qshift);
%
% X -> 2D real matrix/Image
%
% nlevels -> No. of levels of wavelet decomposition
%
% biort -> 'antonini' => Antonini 9,7 tap filters.
%          'legall'   => LeGall 5,3 tap filters.
%          'near_sym_a' => Near-Symmetric 5,7 tap filters.
%          'near_sym_b' => Near-Symmetric 13,19 tap filters.
%
% qshift -> 'qshift_06' => Quarter Sample Shift Orthogonal (Q-
Shift) 10,10 tap filters,
%
%          (only 6,6 non-zero taps).
%          'qshift_a' => Q-shift 10,10 tap filters,
%
%          (with 10,10 non-zero taps, unlike
qshift_06).
%          'qshift_b' => Q-Shift 14,14 tap filters.
%          'qshift_c' => Q-Shift 16,16 tap filters.
%          'qshift_d' => Q-Shift 18,18 tap filters.
%
%
% Yl -> The real lowpass image from the final level
% Yh -> A cell array containing the 6 complex highpass
subimages for each level.
% Yscale -> This is an OPTIONAL output argument, that is a cell
array containing
%          real lowpass coefficients for every scale.
%
%
% Example: [Yl,Yh] = dtwavexfm2(X,3,'near_sym_b','qshift_b');
% performs a 3-level transform on the real image X using the 13,19-
tap filters
% for level 1 and the Q-shift 14-tap filters for levels >= 2.
%

if isstr(biort) & isstr(qshift) %Check if the inputs are strings
    biort_exist = exist([biort '.mat']);
    qshift_exist = exist([qshift '.mat']);
```

```

    if biort_exist == 2 & qshift_exist == 2;           %Check to see
if the inputs exist as .mat files
    load (biort);
    load (qshift);
    else
        error('Please enter the correct names of the Biorthogonal or Q-
Shift Filters, see help DTWAVEXFM2 for details.');
```

```

    end
else
    error('Please enter the names of the Biorthogonal or Q-Shift
Filters as shown in help DTWAVEXFM2.');
```

```

end

original_size = size(X);

if ndims(X) >= 3;
    error(sprintf('The entered image is %dx%dxd, please enter each
image slice
separately.',original_size(1),original_size(2),original_size(3)));
end

% The next few lines of code check to see if the image is odd in
size, if so an extra ...
% row/column will be added to the bottom/right of the image
initial_row_extend = 0; %initialise
initial_col_extend = 0;
if any(rem(original_size(1),2)), %if sx(1) is not divisable by 2 then
we need to extend X by adding a row at the bottom
    X = [X; X(end,:)];           %Any further extension will be done
in due course.
    initial_row_extend = 1;
end
if any(rem(original_size(2),2)), %if sx(2) is not divisable by 2
then we need to extend X by adding a col to the left
    X = [X X(:,end)];           %Any further extension will be done in
due course.
    initial_col_extend = 1;
end
extended_size = size(X);

if nlevels == 0, return; end

%initialise
Yh=cell(nlevels,1);
if nargin == 3
    Yscale=cell(nlevels,1); %this is only required if the user
specifies a third output component.
end

S = [];
sx = size(X);
if nlevels >= 1,
```

```

% Do odd top-level filters on cols.
Lo = colfilter(X,h0o).';
Hi = colfilter(X,h1o).';

% Do odd top-level filters on rows.
LoLo = colfilter(Lo,h0o).';           % LoLo
Yh{1} = zeros([size(LoLo)/2 6]);
Yh{1}(:,:[1 6]) = q2c(colfilter(Hi,h0o).'); % Horizontal
pair
Yh{1}(:,:[3 4]) = q2c(colfilter(Lo,h1o).'); % Vertical
pair
Yh{1}(:,:[2 5]) = q2c(colfilter(Hi,h1o).'); % Diagonal pair
S = [ size(LoLo) ;S];
if nargin == 3
    Yscale{1} = LoLo;
end
end

if nlevels >= 2;
    for level = 2:nlevels;
        [row_size col_size] = size(LoLo);
        if any(rem(row_size,4)), % Extend by 2 rows if no. of rows
of LoLo are divisible by 4;
            LoLo = [LoLo(1,:); LoLo; LoLo(end,:)];
        end
        if any(rem(col_size,4)), % Extend by 2 cols if no. of cols
of LoLo are divisible by 4;
            LoLo = [LoLo(:,1) LoLo LoLo(:,end)];
        end

        % Do even Qshift filters on rows.
Lo = coldfilt(LoLo,h0b,h0a).';
Hi = coldfilt(LoLo,h1b,h1a).';

        % Do even Qshift filters on columns.
LoLo = coldfilt(Lo,h0b,h0a).'; %LoLo
Yh{level} = zeros([size(LoLo)/2 6]);
Yh{level}(:,:[1 6]) = q2c(coldfilt(Hi,h0b,h0a).'); %
Horizontal
Yh{level}(:,:[3 4]) = q2c(coldfilt(Lo,h1b,h1a).'); %
Vertical
Yh{level}(:,:[2 5]) = q2c(coldfilt(Hi,h1b,h1a).'); %
Diagonal
S = [ size(LoLo) ;S];
if nargin == 3
    Yscale{level} = LoLo;
end
end
end

Yl = LoLo;

```

```

if initial_row_extend == 1 & initial_col_extend == 1;
    warning(sprintf(' \r\r The image entered is now a %dx%d NOT a
%dx%d \r The bottom row and rightmost column have been duplicated,
prior to decomposition. \r\r ',...

extended_size(1),extended_size(2),original_size(1),original_size(2));
end

if initial_row_extend == 1 ;
    warning(sprintf(' \r\r The image entered is now a %dx%d NOT a
%dx%d \r Row number %d has been duplicated, and added to the bottom
of the image, prior to decomposition. \r\r',...

extended_size(1),extended_size(2),original_size(1),original_size(2),org
inal_size(1));
end

if initial_col_extend == 1;
    warning(sprintf(' \r\r The image entered is now a %dx%d NOT a
%dx%d \r Col number %d has been duplicated, and added to the right of
the image, prior to decomposition. \r\r',...

extended_size(1),extended_size(2),original_size(1),original_size(2),org
inal_size(2));
end
return

%=====
%
% ***** INTERNAL FUNCTION
% *****
%=====
%=====

function z = q2c(y)

% function z = q2c(y)
% Convert from quads in y to complex numbers in z.

sy = size(y);
t1 = 1:2:sy(1); t2 = 1:2:sy(2);
j2 = sqrt([0.5 -0.5]);

% Arrange pixels from the corners of the quads into
% 2 subimages of alternate real and imag pixels.
% a----b
% |    |
% |    |
% c----d

```

```
% Combine (a,b) and (d,c) to form two complex subimages.  
p = y(t1,t2)*j2(1) + y(t1,t2+1)*j2(2);      % p = (a + jb) / sqrt(2)  
q = y(t1+1,t2+1)*j2(1) - y(t1+1,t2)*j2(2); % q = (d - jc) / sqrt(2)  
  
% Form the 2 subbands in z.  
z = cat(3,p-q,p+q);  
  
return
```

APPENDIX E

Coefficients of the DTCWT Filters:

Antonini 9,7 tap filters. 'antonini'

g_0	g_1	h_0	h_1
-0.04563588155712514	0.026748757410810106	0.026748757410810106	0.04563588155712514
-0.02877176311424934	0.01686411844287467	-0.01686411844287467	-0.02877176311424934
0.295635881557128	-0.07822326652899052	-0.07822326652899052	-0.295635881557128
0.5575435262285023	-0.2668641184428729	0.2668641184428729	0.5575435262285023
0.29563588155712334	0.6029490182363593	0.6029490182363593	-0.29563588155712334
-0.02877176311425308	-0.2668641184428769	0.2668641184428769	-0.02877176311425308
-0.04563588155712608	-0.0782232665289884	-0.0782232665289884	0.04563588155712608
	0.016864118442875293	-0.016864118442875293	
	0.026748757410809648	0.026748757410809648	

LeGall 5,3 tap filters. 'legall'

g_0	g_1	h_0	h_1
0.25	-0.125	-0.125	-0.25
0.5	-0.25	0.25	0.5
0.25	0.75	0.75	-0.25
	-0.25	0.25	
	-0.125	-0.125	

Near-Symmetric 5,7 tap filters. 'near_sym_a'

g₀	g₁	h₀	h₁
-0.010714285714285713	-0.05	-0.05	0.010714285714285713
-0.05357142857142857	-0.25	0.25	-0.05357142857142857
0.26071428571428573	0.6	0.6	-0.26071428571428573
0.6071428571428571	-0.25	0.25	0.6071428571428571
0.26071428571428573	-0.05	-0.05	-0.26071428571428573
-0.05357142857142857			-0.05357142857142857
-0.010714285714285713			0.010714285714285713

Near-Symmetric 13,19 tap filters. 'near_sym_b'

g₀	g₁	h₀	h₁
7.062639508928571E-5	-0.0017578125	-0.0017578125	-7.062639508928571E-5
0.0	-0.0	0.0	0.0
-0.0013419015066964285	0.022265625	0.022265625	0.0013419015066964285
-0.0018833705357142855	0.046875	-0.046875	-0.0018833705357142855
0.007156808035714285	-0.0482421875	-0.0482421875	-0.007156808035714285
0.023856026785714284	-0.296875	0.296875	0.023856026785714284
-0.05564313616071428	0.55546875	0.55546875	0.05564313616071428
-0.05168805803571428	-0.296875	0.296875	-0.05168805803571428
0.29975760323660716	-0.0482421875	-0.0482421875	-0.29975760323660716
0.5594308035714286	0.046875	-0.046875	0.5594308035714286
0.29975760323660716	0.022265625	0.022265625	-0.29975760323660716
-0.05168805803571428	-0.0	0.0	-0.05168805803571428
-0.05564313616071428	-0.0017578125	-0.0017578125	0.05564313616071428
0.023856026785714284			0.023856026785714284
0.007156808035714285			-0.007156808035714285
-0.0018833705357142855			-0.0018833705357142855
-0.0013419015066964285			0.0013419015066964285

0.0			0.0
7.062639508928571E-5			-7.062639508928571E-5

Quarter Sample Shift Orthogonal (Q-Shift) 10,10 tap filters, (only 6,6 non-zero taps).
'qshift_06'

g₀	g₁	h₀	h₁
0.0	-0.03516383657149474	0.03516383657149474	0.0
0.0	0.0	0.0	-0.0
-0.11430183714424873	0.08832942445107285	-0.08832942445107285	0.11430183714424873
0.0	0.23389032060723564	0.23389032060723564	-0.0
0.5875182977235605	-0.7602723690661257	0.7602723690661257	0.5875182977235605
0.7602723690661257	0.5875182977235605	0.5875182977235605	-0.7602723690661257
0.23389032060723564	-0.0	0.0	0.23389032060723564
-0.08832942445107285	-0.11430183714424873	-0.11430183714424873	0.08832942445107285
0.0	-0.0	0.0	0.0
0.03516383657149474	0.0	0.0	0.03516383657149474

Q-shift 10,10 tap filters, (with 10,10 non-zero taps, unlike qshift_06). 'qshift_a'

g₀	g₁	h₀	h₁
-0.006181881892116438	-0.051130405283831656	0.051130405283831656	-0.006181881892116438
-0.0016896812725281543	-0.013975370246888838	-0.013975370246888838	0.0016896812725281543
-0.1002312195074762	0.10983605166597087	-0.10983605166597087	-0.1002312195074762
8.736226952170968E-4	0.26383956105893763	0.26383956105893763	-8.736226952170968E-4
0.5636557101270515	-0.7666284677930372	0.7666284677930372	0.5636557101270515
0.7666284677930372	0.5636557101270515	0.5636557101270515	-0.7666284677930372
0.26383956105893763	-8.736226952170968E-4	8.736226952170968E-4	0.26383956105893763
-0.10983605166597087	-0.1002312195074762	-0.1002312195074762	0.10983605166597087

-0.013975370246888838	0.0016896812725281543	-0.0016896812725281543	-0.013975370246888838
0.051130405283831656	-0.006181881892116438	-0.006181881892116438	-0.051130405283831656

Q-Shift 14,14 tap filters. 'qshift_b'

g_0	g_1	h_0	h_1
-0.004556895628475491	-0.003253142763653182	0.003253142763653182	-0.004556895628475491
-0.005439475937274115	-0.00388321199915849	-0.00388321199915849	0.005439475937274115
0.01702522388155399	-0.03466034684485349	0.03466034684485349	0.01702522388155399
0.023825384794920298	-0.03887280126882779	-0.03887280126882779	-0.023825384794920298
-0.1067118046866654	0.11720388769911527	-0.11720388769911527	-0.1067118046866654
0.011866092033797	0.27529538466888204	0.27529538466888204	-0.011866092033797
0.5688104207121227	-0.7561456438925225	0.7561456438925225	0.5688104207121227
0.7561456438925225	0.5688104207121227	0.5688104207121227	-0.7561456438925225
0.27529538466888204	-0.011866092033797	0.011866092033797	0.27529538466888204
-0.11720388769911527	-0.1067118046866654	-0.1067118046866654	0.11720388769911527
-0.03887280126882779	-0.023825384794920298	0.023825384794920298	-0.03887280126882779
0.03466034684485349	0.01702522388155399	0.01702522388155399	-0.03466034684485349
-0.00388321199915849	0.005439475937274115	-0.005439475937274115	-0.00388321199915849
0.003253142763653182	-0.004556895628475491	-0.004556895628475491	-0.003253142763653182

Q-Shift 16,16 tap filters. 'qshift_c'

g_0	g_1	h_0	h_1
0.002430349945148675	0.0047616119384559135	0.0047616119384559135	0.002430349945148675
-2.276522058977718E-4	-4.4602278926228516E-4	-4.460227892622816E-4	2.276522058977718E-4
-0.0072026778782583465	7.144197327965012E-5	-7.144197327965012E-5	-0.0072026778782583465
0.018498682724156248	0.034914612306842195	0.034914612306842195	-0.018498682724156248
0.02228926326692271	0.03727389579989796	-0.03727389579989796	0.02228926326692271

-0.11255888425752203	-0.11591145742744076	-0.11591145742744076	0.11255888425752203
0.01463740596447335	-0.2763686431330317	0.2763686431330317	0.01463740596447335
0.567134484100133	0.7563937651990367	0.7563937651990367	-0.567134484100133
0.7563937651990367	-0.567134484100133	0.567134484100133	0.7563937651990367
0.2763686431330317	0.01463740596447335	0.01463740596447335	-0.2763686431330317
-0.11591145742744076	0.11255888425752203	-0.11255888425752203	-0.11591145742744076
-0.03727389579989796	0.02228926326692271	0.02228926326692271	0.03727389579989796
0.034914612306842195	-0.018498682724156248	0.018498682724156248	0.034914612306842195
-7.144197327965012E-5	-0.0072026778782583465	0.0072026778782583465	7.144197327965012E-5
-4.4602278926228516E-4	2.276522058977718E-4	-2.276522058977718E-4	-4.4602278926228516E-4
-0.0047616119384559135	0.002430349945148675	0.002430349945148675	0.0047616119384559135

Q-Shift 18,18 tap filters. 'qshift_d'

g_0	g_1	h_0	h_1
0.002411869456666278	0.002284127440270531	-0.002284127440270531	0.002411869456666278
0.0012775586538069982	0.0012098941630734423	0.0012098941630734423	0.0012775586538069982
-0.0025761743066007948	0.011834794515430786	-0.011834794515430786	0.0025761743066007948
-0.006628794612430063	0.0012834569993443994	0.0012834569993443994	0.006628794612430063
0.03152637712208465	-0.044365221606616996	0.044365221606616996	0.03152637712208465
0.018156493945546453	-0.05327610880304726	-0.05327610880304726	-0.018156493945546453
-0.12018854471079482	0.1133058863621428	-0.1133058863621428	-0.12018854471079482
0.024550152433666563	0.2809028632221865	0.2809028632221865	-0.024550152433666563
0.5658080673964587	-0.7528160380878561	0.7528160380878561	0.5658080673964587
0.7528160380878561	0.5658080673964587	0.5658080673964587	-0.7528160380878561
0.2809028632221865	-0.024550152433666563	0.024550152433666563	0.2809028632221865
-0.1133058863621428	-0.12018854471079482	-0.12018854471079482	0.1133058863621428
-0.05327610880304726	-0.018156493945546453	0.018156493945546453	-0.05327610880304726
0.044365221606616996	0.03152637712208465	0.03152637712208465	-0.044365221606616996
0.0012834569993443994	0.006628794612430063	-0.006628794612430063	0.0012834569993443994

-0.011834794515430786	-0.0025761743066007948	-0.0025761743066007948	0.011834794515430786
0.0012098941630734423	-0.0012775586538069982	0.0012775586538069982	0.0012098941630734423
-0.002284127440270531	0.002284127440270531	-0.002284127440270531	0.002284127440270531